The Wiener-Hopf-Hilbert Technique Applied to Problems in Diffraction

a thesis submitted for the degree of

Doctor of Philosophy

by

Peter Geoffrey Barton
Department of Mathematical Sciences
Brunel University

September 1999

Abstract

A number of diffraction problems which have practical applications are examined using the Wiener-Hopf-Hilbert technique. Each problem is formulated as a matrix Wiener-Hopf equation, the solution of which requires the factorisation of a matrix kernel. Since the determinant of the matrix kernel has poles in the cut plane, the Wiener-Hopf-Hilbert technique is modified to allow the usual arguments to follow through. In each case an explicit matrix factorisation is carried out and asymptotic expressions for the field scattered to infinity are obtained.

The first problem solved is that of diffraction by a semi-infinite plane with different face impedances. The solution includes the case of an incident surface wave as well as an incident plane wave for an arbitrary angle of incidence. Graphs of the far-field are provided for various values of the half-plane impedance parameters. The second problem examined is diffraction by a half-plane in a moving fluid. This is solved without restriction on the impedance parameters of the half-plane and includes both the leading edge and trailing edge situations. The final problem is of radiation from an inductive wave-guide. Expressions are obtained for the field radiated at the wave-guide mouth and the field reflected in the duct region.

Acknowledgements

I would like to express my thanks to Dr Tony Rawlins for his help, advice and encouragement, which he has given freely throughout my time at Brunel. My thanks also goes to my former supervisor the late Professor Gerry Wickham. I express my gratitude to the EPSRC for their funding of this work.

Special thanks go to all of my family for their support and for everything they have done for me. Finally, my thanks go to all my friends from Bolton, Oxford and especially to Jo and my friends from Brunel.

Declaration

I declare that this work has not been submitted for a degree at any other university or institution.

Parts of Chapter 2 have been published in the Quarterly Journal of Mechanics and Applied Mathematics as a paper entitled Diffraction by a Semi-Infinite Plane with Different Face Impedances.

PETER BARTON

Contents

Appendices

List of Figures

Chapter 1

Introduction

1.1 The Wiener-Hopf Technique

This work concerns the scattering of acoustic and electromagnetic waves for impedance half-plane type boundary value problems. There are two basic analytical methods used for the solution of diffraction problems of this type. The Maliuzhinets [20] method introduced in 1958 was used to obtain a complete solution to the problem of diffraction of a plane wave by an impedance wedge. On setting the wedge angle to be zero this gives a solution to the problem of the diffraction of a plane wave by a half-plane with different face impedances.

The matrix Wiener-Hopf method employed in this work is a generalization of the Wiener-Hopf [33] technique introduced in 1931. This method is useful for solving boundary value problems on semi-infinite geometries; Noble [27] gives a comprehensive guide to the technique. The matrix method involves the solution of a matrix Wiener-Hopf equation which is defined in a strip (or on a line) τ of the complex α-plane and takes the form

$$G(\alpha)l(\alpha) = u(\alpha) + P(\alpha), \tag{1.1}$$

where $G(\alpha)$ is a known square matrix and $P(\alpha)$ is a known vector. The unknowns $u(\alpha)$ and $l(\alpha)$ have elements that are analytic in an upper (τ_+) and lower (τ_-) halves of the complex plane respectively. $G(\alpha)$ and $P(\alpha)$ are analytic in the strip (or on the line) $\tau = \tau_+ \cap \tau_-$. The solution of such an equation requires the factorisation of the matrix kernel $G(\alpha)$ such that

$$G(\alpha) = G_+(\alpha)\, G_-(\alpha), \tag{1.2}$$

where G_+ and G_- and their inverses are regular and analytic in τ_+ and τ_- respectively, and their elements have algebraic behaviour at infinity. In the scalar case this can be done by taking logarithms and sum splitting the kernel using Cauchy's theorem. However, in the case of matrices this does not apply due to the non-commutativity of the matrices involved, or the exponential behaviour of the matrix elements at infinity. This is the main obstacle in solving matrix Wiener-Hopf problems and three main methods of factorisation have been developed. Following is a summary to these three techniques, a comprehensive guide with worked examples can be found in [7].

The weak factorisation method was developed independently by Idemen and Abrahams. Although this method does not require the non-singularity of G_+ and G_- it does require the solution of an infinite system of linear algebraic equations. This method has been applied to several half-plane problems, including scattering of acoustic waves by Abrahams and Wickham [1], [2] and [3].

The Daniele/Khrapkov method is based on a basic idea by Heins [10]. It was developed independently by Khrapkov [17] and later by Daniele [5] who overcame the problems with exponential growth of the split matrices. More recently, work has been

carried out by Meister and Speck [22] based on factorizations of this form. Formulating the problems in a Sobolev space setting, their work includes the impedance problem and a general problem involving second order boundary conditions.

The method adopted in this work is the Wiener-Hopf-Hilbert method introduced by Hurd in 1976 [11]. A criterion for the range of applicability of this method was given by Hurd and includes that of Rawlins and Williams [30]. Examples of problems solved using the Wiener-Hopf-Hilbert method include Hurd and Przeździecki [13], [14] and Lüneburg and Hurd [18]. The gist of this method is to reduce the matrix Wiener-Hopf equation to a pair of coupled Hilbert equations. The matrix in this case is considerably simpler and can be solved using Muskhelishvili's theory [26]. It will be seen that the determinants of the matrices in the problems considered have poles in the cut plane. The Wiener-Hopf-Hilbert technique is therefore modified to allow the usual arguments to follow through.

1.2 Structure of the Thesis

The structure of each of the following chapters follows the same basic pattern. In each case the boundary value problem is set up and from this a matrix Wiener-Hopf equation is derived. The matrix kernel is then factorised and an expression for the far-field is established. A discussion is then given of any graphical results obtained.

In Chapter 2 the problem of the diffraction of a plane acoustic wave incident on a semi-infinite plane is solved. The upper and lower surfaces of the half-plane are lined with materials with different absorbing properties and the solution given is valid

for an arbitrary angle of incidence. Expressions are obtained for the reflected and diffracted fields as well as arising surface waves. Graphs of the far-field are given for a range of values of the angle of incidence and specific admittance of the half-plane surfaces. It is shown that this solution is valid for an incident surface wave. Graphs of a diffracted 'lobe' are obtained and the reflected and transmitted surface waves are examined. This problem generalizes that solved by Trenev [32] for an electromagnetic application.

A more general boundary condition is considered in Chapter 3. This is equivalent to the problem of the diffraction of sound by a half-plane in a moving fluid and the solution reduces, in a special situation, to that given by Rawlins [29]. The solution given includes both the leading edge and trailing edge situation, where a Kutta-Joukowski edge condition is imposed. Graphs of the far-field are plotted for both absorbent and wave-bearing half-planes. It can be seen that special cases of this solution agree with results from Chapter 2.

In Chapter 4 the problem of electromagnetic radiation from an inductive waveguide is solved. An exact closed form solution is obtained for the problem of a radiating parallel plate waveguide when the inside walls are inductively loaded and the outside walls are capacitively loaded. This mathematical problem serves as a model for an inductively loaded horn antenna. Expressions are computed for the reflection coefficient at the waveguide mouth and the radiation diagrams of the far-field.

At the end of each chapter, conclusions are drawn from the results obtained in solving these problems. Suggestions are also made as to possible further developments

in the use of the Wiener-Hopf-Hilbert technique to solve diffraction problems.

Appendix A gives an alternative expression for the diffracted field to give uniform asympotics across the geometrical optics boundaries. Appendix B gives an analysis of the incident field used in the wave-guide problem (Chapter 4). A selection of the Mathematica programs used to obtain the graphical plots are given in Appendix C. Finally, in Appendices D and E, contour integrations are carried out that are required in Chapters 2-4.

Chapter 2

Diffraction by a Half-Plane with Different Face Impedances

2.1 Introduction

The problem of diffraction of a plane wave by a semi-infinite plane with different impedance boundary conditions on each face was first solved by Maliuzhinets [20] using a Sommerfeld integral representation for the field. It is also possible to formulate the problem as a pair of simultaneous Wiener-Hopf equations that were thought to be insoluble until Hurd [11] introduced the powerful Wiener-Hopf-Hilbert technique. This method involves transforming the Wiener-Hopf equations into pair of coupled Hilbert equations, which can be solved using Muskhelishvili's theory [26]. The crux of this method requires that the determinant of the Wiener-Hopf kernel does not vanish in the cut plane. In the case where the impedance parameters are such that the half-plane is absorbent, the determinant of the matrix kernel is non-zero. Rawlins [31] obtained explicit expressions for the diffracted and geometrical acoustic field for the diffraction of waves from a line source by an impedance half-plane. However, for wave bearing surfaces, where the impedance parameter can be purely imaginary,

the determinant of the matrix kernel has zeros in the cut plane. Here the Wiener-Hopf-Hilbert approach is generalised to deal with both wave-bearing and absorbent surfaces.

The present work has applications in acoustics and electromagnetics. The half-plane problem with absorbing boundary conditions forms a mathematical model for a noise barrier lined with different materials on its upper and lower surfaces. Such barriers can be used to reduce noise levels from airports or motorways. Only the field radiated from the edge of the barrier affects a receiver in the shadow region of such a barrier. This can be reduced by lining the barrier with different acoustically absorbent materials. In the case where the impedance parameters are purely imaginary, the half-plane can be considered as a directional wave launcher. The present work also has applications in electromagnetism where a thin dielectric layer above a perfectly conducting half-plane acts as a waveguide launcher.

In Section 2.2 the mathematical boundary value problem is formulated. The problem is then solved in Section 2.3 by an application of complex Fourier transforms, this results in a pair of Wiener-Hopf equations. The important step in any Wiener-Hopf problem is the factorisation of the Wiener-Hopf matrix kernel, this is carried out in Section 2.4. Although the determinant of the matrix kernel contains singularities, by performing the factorisation on a matrix $K(\alpha)$ with a constant determinant, the problem of factorisation of the matrix kernel can be reduced to pair of coupled Hilbert equations in the usual way. In Section 2.5 asymptotic approximations for the far-field are obtained. Explicit expressions are given for the diffracted and geometrical acous-

tic field and graphs of the far-field are plotted. Graphical results for various angles of incidence and impedance values are given in Section 2.6. These results are followed by an examination of some special cases that are of particular interest. The special case of a rigid half-plane is examined in detail in Section 2.7. The expressions for the far-field simplify considerably in this case and are clearly in agreement with earlier work done on this problem. Section 2.8 looks at the case of a semi-rigid half-plane, that is a half-plane with one zero and one none zero impedance parameter. How such a barrier could be best used to reduce the sound intensity between a source and receiver is discussed.

Surface waves are examined in Section 2.9. In the particular case where the specific admittance of the half-plane surfaces is wholly imaginary, it is shown that surface waves arise. Moreover, the solution given in Section 2.5 is valid for complex values of the incident wave angle (i.e. the problem of an incident surface wave). Diffracted lobes are obtained and the reflected and transmitted surface waves are examined. Two special cases are then examined for the case of a surface wave incident upon a half-plane. In Section 2.10 an inductive half-plane with the same impedance parameters on its upper and lower surfaces is considered. In Section 2.11 is examined a half-plane whose impedance parameters vary only in sign. It will be seen that the radiated lobes are identical in these two cases, though the reflected and transmitted surface waves are not. Conclusions are drawn and further work discussed in Section 2.12.

2.2 Formulation of the Boundary Value Problem

To begin with, the basic equations governing propagation through a homogeneous medium are introduced. The density field, ρ and velocity field, $\mathbf{u}$ satisfy the continuity equation

$$\frac{\partial \rho}{\partial t} + \nabla.(\rho \mathbf{u}) = 0. \tag{2.1}$$

An equation of state, which describes the compressibility properties of the medium, is also required. It will be assumed that the pressure, p depends only on the local density

$$p = p(\rho). \tag{2.2}$$

When the medium is inviscid and in the absence of external forces, the Navier-Stokes equation of motion reduces to Euler's equation

$$\frac{\partial \mathbf{u}}{\partial t} + (\mathbf{u}.\nabla)\mathbf{u} = -\frac{1}{\rho}\nabla p. \tag{2.3}$$

These three equations are linearised by regarding as small all perturbations from a state in which the medium is at rest and has uniform density ρ_o and pressure p. By retaining only first order terms the following linearised equations are formed

$$\frac{\partial \rho}{\partial t} = -\rho_o \nabla.\mathbf{u}, \tag{2.4}$$

$$\frac{\partial \mathbf{u}}{\partial t} = -\frac{1}{\rho_o}\nabla p, \tag{2.5}$$

$$\frac{\partial p}{\partial t} = c^2 \frac{\partial \rho}{\partial t}, \tag{2.6}$$

where c is the speed of sound. By taking the curl of equation (2.5) it can be seen that the vorticity $\mathbf{\Omega} = \nabla \wedge \mathbf{u}$ is independent of time. Thus, for an initially irrotational

flow, $\mathbf{\Omega} = 0$ for all time and there exists a velocity potential $\psi(\mathbf{x}, t)$ such that

$$\mathbf{u} = \nabla\psi. \tag{2.7}$$

Eliminating ρ and p from equations (2.4)-(2.6) gives the wave equation

$$\frac{\partial^2\psi}{\partial t^2} = c^2\nabla^2\psi. \tag{2.8}$$

Writing $\psi(x, y, t) = \text{Re}\{\psi(x, y)e^{-i\omega t}\}$ and suppressing the time factor $e^{-i\omega t}$ throughout results in the Helmholtz equation

$$\left(\nabla^2 + k^2\right)\psi(x, y) = 0. \tag{2.9}$$

The acoustic wave number k is related to the angular frequency ω by the identity $\omega = kc$.

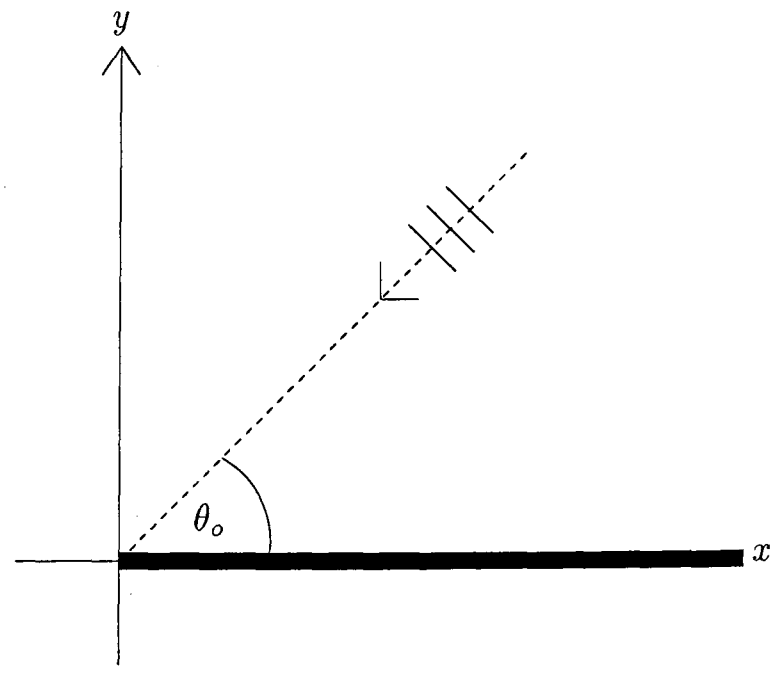

Figure 2.1: A plane wave incident on a half-plane.

It is assumed that the half-plane occupies the region $x \geq 0,\ y = 0$ (see Figure 2.1) and the surfaces are lined with materials such that β_1 and β_2 are the complex specific

admittances of the upper and lower surfaces of the half-plane respectively. It is noted that for Re $\beta_{1,2} > 0$ the surface is absorbent. For Re $\beta_{1,2} = 0$ the surface no longer absorbs energy and can support surface waves provided $\beta_{1,2} = -iX_{1,2}, X_{1,2} > 0$. The problem is one of solving the Helmholtz equation

$$\frac{\partial^2\psi}{\partial x^2} + \frac{\partial^2\psi}{\partial y^2} + k^2\psi = 0, \tag{2.10}$$

subject to the boundary conditions (see [24])

$$\frac{\partial\psi}{\partial y}(x, 0^+) + ik\beta_1\psi(x, 0^+) = 0, \quad x > 0, \tag{2.11}$$

$$\frac{\partial\psi}{\partial y}(x, 0^-) - ik\beta_2\psi(x, 0^-) = 0, \quad x > 0. \tag{2.12}$$

The potential ψ must also satisfy the continuity conditions

$$\frac{\partial\psi}{\partial y}(x, 0^+) = \frac{\partial\psi}{\partial y}(x, 0^-), \quad x < 0, \tag{2.13}$$

$$\psi(x, 0^+) = \psi(x, 0^-), \quad x < 0, \tag{2.14}$$

and the edge condition

$$\psi = O(1), \quad \frac{\partial\psi}{\partial y} = O(x^{-1/2}), \quad \text{as } x \to 0. \tag{2.15}$$

Combined with the condition that the diffracted field is outgoing at infinity, these conditions ensure that the boundary value problem has a unique solution.

2.3 Reduction to a Matrix Wiener-Hopf Equation

Define the complex Fourier transform $\hat{\psi}(\alpha, y)$ by

$$\hat{\psi}(\alpha, y) = \frac{1}{2\pi}\int_{-\infty}^{\infty}\psi(x, y)e^{-i\alpha x}dx. \tag{2.16}$$

Applying this transform to the Helmholtz equation (2.10) gives

$$\frac{d^2\hat{\psi}}{dy^2} + \kappa^2\hat{\psi} = 0. \tag{2.17}$$

The branch of $\kappa = (k^2 - \alpha^2)^{1/2}$ is chosen such that $\kappa = +k$ for $\alpha = 0$. It can now be seen that a solution to the boundary value problem is given by

$$\psi = \psi_{go} + \int_{-\infty}^{\infty} A(\alpha)e^{i(\alpha x+\kappa y)}\, d\alpha, \quad y > 0, \tag{2.18}$$

$$= \int_{-\infty}^{\infty} B(\alpha)e^{i(\alpha x-\kappa y)}\, d\alpha, \qquad y < 0. \tag{2.19}$$

For convenience it is assumed that ψ_{go} consists of the incident plane wave and a reflected wave thus

$$\psi_{go} = e^{-ik(x\cos\theta_o+y\sin\theta_o)} + Re^{-ik(x\cos\theta_o-y\sin\theta_o)}, \tag{2.20}$$

where

$$R = \left(\frac{\sin\theta_o - \beta_1}{\sin\theta_o + \beta_1}\right), \quad 0 < \theta_o < \pi. \tag{2.21}$$

Applying the continuity conditions (2.13) and (2.14) leads to

$$A(\alpha) - B(\alpha) = l_1(\alpha) - \frac{\sin\theta_o}{\pi i(\beta_1 + \sin\theta_o)(\alpha + k_o)}, \tag{2.22}$$

$$\kappa(A(\alpha) + B(\alpha)) = l_2(\alpha) + \frac{k\beta_1\sin\theta_o}{\pi i(\beta_1 + \sin\theta_o)(\alpha + k_o)}, \tag{2.23}$$

where $\alpha = -k_o = -k\cos\theta_o$ lies in the lower half of the α-plane (τ_- =Im(α) ≤ 0) and $l_1(\alpha)$ and $l_2(\alpha)$ are analytic in this region. The capture of the pole at $\alpha = -k_o$ in the lower half plane is shown in Figure 2.2. The boundary conditions (2.11) and (2.12) lead to

$$(k\beta_1 + \kappa)A(\alpha) = u_1(\alpha), \tag{2.24}$$

$$(k\beta_2 + \kappa)B(\alpha) = u_2(\alpha), \tag{2.25}$$

where $u_1(\alpha)$ and $u_2(\alpha)$ are analytic in the upper half of the α-plane ($\tau_+ = \mathrm{Im}(\alpha) \geq 0, \alpha \neq -k_o$).

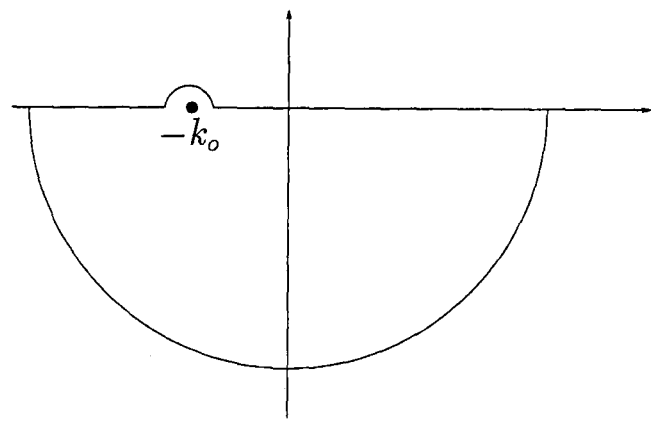

Figure 2.2: The complex plane.

Eliminating the unknowns $A(\alpha), B(\alpha)$ gives

$$(k\beta_1 + \kappa)\frac{1}{2}\left(l_1 + \frac{l_2}{\kappa}\right) = u_1 + \frac{\sin\theta_o(\kappa + k\beta_1)(1 - k\beta_1/\kappa)}{2\pi i(\beta_1 + \sin\theta_o)(\alpha + k_o)}, \tag{2.26}$$

$$(k\beta_2 + \kappa)\frac{1}{2}\left(-l_1 + \frac{l_2}{\kappa}\right) = u_2 - \frac{\sin\theta_o(\kappa + k\beta_2)(1 + k\beta_1/\kappa)}{2\pi i(\beta_1 + \sin\theta_o)(\alpha + k_o)}, \tag{2.27}$$

which leads to the matrix Wiener-Hopf equation

$$G(\alpha)l(\alpha) = u(\alpha) + G(\alpha)\frac{P}{(\alpha + k_o)}, \tag{2.28}$$

where

$$G(\alpha) = \frac{1}{2}\begin{pmatrix} \kappa + k\beta_1 & (\kappa + k\beta_1)/\kappa \\ -\kappa - k\beta_2 & (\kappa + k\beta_2)/\kappa \end{pmatrix}, \tag{2.29}$$

$$P = \frac{\sin\theta_o}{\pi i(\beta_1 + \sin\theta_o)}\begin{pmatrix} 1 \\ -k\beta_1 \end{pmatrix}, \quad l(\alpha) = \begin{pmatrix} l_1 \\ l_2 \end{pmatrix}, \quad u(\alpha) = \begin{pmatrix} u_1 \\ u_2 \end{pmatrix}. \tag{2.30}$$

Define $D(\alpha)$ such that

$$D^2(\alpha) = \det G(\alpha) = \frac{1}{2\kappa}(\kappa + k\beta_1)(\kappa + k\beta_2),$$

and define $K(\alpha)$ by

$$G(\alpha) = D(\alpha)K(\alpha). \tag{2.31}$$

Then

$$K(\alpha) = \left\{\frac{\kappa}{2(\kappa+k\beta_1)(\kappa+k\beta_2)}\right\}^{\frac{1}{2}} \begin{pmatrix} \kappa+k\beta_1 & (\kappa+k\beta_1)/\kappa \\ -(\kappa+k\beta_2) & (\kappa+k\beta_2)/\kappa \end{pmatrix}, \tag{2.32}$$

and

$$\det K(\alpha) = 1.$$

The factorisation of $G(\alpha)$ now follows directly from the factorisation of $K(\alpha)$ and $D(\alpha)$.

2.4 Factorisation of the Matrix Kernel

Factorisation of $K(\alpha)$

The required factorisation is $K(\alpha) = U(\alpha)L^{-1}(\alpha)$ where $L(\alpha)$ is analytic everywhere except $k < \alpha < \infty$, $\mathrm{Im}(\alpha) = 0$ and $U(\alpha)$ is analytic everywhere except $-\infty < \alpha < -k$, $\mathrm{Im}(\alpha) = 0$. Then it can be seen that

$$\left.\begin{aligned} K^+(\xi) &= U^+(\xi)L^{-1}(\xi) \\ K^-(\xi) &= U^-(\xi)L^{-1}(\xi) \end{aligned}\right\} \quad -\infty < \xi < -k, \tag{2.33}$$

since L is continuous across this region. Eliminating $L^{-1}(\xi)$ gives

$$U^+(\xi) = K^+(\xi)[K^{-1}(\xi)]^- U^-(\xi), \tag{2.34}$$

where F^+ denotes values of F on the upper side of the cut and F^- denotes values of F on the lower side of the cut. From equation (2.32) it follows that

$$K^+(\xi) = \left\{\frac{i|\kappa|}{2(i|\kappa|+k\beta_1)(i|\kappa|+k\beta_2)}\right\}^{\frac{1}{2}} \begin{pmatrix} i|\kappa|+k\beta_1 & \dfrac{i|\kappa|+k\beta_1}{i|\kappa|} \\ -(i|\kappa|+k\beta_2) & \dfrac{i|\kappa|+k\beta_2}{i|\kappa|} \end{pmatrix}, \tag{2.35}$$

$$[K^{-1}(\xi)]^- = \left\{\frac{-i|\kappa|}{2(-i|\kappa|+k\beta_1)(-i|\kappa|+k\beta_2)}\right\}^{\frac{1}{2}} \begin{pmatrix} \frac{-i|\kappa|+k\beta_2}{-i|\kappa|} & \frac{-i|\kappa|+k\beta_1}{i|\kappa|} \\ -i|\kappa|+k\beta_2 & -i|\kappa|+k\beta_1 \end{pmatrix}. \quad (2.36)$$

Equation (2.34) then becomes

$$U^+(\xi) = \left\{\frac{1}{(k^2\beta_1^2+|\kappa|^2)(k^2\beta_2^2+|\kappa|^2)}\right\}^{\frac{1}{2}} \begin{pmatrix} 0 & -i(k^2\beta_1^2+|\kappa|^2) \\ -i(k^2\beta_2^2+|\kappa|^2) & 0 \end{pmatrix} U^-(\xi).$$

This simplifies to

$$U^+(\xi) = \begin{pmatrix} 0 & -i\left(\frac{k^2\beta_1^2+|\kappa|^2}{k^2\beta_2^2+|\kappa|^2}\right)^{1/2} \\ -i\left(\frac{k^2\beta_2^2+|\kappa|^2}{k^2\beta_1^2+|\kappa|^2}\right)^{1/2} & 0 \end{pmatrix} U^-(\xi). \quad (2.37)$$

It is apparent that the above equation necessitates the solution of the following coupled Hilbert problems

$$U_1^+(\xi) = -i\left(\frac{k^2\beta_1^2+|\kappa|^2}{k^2\beta_2^2+|\kappa|^2}\right)^{\frac{1}{2}} U_2^-(\xi), \quad (2.38)$$

$$U_2^+(\xi) = -i\left(\frac{k^2\beta_2^2+|\kappa|^2}{k^2\beta_1^2+|\kappa|^2}\right)^{\frac{1}{2}} U_1^-(\xi). \quad (2.39)$$

The substitutions $V(\xi) = U_1(\xi)U_2(\xi)$ and $W(\xi) = \dfrac{U_1(\xi)}{U_2(\xi)}$, upon multiplying and dividing the Hilbert equations, produce

$$V^+(\xi)/V^-(\xi) = -1, \quad (2.40)$$

$$[\log W(\xi)]^+ + [\log W(\xi)]^- = \log\left[\frac{|\kappa|^2+k^2\beta_1^2}{|\kappa|^2+k^2\beta_2^2}\right]. \quad (2.41)$$

By inspection, it can be seen that equation (2.40) has a particular solution

$$V(\alpha) = (k+\alpha)^{-\frac{1}{2}}. \quad (2.42)$$

By using the result $[\sqrt{k+\xi}]^{\pm} = \pm i|k+\xi|^{\frac{1}{2}}$, equation (2.41) can be written in the form

$$\left[\frac{\log W(\xi)}{\sqrt{k+\xi}}\right]^+ - \left[\frac{\log W(\xi)}{\sqrt{k+\xi}}\right]^- = \frac{-i}{|k+\xi|^{\frac{1}{2}}} \log\left[\frac{|\kappa|^2+k^2\beta_1^2}{|\kappa|^2+k^2\beta_2^2}\right]. \quad (2.43)$$

This standard Hilbert problem has a solution (see Appendix E)

$$W(\alpha) = \exp\left[-\frac{\sqrt{k+\alpha}}{2\pi}\int_{-\infty}^{-k}\frac{1}{|k+t|^{\frac{1}{2}}}\log\left[\frac{|\kappa|^2+k^2\beta_1^2}{|\kappa|^2+k^2\beta_2^2}\right]\frac{dt}{t-\alpha}\right]. \tag{2.44}$$

By manipulating the integrand, this reduces to

$$W(\alpha) = \exp\left[\frac{\sqrt{k+\alpha}}{2\pi}\int_0^{\infty}\Big\{\log[t+kB_1(+)]+\log[t+kB_1(-)] - \log[t+kB_2(+)]-\log[t+kB_2(-)]\Big\}\frac{dt}{t^{\frac{1}{2}}(t+k+\alpha)}\right],$$

where $B_{1,2}(\pm) = 1 \pm \sqrt{1-\beta_{1,2}^2}$. Using the result (see Appendix D)

$$\int_0^{\infty}\frac{\log(t+\delta)}{t^{\frac{1}{2}}(t+\gamma)}dt = \frac{2\pi}{\sqrt{\gamma}}\log(\sqrt{\gamma}+\sqrt{\delta}),\quad |\arg\gamma|<\pi,\quad |\arg\delta|\le\pi, \tag{2.45}$$

enables a solution of (2.41) to be written as

$$W(\alpha) = \frac{\left(\sqrt{k+\alpha}+\sqrt{kB_1(+)}\right)\left(\sqrt{k+\alpha}+\sqrt{kB_1(-)}\right)}{\left(\sqrt{k+\alpha}+\sqrt{kB_2(+)}\right)\left(\sqrt{k+\alpha}+\sqrt{kB_2(-)}\right)}. \tag{2.46}$$

Particular solutions of (2.38) and (2.39) are now given by

$$U_1(\alpha) = -[V(\alpha)]^{\frac{1}{2}}[W(\alpha)]^{\frac{1}{2}},$$

$$U_2(\alpha) = -[V(\alpha)]^{\frac{1}{2}}[W(\alpha)]^{-\frac{1}{2}}.$$

A general solution can be obtained by following the method given by Rawlins [31]. This is done by imposing further conditions on the functions $U_1(\alpha)$ and $U_2(\alpha)$. First it is required that

$$U_1(\alpha) = O((k+\alpha)^n),\quad U_2(\alpha) = O((k+\alpha)^{1/2+m}),\quad \text{as } \alpha\to -k,$$

for some $n, m > -1$. Secondly it is required that $U_1(\alpha)$ and $U_2(\alpha)$ have finite degree at infinity. These conditions lead to

$$U(\alpha) = U^{(0)}(\alpha)P(\alpha),$$

where $P_{ij}(i,j=1,2)$ are arbitrary polynomials and

$$U^{(0)}(\alpha) = \begin{pmatrix} -[V(\alpha)]^{\frac{1}{2}}[W(\alpha)]^{\frac{1}{2}} & [V(\alpha)]^{\frac{1}{2}}[W(\alpha)]^{\frac{1}{2}}[k+\alpha]^{\frac{1}{2}} \\ -[V(\alpha)]^{\frac{1}{2}}[W(\alpha)]^{-\frac{1}{2}} & -[V(\alpha)]^{\frac{1}{2}}[W(\alpha)]^{-\frac{1}{2}}[k+\alpha]^{\frac{1}{2}} \end{pmatrix}.$$

To ensure that U is non-singular in the cut plane $\det U$ and hence $\det P$ must be non-zero for all α. Since $\det P$ is a polynomial, it follows that $\det P=$ constant. For simplicity, P is chosen to be the identity matrix. This gives a final expression of

$$U(\alpha) = \begin{pmatrix} -[k+\alpha]^{-\frac{1}{4}}[W(\alpha)]^{\frac{1}{2}} & [k+\alpha]^{\frac{1}{4}}[W(\alpha)]^{\frac{1}{2}} \\ -[k+\alpha]^{-\frac{1}{4}}[W(\alpha)]^{-\frac{1}{2}} & -[k+\alpha]^{\frac{1}{4}}[W(\alpha)]^{-\frac{1}{2}} \end{pmatrix}. \tag{2.47}$$

The matrix $L(\alpha)$ can be found from the expression

$$L(\alpha) = K^{-1}(\alpha)\, U(\alpha).$$

Factorisation of $D(\alpha)$

The function $D(\alpha)$ can be written as

$$\begin{aligned} D(\alpha) &= \sqrt{\frac{(\kappa+k\beta_1)(\kappa+k\beta_2)}{2\kappa}}, \\ &= \left(\frac{\kappa}{2}\right)^{1/2}\left(\frac{\kappa+k\beta_1}{\kappa}\right)^{1/2}\left(\frac{\kappa+k\beta_2}{\kappa}\right)^{1/2}. \end{aligned}$$

Consider factorising the function $d^n(\alpha)$ given by

$$d^n(\alpha) = \frac{\kappa+k\beta_n}{\kappa}. \tag{2.48}$$

Using calculations given in Rawlins [29] it is noted that

$$d^n_+(\nu) = \frac{\sqrt{1+\beta_n}}{\sqrt{1+\nu/k}} \exp\left\{\frac{\beta_n}{2\pi\sqrt{1-\beta_n^2}}\left[F(\sqrt{1-\beta_n^2}) - F(-\sqrt{1-\beta_n^2})\right]\right\},$$

where

$$F(v) = -v\int_{\pi/2}^{\arccos(\nu/k)} \frac{u - (1-v^2)^{-1/2}\arccos v \sin u\; du}{(v-\cos u)}. \tag{2.49}$$

It now follows that

$$D_+(\alpha) = \left\{ \sqrt{\frac{k+\alpha}{2}}\, d_+^1(\alpha)\, d_+^2(\alpha) \right\}^{1/2}. \tag{2.50}$$

This completes the factorisation of $D(\alpha)$.

2.5 Asymptotic Expressions for the Far-Field

It is noted that

$$\begin{aligned} G(\alpha) &= D(\alpha)K(\alpha) \\ &= D_+(\alpha)D_-(\alpha)U(\alpha)L^{-1}(\alpha) \\ &= D_+(\alpha)U(\alpha)D_-(\alpha)L^{-1}(\alpha) \\ &= G_+(\alpha)G_-(\alpha). \end{aligned}$$

With the factorisation of $G(\alpha)$ complete, proceeding from equation (2.28) gives

$$\begin{aligned} G(\alpha)l(\alpha) &= u(\alpha) + G(\alpha)\frac{P}{(\alpha+k_o)}, \\ G_+(\alpha)G_-(\alpha)l(\alpha) &= u(\alpha) + G_+(\alpha)G_-(\alpha)\frac{P}{(\alpha+k_o)}, \\ G_-(\alpha)l(\alpha) &= G_+^{-1}(\alpha)u(\alpha) + G_-(\alpha)\frac{P}{(\alpha+k_o)}, \\ G_-(\alpha)l(\alpha) - \Big[G_-(\alpha) - G_-(-k_o)\Big]\frac{P}{(\alpha+k_o)} &= G_+^{-1}(\alpha)u(\alpha) + G_-(-k_o)\frac{P}{(\alpha+k_o)}. \end{aligned} \tag{2.51}$$

The left hand side of this expression is analytic in $\mathrm{Im}(\alpha) \leq 0$ and the right hand side is analytic in $\mathrm{Im}(\alpha) \geq 0, \alpha \neq -k_o$. Hence both sides of equation (2.51) are equal to an entire function $\mathbf{Q}(\alpha)$. From equations (2.42) and (2.46) it follows that

$$V(\alpha) = O(\alpha^{-\frac{1}{2}}), \quad W(\alpha) = O(1), \quad |\alpha| \to \infty.$$

This implies that

$$G_+(\alpha) = O\begin{pmatrix} 1 & \alpha^{\frac{1}{2}} \\ 1 & \alpha^{\frac{1}{2}} \end{pmatrix}, \quad G_-(\alpha) = O\begin{pmatrix} \alpha^{-\frac{1}{2}} & 1 \\ \alpha^{\frac{1}{2}} & \alpha^{-1} \end{pmatrix}, \quad |\alpha| \to \infty.$$

Combining the edge condition (2.15) with (2.24) it can be shown that the terms of $u(\alpha)$ are $O(\alpha^{-1/2})$ at worst. Using Liouville's theorem it now follows that $\mathbf{Q}(\alpha) = 0$.

Thus

$$l(\alpha) = \left[\mathrm{I} - G_-^{-1}(\alpha)G_-(-k_o)\right]\frac{P}{(\alpha + k_o)}, \tag{2.52}$$

$$u(\alpha) = -G_+(\alpha)G_-(-k_o)\frac{P}{(\alpha + k_o)}. \tag{2.53}$$

Combining (2.53) with (2.24) and (2.18) gives

$$\psi_s(x,y) = \int_{-\infty}^{\infty} \frac{u_1(\alpha)}{(\kappa + k\beta_1)}\, e^{i(\alpha x + \kappa y)} d\alpha, \quad y > 0. \tag{2.54}$$

From (2.25) and (2.19) it can be seen that

$$\psi_s(x,y) = \int_{-\infty}^{\infty} \frac{u_2(\alpha)}{(\kappa + k\beta_2)}\, e^{i(\alpha x - \kappa y)} d\alpha, \quad y < 0. \tag{2.55}$$

The path of integration is indented below at $\alpha = k$ and above at $\alpha = -k, -k_o$, for real k and $0 < \theta_o < \pi$. These integrals are of the type examined in Noble [27] and the method described there is adopted by considering a shift of contour in the α-plane given by

$$\alpha = k\cos(\theta + it), \quad (-\infty < t < \infty). \tag{2.56}$$

Expression (2.56) represents one half of a hyperbola. For $0 < \theta < \pi/2$, this represents the half of the hyperbola in the right-hand half-plane (Figure 2.3), and for $\pi/2 < \theta < \pi$, the half in the left-hand half-plane (Figure 2.4). It can be seen that the pole at $\alpha = -k_o$ is captured for $\theta > \pi - \theta_o$. Noting that $u_1(\alpha)$ is given by expression (2.53) and P is defined by (2.30), the contribution from the pole at $\alpha = -k_o$ is

$$\begin{aligned} -\psi_r(r,\theta) &= 2\pi i \lim_{\alpha \to -k_o} (\alpha + k_o)\frac{u_1(\alpha)}{(\kappa + k\beta_1)}\, e^{i\alpha x + i\kappa y}, \\ &= -\frac{\sin\theta_o}{(\beta_1 + \sin\theta_o)^2}\left\{(\beta_1 + \sin\theta_o) - \frac{\beta_1(\beta_1 + \sin\theta_o)}{\sin\theta_o}\right\} e^{-ik(x\cos\theta_o - y\sin\theta_o)}, \\ &= -\left(\frac{\sin\theta_o - \beta_1}{\sin\theta_o + \beta_1}\right) e^{-ikr\cos(\theta + \theta_o)}, \quad \theta > \pi - \theta_o. \end{aligned} \tag{2.57}$$

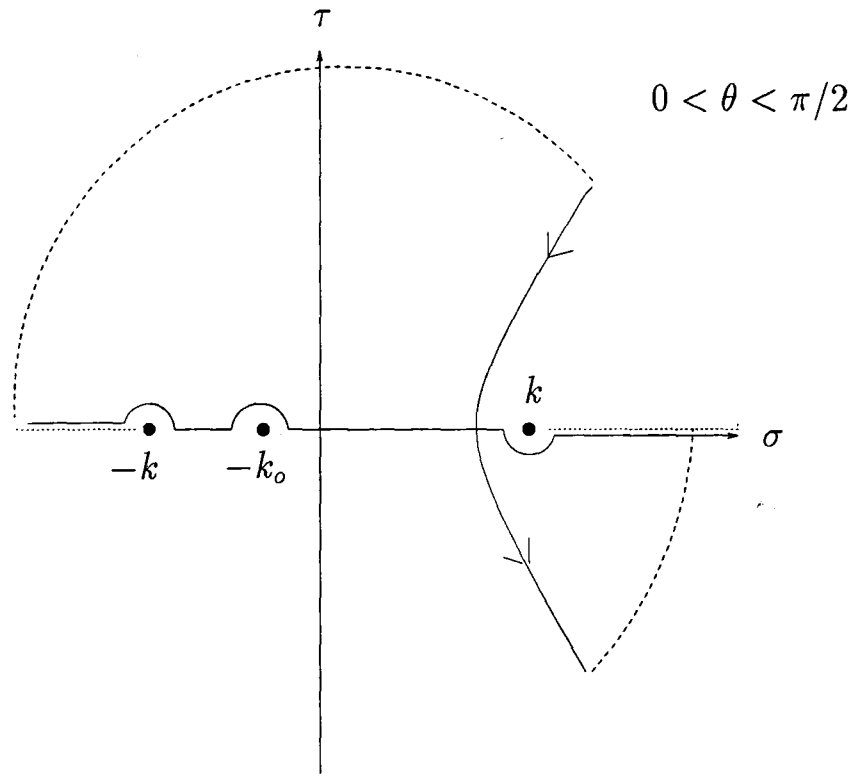

Figure 2.3: The pole at $-k_o$ is not captured.

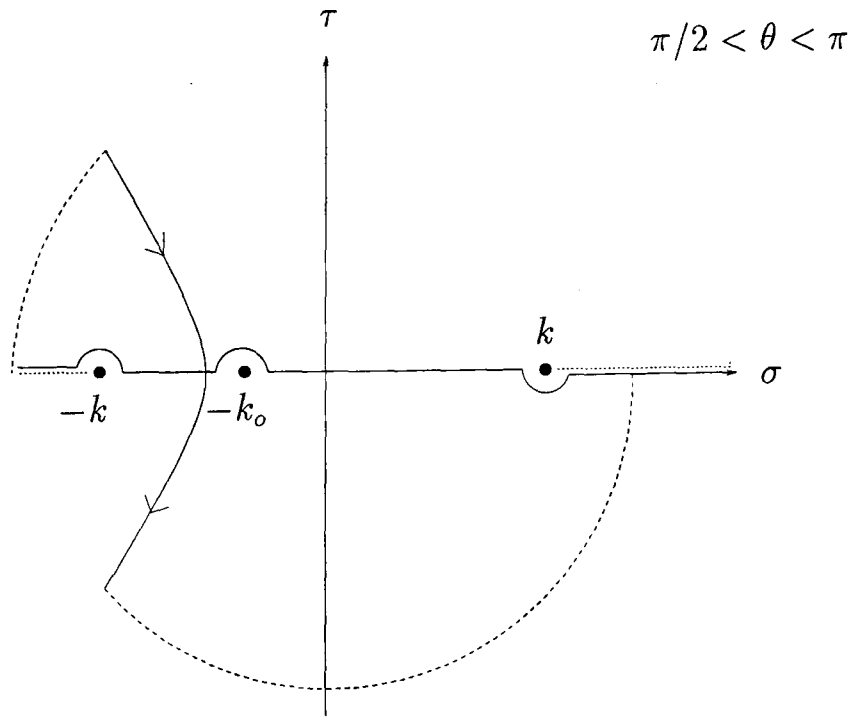

Figure 2.4: The pole at $-k_o$ is captured for $\theta > \pi - \theta_o$.

This cancels the reflected wave in the region $\theta > \pi - \theta_o$. As expected, the reflected wave exists only in the region $\theta < \pi - \theta_o$. On applying (2.56) to equation (2.54), the scattered field becomes

$$\psi_s(r,\theta) = \int_{-\infty}^{\infty} \frac{-i\sin(\theta+it)}{\beta_1 + \sin(\theta+it)} u_1[k\cos(\theta+it)] e^{ikr\cosh t} dt, \quad 0 < \theta < \pi, \tag{2.58}$$

$$= \int_{-\infty}^{\infty} \frac{i\sin(\theta+it)}{\beta_2 - \sin(\theta+it)} u_2[k\cos(\theta+it)] e^{ikr\cosh t} dt, \quad -\pi < \theta < 0. \tag{2.59}$$

ψ_s is now of the form examined by Copson [4] using the method of stationary phase. Following this method gives

$$\psi_{d_+}(r,\theta) = 2i\sqrt{\frac{\pi}{2kr}} \left(\frac{\sin\theta}{\sin\theta + \beta_1} \right) u_1[k\cos\theta] e^{ikr + \frac{\pi i}{4}}, \quad 0 < \theta < \pi. \tag{2.60}$$

Similarly, in the lower half-plane

$$\psi_{d_-}(r,\theta) = -2i\sqrt{\frac{\pi}{2kr}} \left(\frac{\sin\theta}{-\sin\theta + \beta_2} \right) u_2[k\cos\theta] e^{ikr + \frac{\pi i}{4}}, \quad -\pi < \theta < 0. \tag{2.61}$$

Applying (2.56) to the incident plane wave gives

$$\psi_i(r,\theta) = e^{-ikr\cos(\theta - \theta_o)}. \tag{2.62}$$

Combining these expressions for the incident plane wave, the wave reflected from the half-plane and the scattered field, the final expression for the far-field is

$$\psi(r,\theta) = \psi_i(r,\theta) + \psi_r(r,\theta) + \psi_{d+}(r,\theta), \qquad 0 < \theta < \pi - \theta_o, \tag{2.63}$$

$$= \psi_i(r,\theta) + \psi_{d+}(r,\theta), \qquad \pi - \theta_o < \theta < \pi, \tag{2.64}$$

$$= \psi_i(r,\theta) + \psi_{d-}(r,\theta), \qquad -\pi < \theta < \theta_o - \pi, \tag{2.65}$$

$$= \psi_{d-}(r,\theta), \qquad \theta_o - \pi < \theta < 0, \tag{2.66}$$

where

$$\psi_i(r,\theta) = e^{-ikr\cos(\theta-\theta_o)}, \tag{2.67}$$

$$\psi_r(r,\theta) = \left(\frac{\sin\theta_o - \beta_1}{\sin\theta_o + \beta_1}\right) e^{-ikr\cos(\theta+\theta_o)}, \tag{2.68}$$

$$\psi_{d+}(r,\theta) = 2i\sqrt{\frac{\pi}{2kr}}\left(\frac{\sin\theta}{\beta_1 + \sin\theta}\right) u_1[k\cos\theta]e^{ikr+\frac{\pi i}{4}}, \tag{2.69}$$

$$\psi_{d-}(r,\theta) = -2i\sqrt{\frac{\pi}{2kr}}\left(\frac{\sin\theta}{\beta_2 - \sin\theta}\right) u_2[k\cos\theta]e^{ikr+\frac{\pi i}{4}}. \tag{2.70}$$

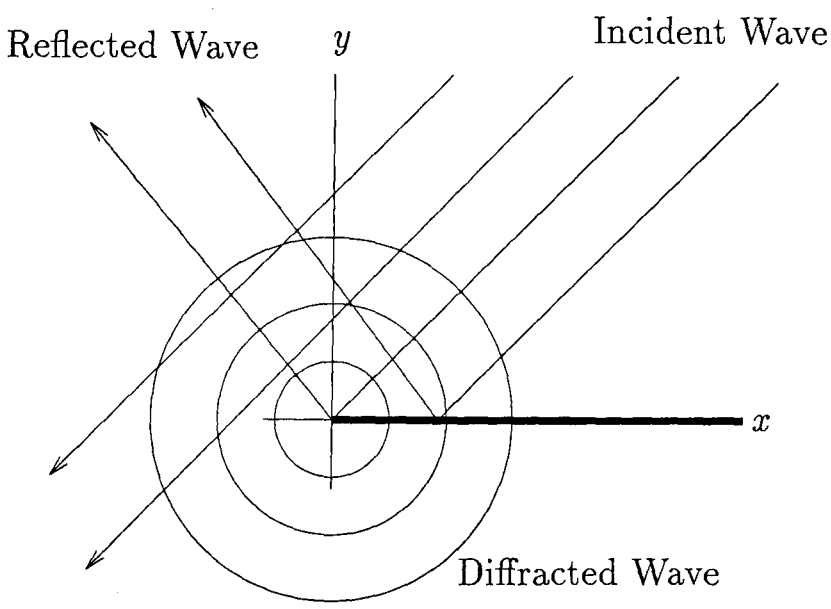

Figure 2.5: Diffraction of waves by a half-plane.

Expression (2.67) represents the incident plane wave. Along with (2.68), the reflected wave, this makes up the geometrical acoustic field. Terms (2.69) and (2.70) represent the diffracted wave in the upper and lower halves of the plane respectively. This wave radiates from the edge of the half-plane to all points in space. These three waves are shown in Figure 2.5.

2.6 Graphical Results

This section contains graphs of the far-field for various values of θ_o, β_1 and β_2. These were obtained by using the expressions given for the far-field in the mathematics software package Mathematica. In fact, the diffracted field given in expressions (2.69) and (2.70) becomes infinite on the boundaries $\theta = \pi - \theta_o$ and $\theta = \pi + \theta_o$ so an alternate expression has been used to give uniform asymptotics across these boundaries. These expressions can be found in Appendix A by putting $M = 0$.

Figures 2.6-2.8 show the modulus of the total far-field for a wave-bearing half-plane ($\beta_1 = \beta_2 = -i$) and Figures 2.9-2.11 show the far-field for an absorbing half-plane ($\beta_1 = \beta_2 = 1/2 - i$). In both cases the angle of incidence is taken to be $\pi/2$, $\pi/3$ and $\pi/4$. There are apparent differences between the two sets of graphs in the region $0 < \theta < \pi/2$. The modulus of the reflection coefficient is given by expression (2.68), when $\beta_1 = \beta_2 = -i$, $|\psi_r|$=1 and when $\beta_1 = \beta_2 = 1/2 - i$, $|\psi_r|$=0.62. It can be seen that in the region $0 < \theta < \pi/2$ the oscillations about the incident wave magnitude of unity are of the order $|\psi_r|$. The field in this region is due primarily to interference between the incident plane wave and the wave reflected from the half-plane. When β_1=1 the reflection coefficient is zero thus minimising the intensity of sound in this region. In Figure 2.12 ($\beta_1 = \beta_2 = 1$) and Figure 2.13 ($\beta_1 = 1, \beta_2 = -i$) it can be seen that there is only a slight deviation about the incident field magnitude of unity in this region (this deviation is due to the diffracted field). These are equivalent to half-planes that absorb all of the sound energy and reflect none.

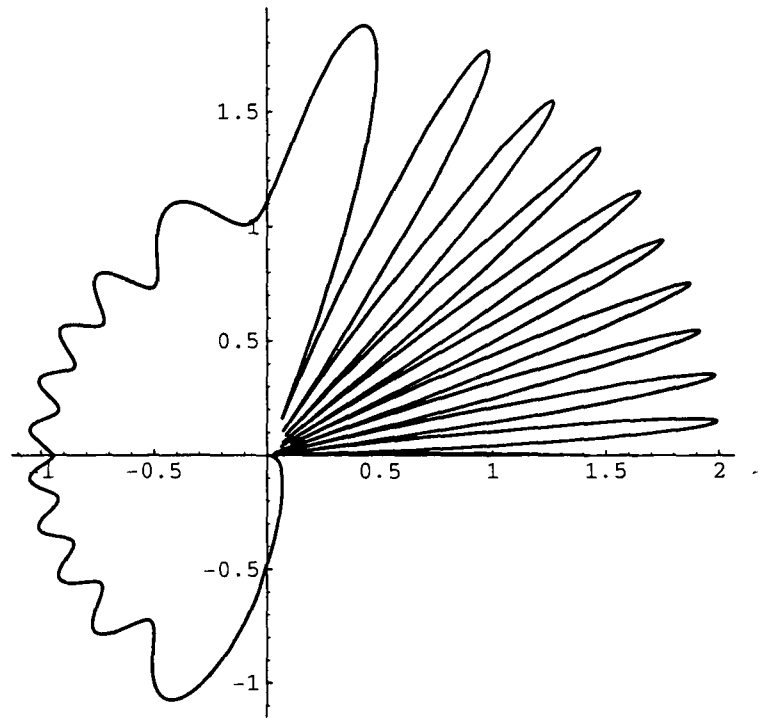

Figure 2.6: $\theta_o = \pi/2$, $\beta_1 = \beta_2 = -i$.

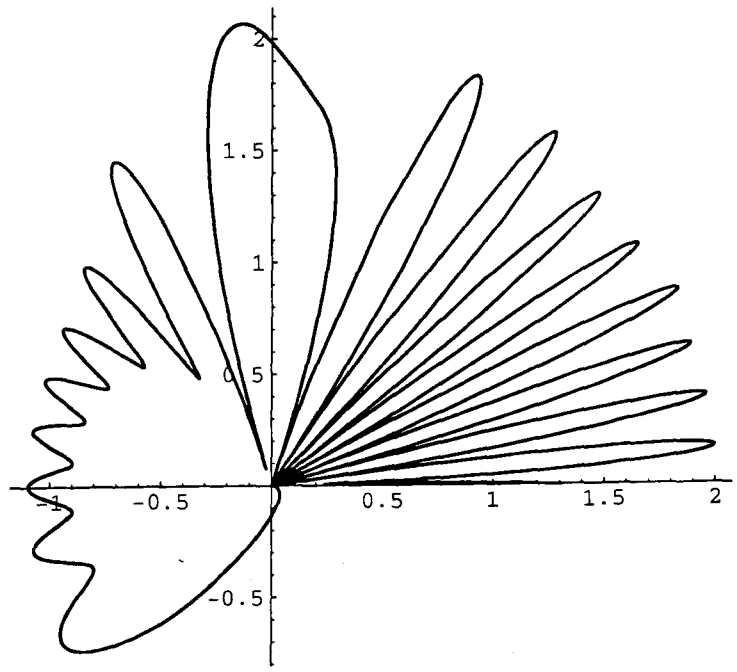

Figure 2.7: $\theta_o = \pi/3$, $\beta_1 = \beta_2 = -i$.

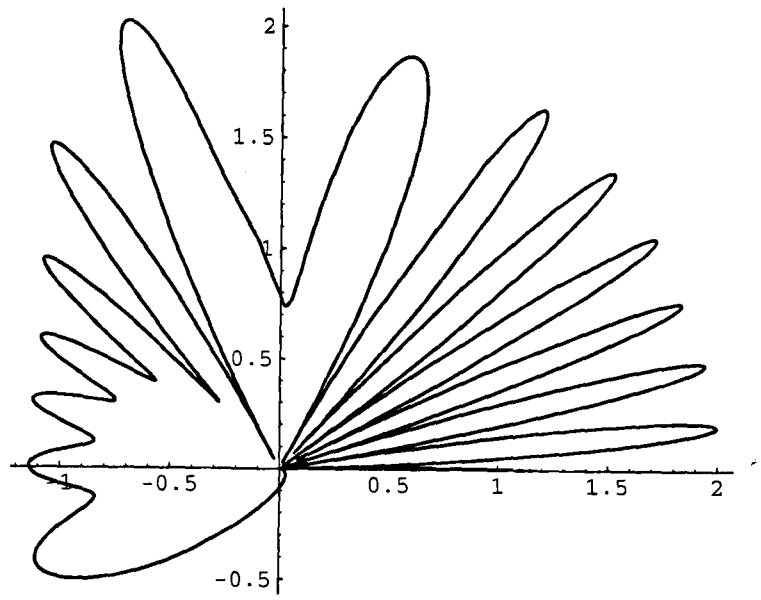

Figure 2.8: $\theta_o = \pi/4$, $\beta_1 = \beta_2 = -i$.

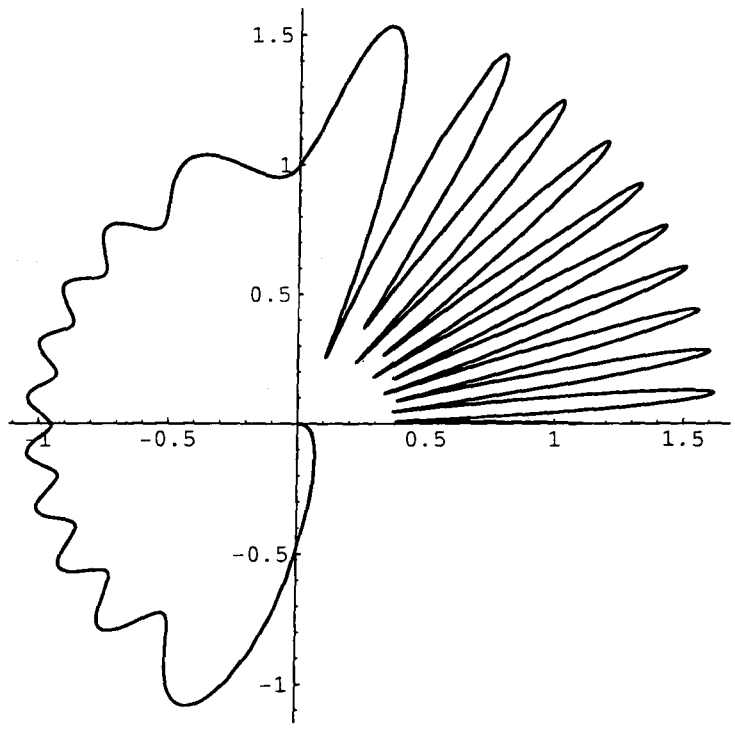

Figure 2.9: $\theta_o = \pi/2$, $\beta_1 = \beta_2 = \frac{1}{2} - i$.

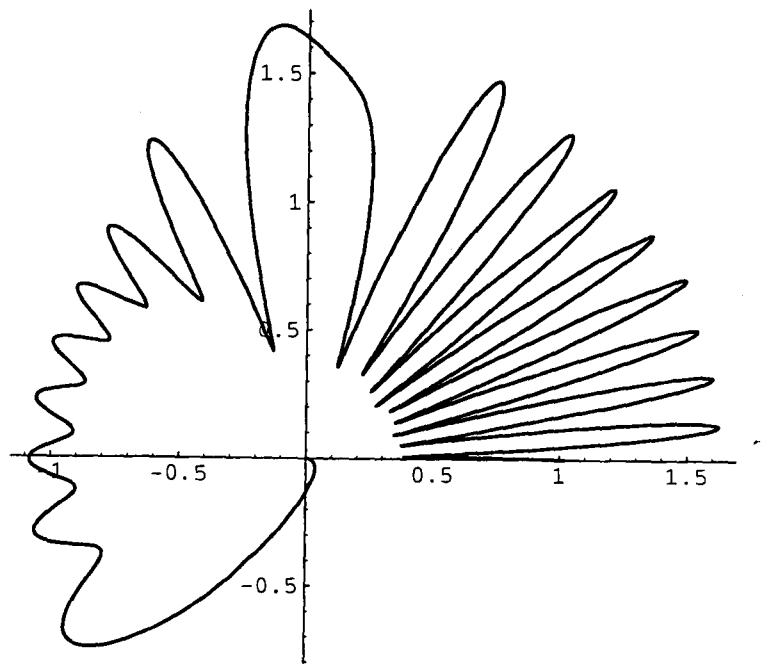

Figure 2.10: $\theta_o = \pi/3$, $\beta_1 = \beta_2 = \frac{1}{2} - i$.

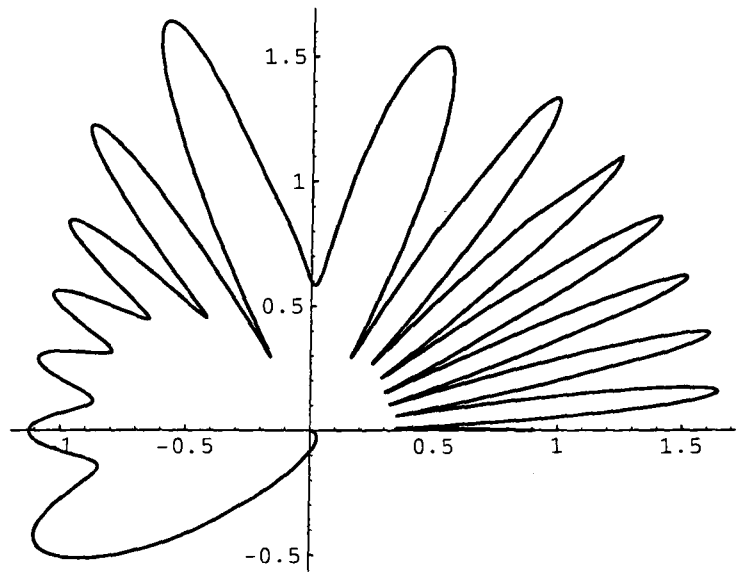

Figure 2.11: $\theta_o = \pi/4$, $\beta_1 = \beta_2 = \frac{1}{2} - i$.

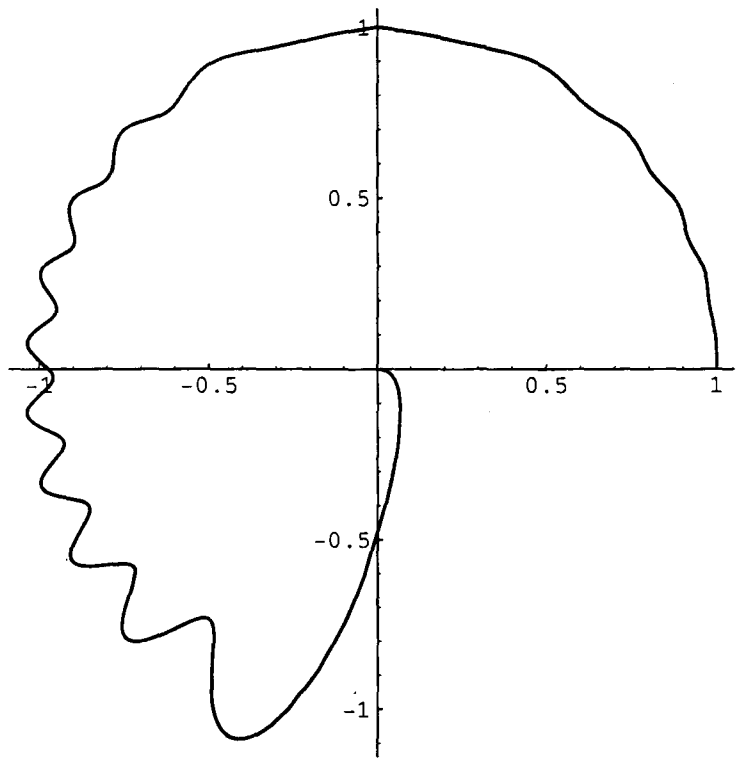

Figure 2.12: $\theta_o = \pi/2$, $\beta_1 = \beta_2 = 1$.

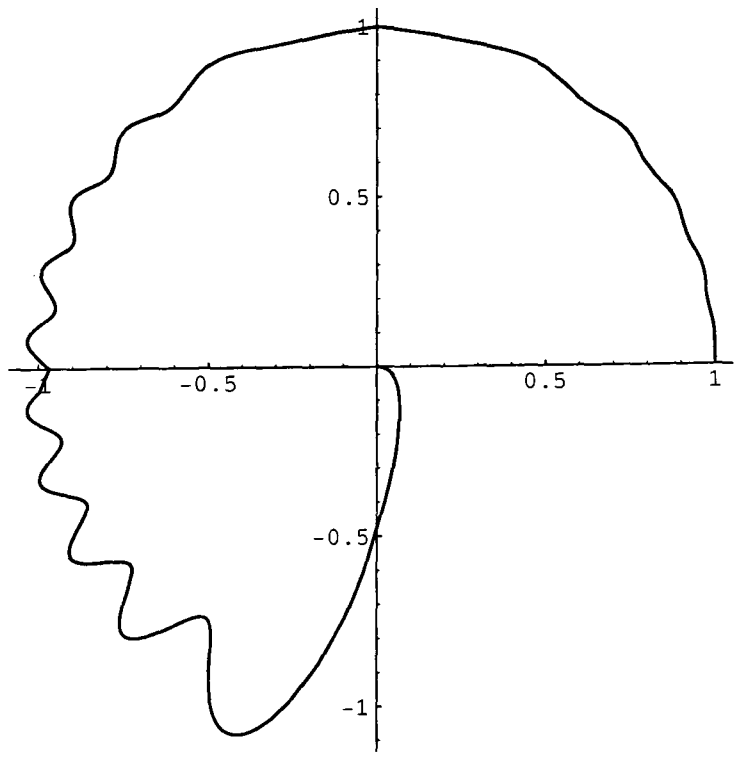

Figure 2.13: $\theta_o = \pi/2$, $\beta_1 = 1, \beta_2 = -i$.

2.7 A Rigid Half-Plane.

In this section the results from Section 2.5 are used to look at the special case of a rigid half-plane ($\beta_1 = \beta_2 = 0$). As well as being of physical interest, this will also provide a useful check for the results to the general problem. For the problem of a plane wave incident on a rigid half-plane the expressions for the far-field simplify considerably. The matrix kernel reduces to

$$G(\alpha) = \frac{1}{2}\begin{pmatrix} \kappa & 1 \\ -\kappa & 1 \end{pmatrix}. \tag{2.71}$$

The split functions can be written as

$$G_+(\alpha) = \begin{pmatrix} -1 & (k+\alpha)^{1/2} \\ -1 & -(k+\alpha)^{1/2} \end{pmatrix}, \quad G_-(\alpha) = \frac{1}{2}\begin{pmatrix} 0 & -1 \\ (k-\alpha)^{1/2} & 0 \end{pmatrix}, \tag{2.72}$$

and equations (2.54) and (2.55) for the scattered field are

$$\begin{aligned} \psi_s(x,y) &= \int_{-\infty}^{\infty} \frac{u_1(\alpha)}{\kappa} e^{i(\alpha x + \kappa y)} d\alpha, \quad y > 0, \\ &= \int_{-\infty}^{\infty} \frac{u_2(\alpha)}{\kappa} e^{i(\alpha x - \kappa y)} d\alpha, \quad y < 0. \end{aligned}$$

Using the kernel split functions given above this simplifies to

$$\psi_s(x,y) = -\frac{(k+k_o)^{1/2}}{2\pi i} \int_{-\infty}^{\infty} \frac{e^{i(\alpha x + \kappa y)}}{(k-\alpha)^{1/2}(\alpha + k_o)} d\alpha, \quad y > 0, \tag{2.73}$$

$$= \frac{(k+k_o)^{1/2}}{2\pi i} \int_{-\infty}^{\infty} \frac{e^{i(\alpha x - \kappa y)}}{(k-\alpha)^{1/2}(\alpha + k_o)} d\alpha, \quad y < 0. \tag{2.74}$$

This is clearly consistent with Equation 2.32a in Noble [27] obtained by Jones' method.

The far-field components are

$$\psi_i(r,\theta) = e^{-ikr\cos(\theta-\theta_o)}, \tag{2.75}$$

$$\psi_r(r,\theta) = e^{-ikr\cos(\theta+\theta_o)}, \tag{2.76}$$

$$\psi_{d+}(r,\theta) = \sqrt{\frac{1}{2\pi kr}}\frac{(1+\cos\theta_o)^{1/2}(1+\cos\theta)^{1/2}}{(\cos\theta+\cos\theta_o)}e^{ikr+\frac{\pi i}{4}}, \tag{2.77}$$

$$\psi_{d-}(r,\theta) = -\sqrt{\frac{1}{2\pi kr}}\frac{(1+\cos\theta_o)^{1/2}(1+\cos\theta)^{1/2}}{(\cos\theta+\cos\theta_o)}e^{ikr+\frac{\pi i}{4}}. \tag{2.78}$$

Figure 2.14 shows the far-field for a plane wave incident on a rigid half-plane with $\theta_o = \pi/2$. The numerical results in the previous section tend to this result as $\beta_{1,2} \to 0$. It can be seen that the field in the region $0 < \theta < \pi/2$ varies between 0 and 2 since $|\psi_r| = 1$, thus all of the energy is reflected and none is absorbed. A large amount of energy is diffracted into the shadow region in this case. It can be seen that the field does not tend to zero as $\theta \to 0$ from below.

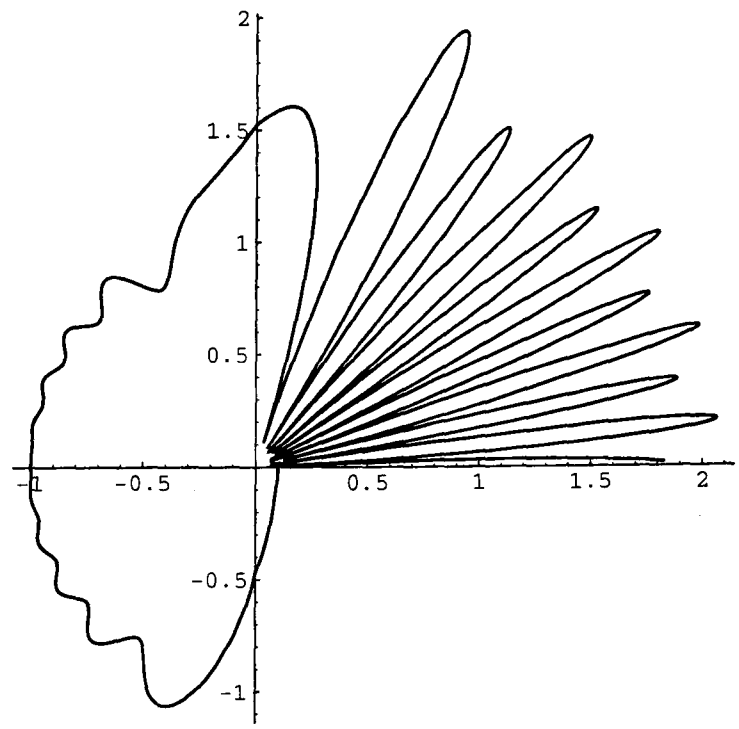

Figure 2.14: $\theta_o = \pi/2, \beta_1 = \beta_2 = 0$.

2.8 A Semi-Rigid Half-Plane.

In this section the problem of a fixed source and a receiver separated by a semi-rigid half-plane (a half-plane with one rigid and one absorbent surface) is examined. The receiver is assumed to be in the shadow region so that the half-plane acts as a noise barrier. It is to be ascertained whether the barrier is more effective with the rigid surface facing the source (Case 1) or facing the receiver (Case 2). These two situations are shown in Figure 2.15.

Figure 2.17 shows the far-field for a plane wave incident at an angle $\theta_o = \pi/4$ on a half-plane with $\beta_1 = 0$ and $\beta_2 = 1.5$ (Case 1). Figure 2.18 shows the far-field for a half-plane with the admittances reversed, that is $\beta_1 = 1.5$ and $\beta_2 = 0$ (Case 2). The diffracted field in the shadow region ($-3\pi/4 < \theta < 0$) is shown in Figure 2.16.

The amount of energy radiated from the edge into the shadow region is the same in both cases when $\theta = -\pi/4$ due to the symmetry of the problems and from the reciprocity theorem, which states that the ratio of pressure amplitude to source strength remains the same if the locations of the source and receiver are interchanged. For a receiver in the region $-3\pi/4 < \theta < -\pi/4$ it can be seen from Figure 2.16 that Case 2 produces the least amount of noise. However a half-plane with admittances as defined in Case 1 is preferable if the receiver is situated in the region $-\pi/4 < \theta < 0$. In both cases the noise level is reduced as the receiver moves closer to the barrier.

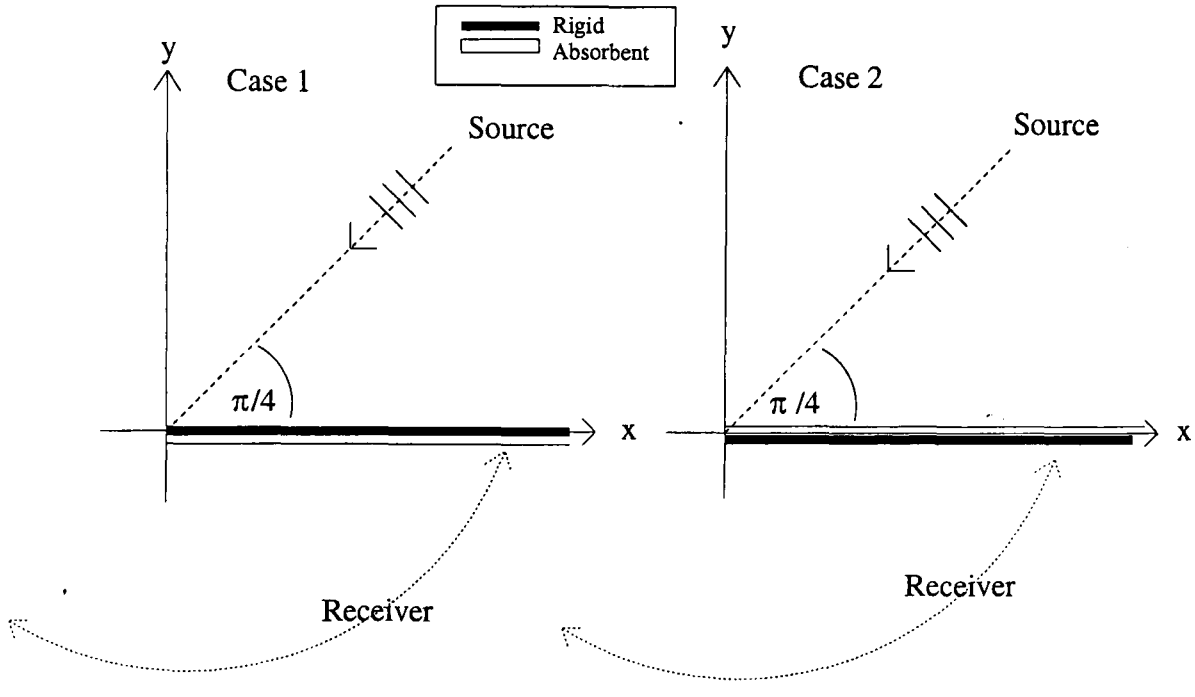

Figure 2.15: A source and receiver separated by a semi-rigid half-plane.

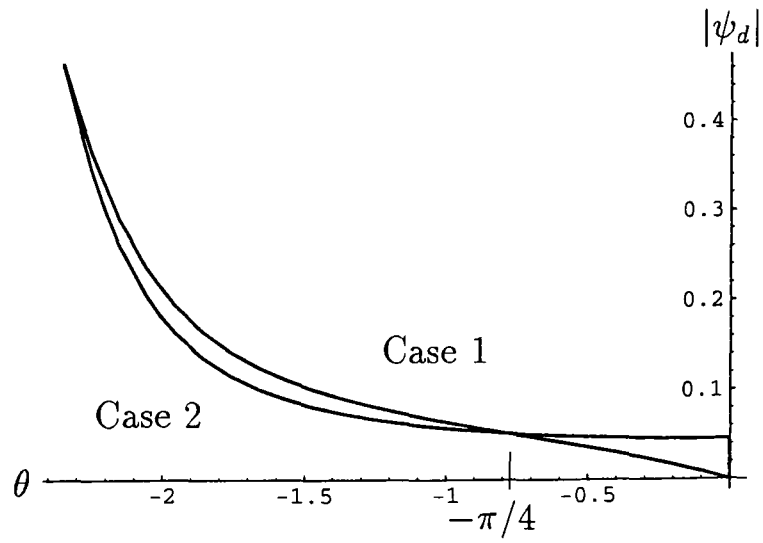

Figure 2.16: Modulus of the diffracted field in the shadow region.

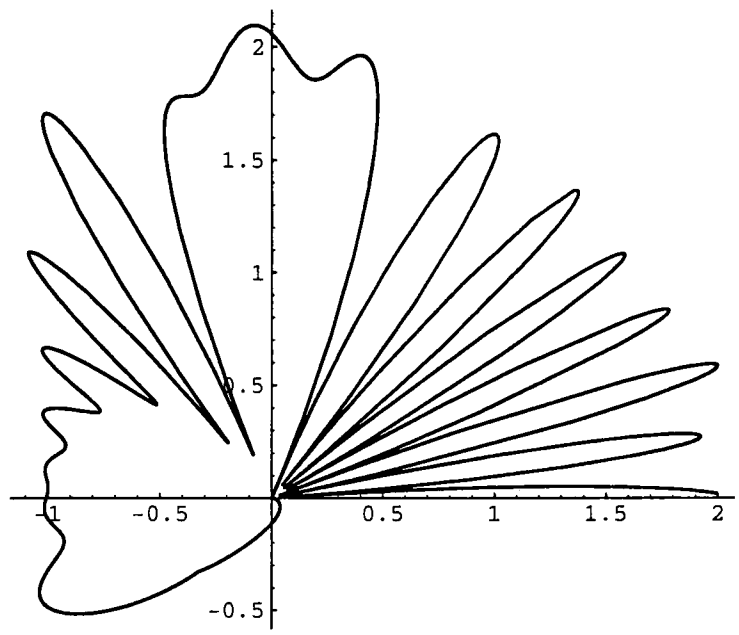

Figure 2.17: $\theta_o = \pi/4$, $\beta_1 = 0, \beta_2 = 1.5$ (Case 1).

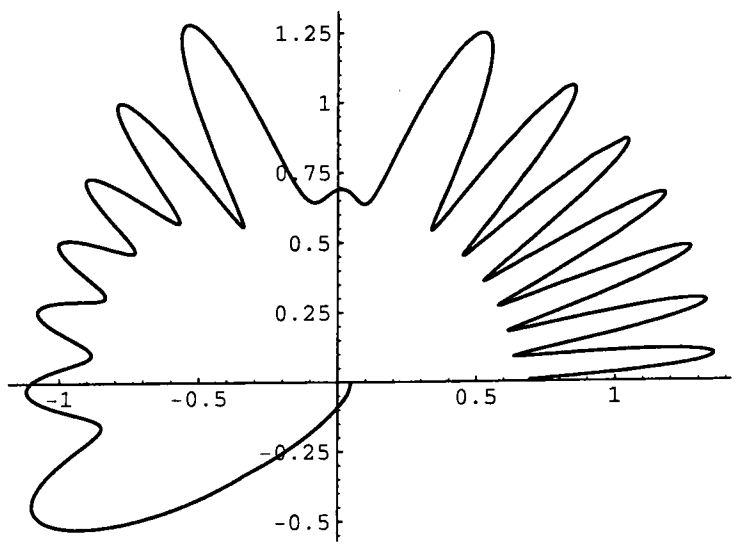

Figure 2.18: $\theta_o = \pi/4$, $\beta_1 = 1.5, \beta_2 = 0$ (Case 2).

2.9 An Incident Surface Wave

Let $\beta_1 = -iX_1$ and $\beta_2 = -iX_2$, where the parameters $X_1, X_2 > 0$. In this case the poles at $\alpha = k\sqrt{1+X_1^2}$ and $\alpha = k\sqrt{1+X_2^2}$ are captured in the integrals (2.54) and (2.55), giving

$$\psi_{surf}(x,0^+) = \frac{2\pi X_1}{\sqrt{1+X_1^2}}\, u_1[k\sqrt{1+X_1^2}]e^{ik\sqrt{1+X_1^2}x - kX_1 y}, \quad x > 0, \tag{2.79}$$

$$\psi_{surf}(x,0^-) = \frac{2\pi X_2}{\sqrt{1+X_2^2}}\, u_2[k\sqrt{1+X_2^2}]e^{ik\sqrt{1+X_2^2}x + kX_2 y}, \quad x > 0. \tag{2.80}$$

These represent surface waves on the upper and lower surfaces of the half-plane respectively.

Now consider an incident wave of the form

$$\phi_i = e^{-ik\left\{\sqrt{1+X_1^2}x - iX_1 y\right\}}. \tag{2.81}$$

This is equivalent to an angle of incidence satisfying $\cos\theta_o = \sqrt{1+X_1^2}$ and $\sin\theta_o = -iX_1$. Substituting these into the expressions for the total far-field gives

$$\phi_D(r,\theta) = 2i\sqrt{\frac{\pi}{2kr}}\left(\frac{\sin\theta}{\beta_1 + \sin\theta}\right)u_1[k\cos\theta]e^{ikr+\frac{\pi i}{4}}, \quad 0 < \theta < \pi, \tag{2.82}$$

$$= -2i\sqrt{\frac{\pi}{2kr}}\left(\frac{\sin\theta}{\beta_2 - \sin\theta}\right)u_2[k\cos\theta]e^{ikr+\frac{\pi i}{4}}, \quad -\pi < \theta < 0. \tag{2.83}$$

The arising surface waves are given by

$$\phi_R(x,0^+) = \frac{2\pi X_1}{\sqrt{1+X_1^2}}u_1[k\sqrt{1+X_1^2}]\; e^{ik\sqrt{1+X_1^2}x - kX_1 y}, \quad x > 0, \tag{2.84}$$

$$\phi_T(x,0^-) = \frac{2\pi X_2}{\sqrt{1+X_2^2}}u_2[k\sqrt{1+X_2^2}]e^{ik\sqrt{1+X_2^2}x + kX_2 y}, \quad x < 0. \tag{2.85}$$

In the case of an incident surface wave the far-field consists only of a wave diffracted from the edge of the half-plane (2.82) and (2.83). Expression (2.84) represents the

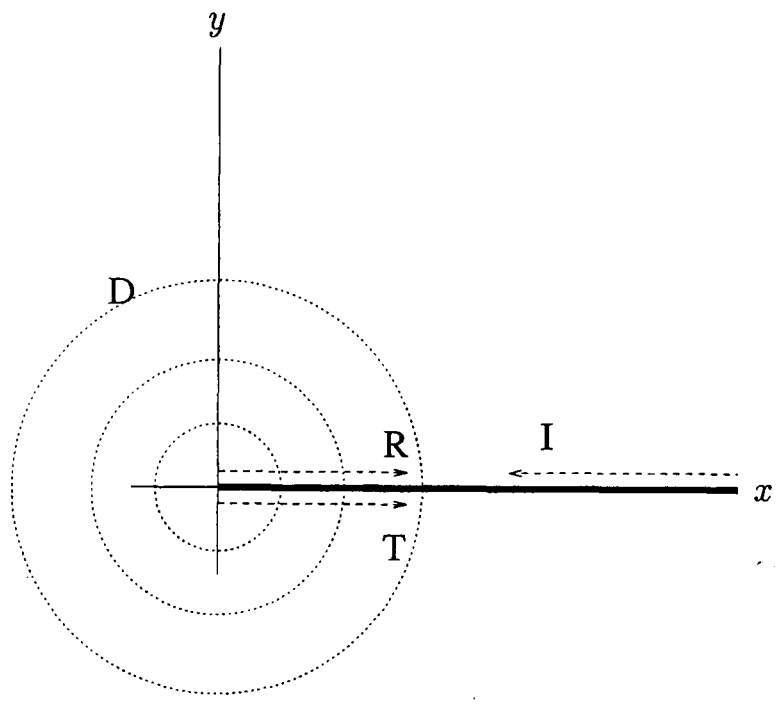

Figure 2.19: A surface wave incident on a half-plane.

reflected wave and takes the form of a surface wave on the upper face of the half-plane. The transmitted wave (2.85) is a surface wave on the lower face of the half-plane (Figure 2.19).

Expressions (2.82)-(2.85) were used to obtain a selection of graphs representing the radiated field and the reflected and transmitted surface waves. Figures 2.20-2.22 were obtained by plotting the function $kr|\phi_D(r,\theta)|^2$ and have been normalised for clarity. These graphs represent the energy radiated by the diffracted field for a surface wave incident on the upper face of the half-plane with $X_1 = 1$ and X_2 varying. These have the form of a lobe oriented toward $\theta = \pi$. When $X_2 > X_1$ ($X_1 > X_2$) the size of the lobe in the region $0 < \theta < \pi/2$ is greater than (less than) the size of the lobe in the region $-\pi/2 < \theta < 0$.

In applying the problem to act as a waveguide launcher it is of interest to maximise

the magnitude of the diffracted field when a surface wave is incident on the half-plane. Figures 2.23, 2.24 and 2.25 show the magnitude of the reflection coefficient, transmission coefficient and the diffracted field for a range of values of X_2 with $X_1 = 1$ (thus fixing the incident surface wave). $|\phi_R|$ and $|\phi_T|$ were obtained from expressions (2.84) and (2.85), with $|\phi_D|$ calculated using the fact that $|\phi_R|^2 + |\phi_T|^2 + |\phi_D|^2 = 1$. It can be seen that the magnitude of the diffracted field is greatest when $X_2 = 0$. Intuitively, this comes from the fact that there is no transmitted wave on the lower face of the half-plane ($|\phi_T| = 0$) and therefore more energy is diffracted from the edge. It can also be seen that when $X_2 = X_1$ the reflection coefficient is minimised and is equal to the transmission coefficient. It is also noted that as $X_2 \to \infty$: $|\phi_T| \to 0, |\phi_R| \to R\sqrt{2}$ and $|\phi_D| \to D$ where R and D are the values of $|\phi_R|$ and $|\phi_D|$ when $X_2 = X_1$.

Figures 2.26, 2.27 and 2.28 show the magnitude of the reflection coefficient, transmission coefficient and the diffracted field for a range of values of X_1 (thus varying the incident surface wave) with $X_2 = 1$.

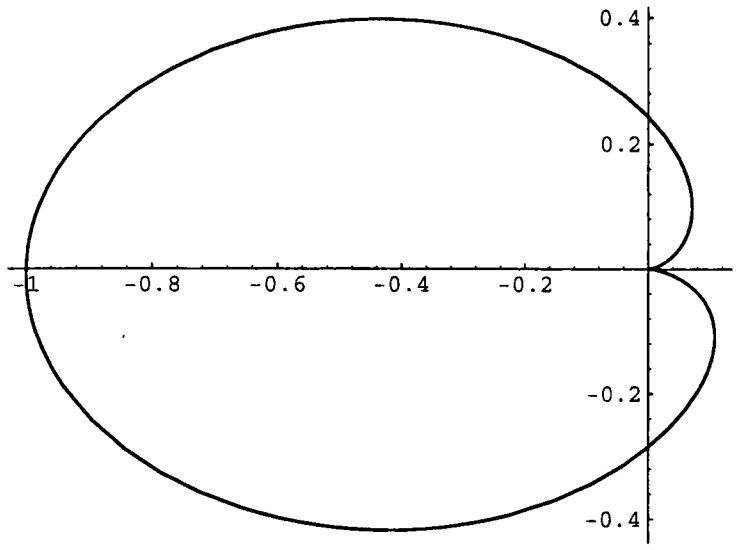

Figure 2.20: Radiation diagram for an incident surface wave, $X_1 = 1, X_2 = \frac{1}{2}$.

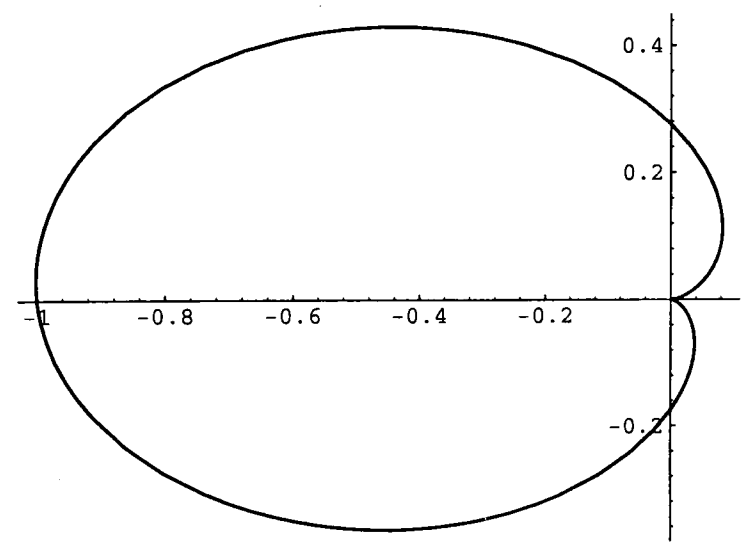

Figure 2.21: Radiation diagram for an incident surface wave, $X_1 = 1, X_2 = 3$.

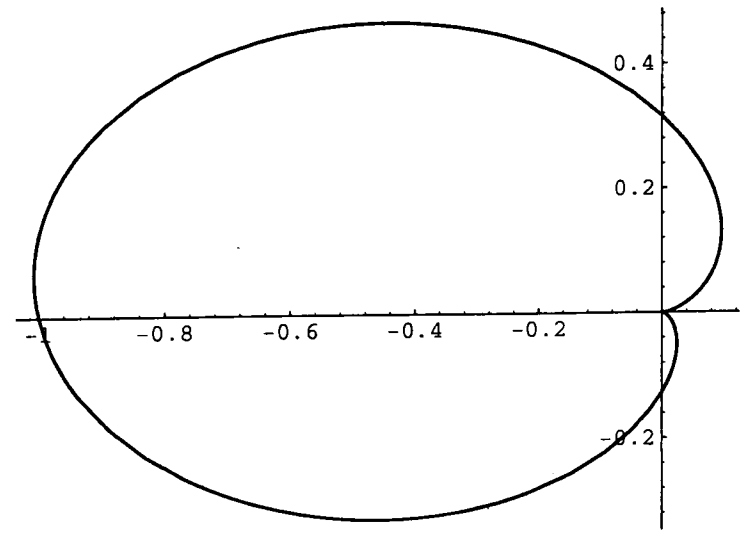

Figure 2.22: Radiation diagram for an incident surface wave, $X_1 = 1, X_2 = 10$.

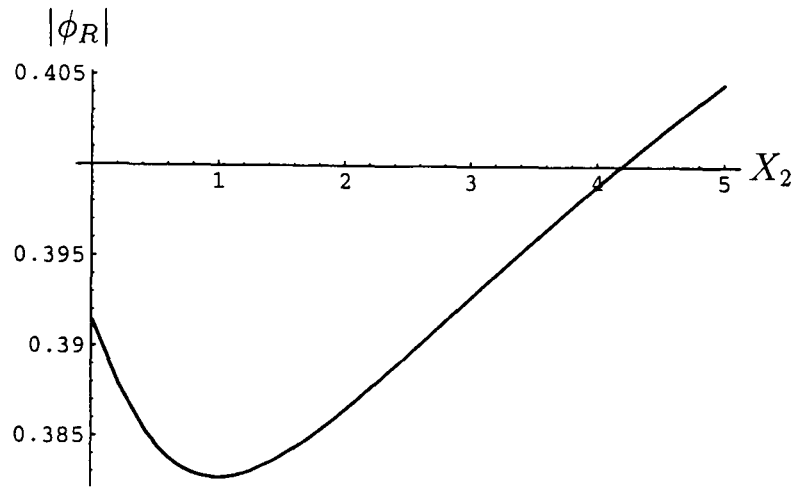

Figure 2.23: Coefficient of reflection for an incident surface wave $X_1 = 1$.

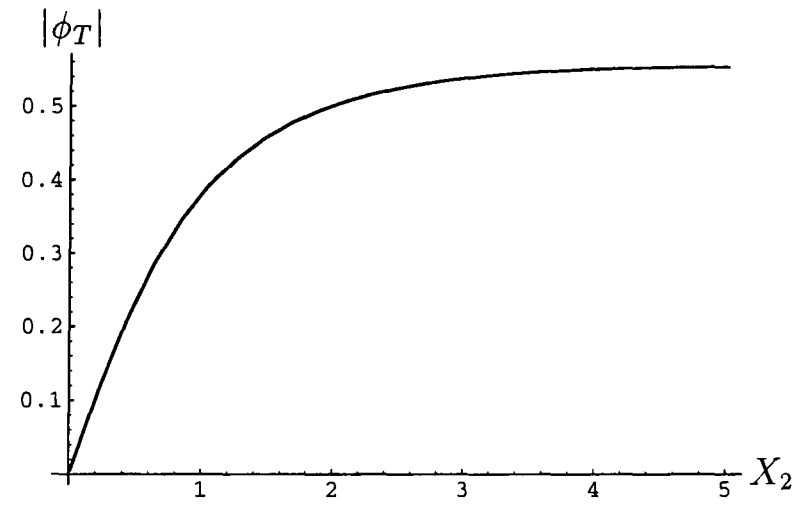

Figure 2.24: Transmission coefficient for an incident surface wave $X_1 = 1$.

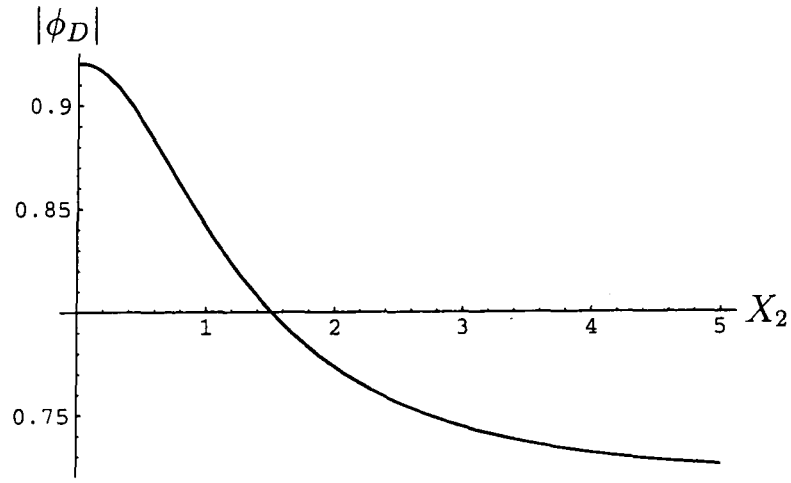

Figure 2.25: Diffracted field for an incident surface wave $X_1 = 1$.

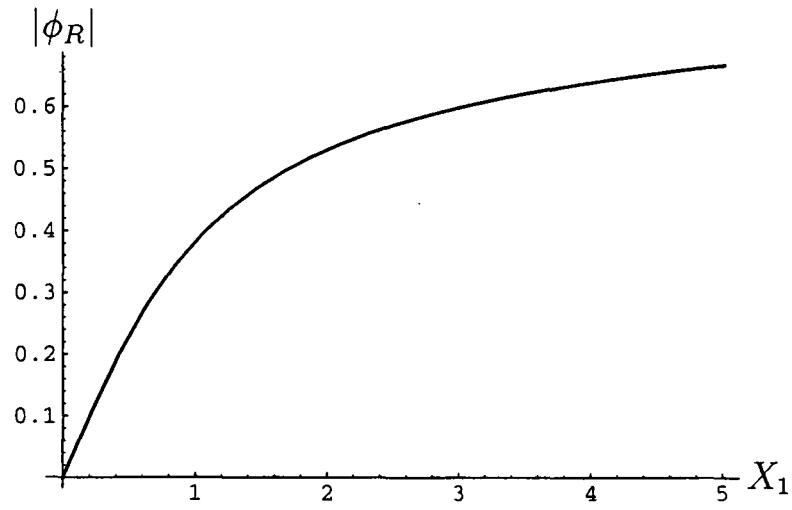

Figure 2.26: Coefficient of reflection of an incident surface wave $X_2 = 1$.

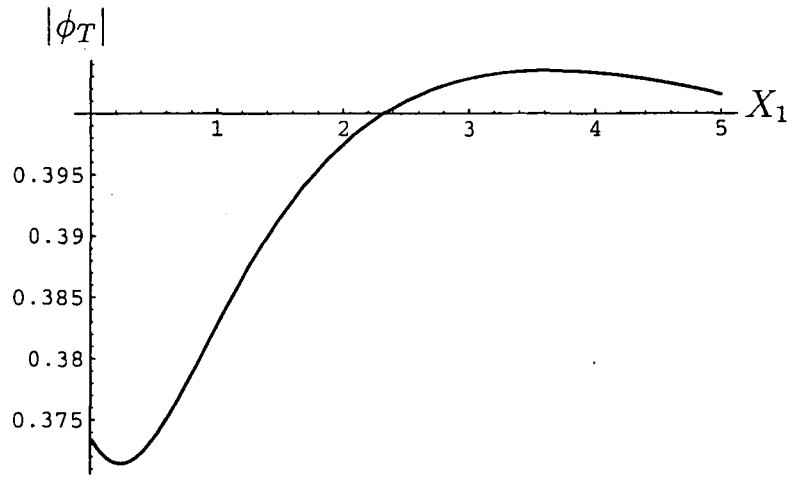

Figure 2.27: Transmission coefficient for an incident surface wave $X_2 = 1$.

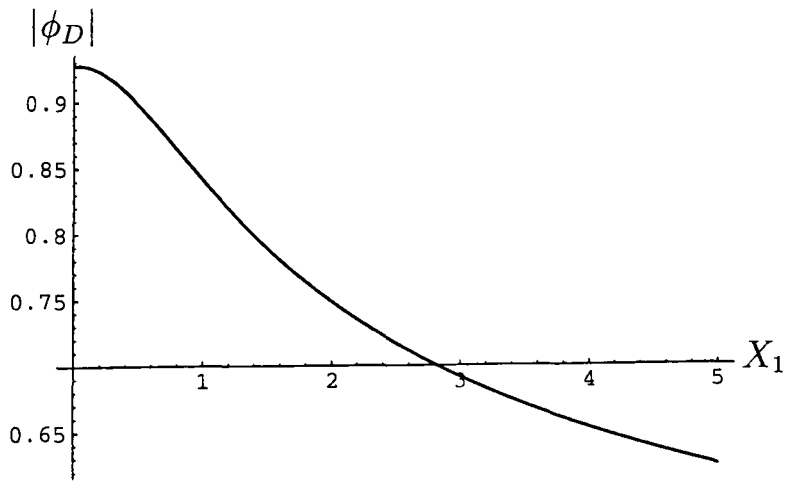

Figure 2.28: Diffracted field for an incident surface wave $X_2 = 1$.

2.10 A Surface Wave Incident on an Inductive Half-Plane.

In this section, the specific case of a surface wave incident on a half-plane with the same impedance on its upper and lower surfaces (Figure 2.29) is considered. The results that follow agree with those of Trenev [32].

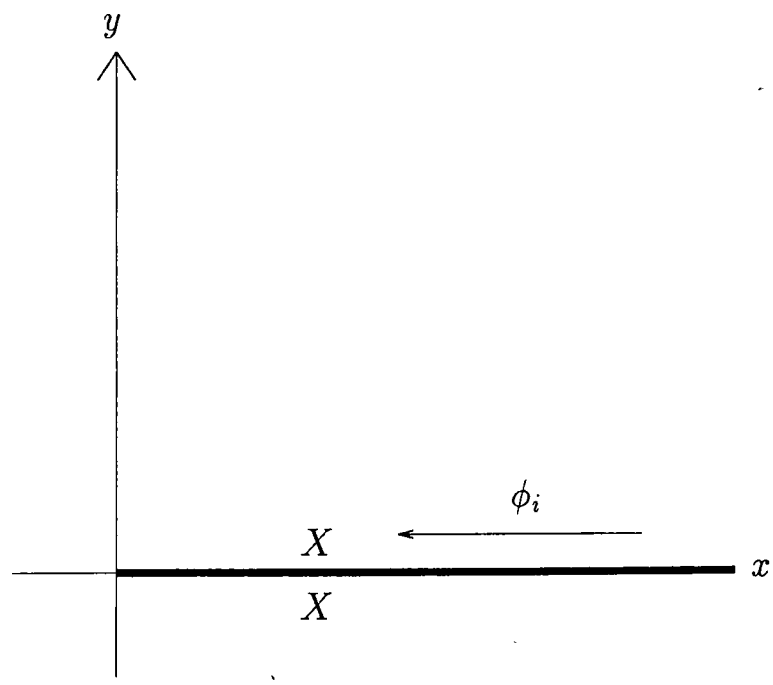

Figure 2.29: A surface wave incident on a half-plane with equal impedance parameters.

In the particular case $X_1 = X_2 = X$, the split functions $U(\alpha)$ and $L^{-1}(\alpha)$ simplify considerably to

$$U(\alpha) = \begin{pmatrix} -(k+\alpha)^{-1/4} & (k+\alpha)^{1/4} \\ -(k+\alpha)^{-1/4} & -(k+\alpha)^{1/4} \end{pmatrix},$$

$$L^{-1}(\alpha) = \frac{1}{\sqrt{2}} \begin{pmatrix} 0 & -(k+\alpha)^{-1/4} \\ (k+\alpha)^{1/4} & 0 \end{pmatrix}.$$

Upon making the substitution $h = \sqrt{1+X^2}$ then, after much algebra (2.84) and (2.85) simplify to give

$$|\phi_R| = |\phi_T| = \sqrt{\frac{h-1}{2h}}.$$

Figures 2.30 and 2.31 shows the dependence of the coefficients of reflection and transmission on impedance for an incident surface wave. With the same impedance on the upper and lower surfaces of the half-plane, the reflection coefficient is equal to the transmission coefficient and approaches $1/\sqrt{2}$ as X increases. This implies that $|\phi_D| \to 0$ as $X \to \infty$ which is in agreement with Figure 2.32 which shows the modulus of the diffracted field.

Figures 2.35-2.33 show the diffracted field for various values of X. It can be seen that the radiated lobes for this problem are symmetrical and that the lobes narrow as the impedance decreases. However, it can be seen from Figure 2.32 that the modulus of the diffracted field increases as X decreases. Thus, for a waveguide launcher with equal impedance parameters on its upper and lower surfaces the amount of energy diffracted is maximised by minimising the impedance, moreover the diffracted lobe is stretched in the forward direction.

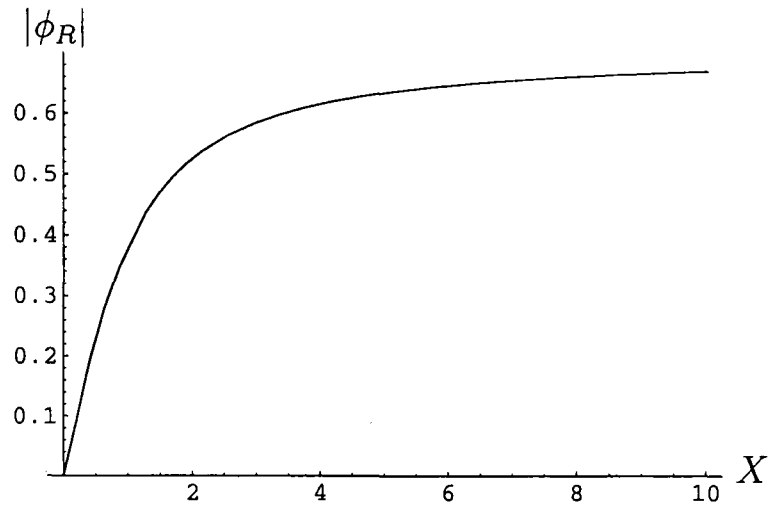

Figure 2.30: Dependence of the reflection coefficient on impedance $X_1 = X_2 = X$.

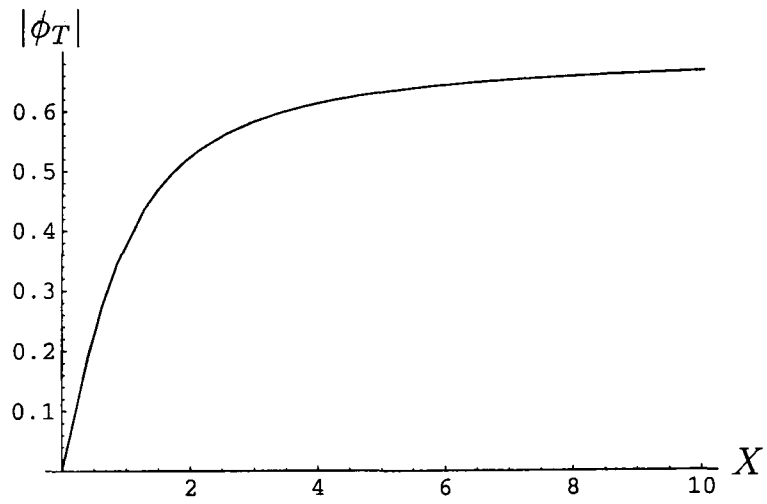

Figure 2.31: Dependence of the transmission coefficient on impedance $X_1 = X_2 = X$.

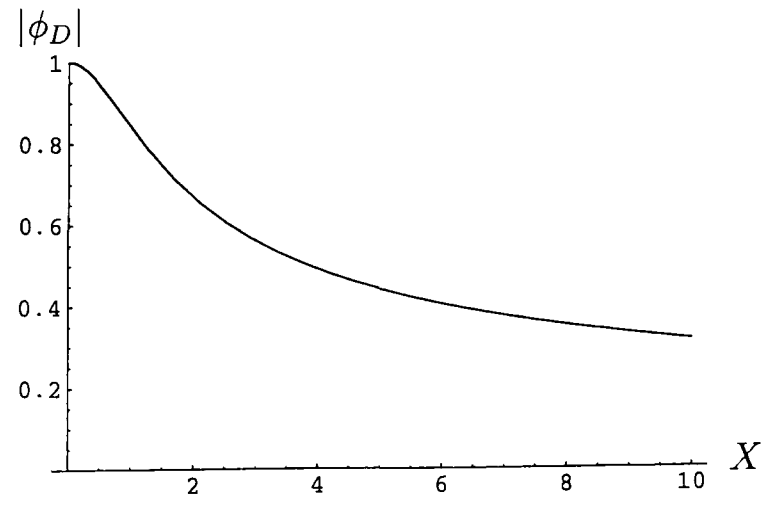

Figure 2.32: Dependence of the diffracted field on impedance $X_1 = X_2 = X$.

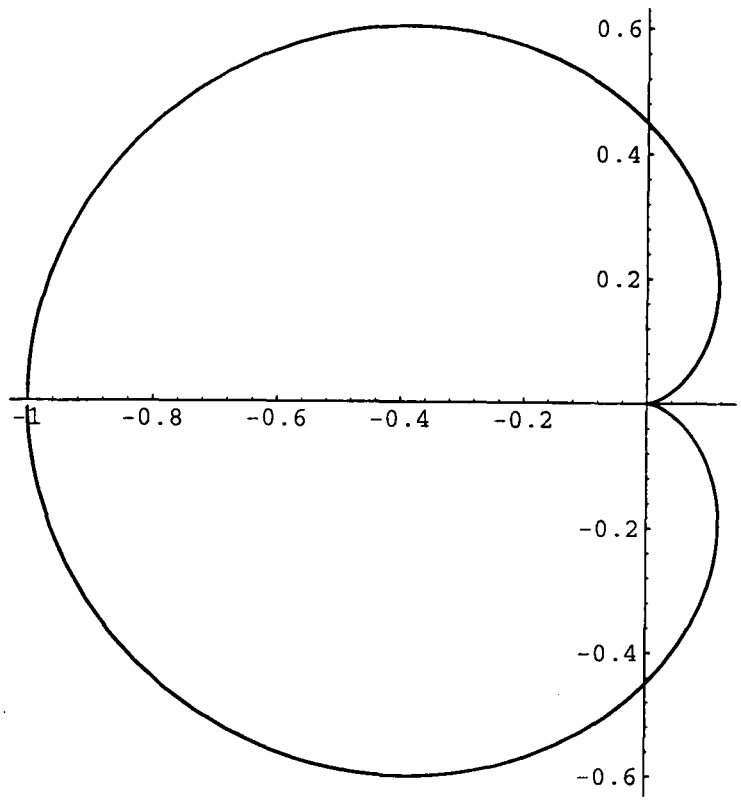

Figure 2.33: Radiation diagram for an incident surface wave, $X_1 = X_2 = 3$.

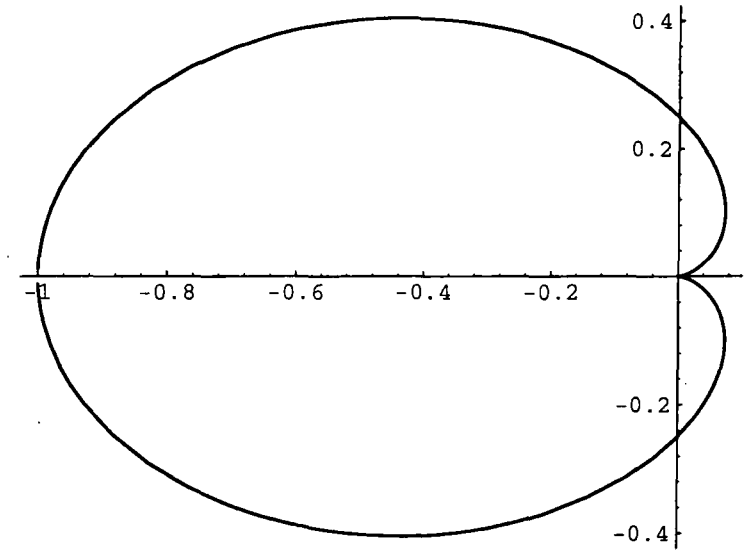

Figure 2.34: Radiation diagram for an incident surface wave, $X_1 = X_2 = 1$.

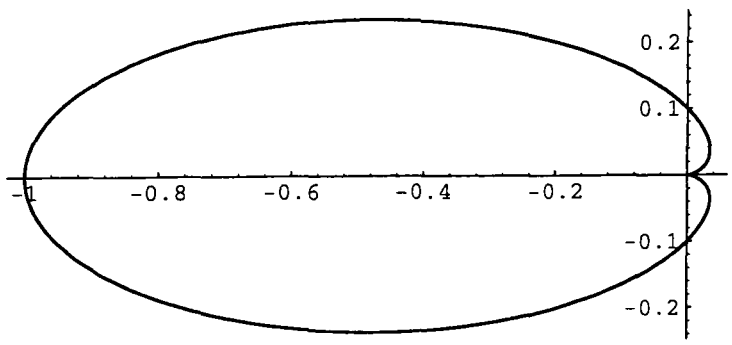

Figure 2.35: Radiation diagram for an incident surface wave, $X_1 = X_2 = \frac{1}{2}$.

2.11 An Inductive/Reactive Half-Plane.

Although this special case is difficult to resolve from our previous solution it is readily solved as a scalar problem. Upon making the substitutions $\beta_1 = -iX$ and $\beta_2 = iX$, equations (2.26) and (2.27) read

$$(\kappa - ikX)\frac{1}{2}\left(l_1 + \frac{l_2}{\kappa}\right) = u_1 + \frac{\kappa^2 + k^2X^2}{2\pi i(\alpha + k_o)2\kappa}, \tag{2.86}$$

$$(\kappa + ikX)\frac{1}{2}\left(-l_1 + \frac{l_2}{\kappa}\right) = u_2 - \frac{\kappa^2 + k^2X^2}{2\pi i(\alpha + k_o)2\kappa}. \tag{2.87}$$

Adding these equations gives

$$l_2 - ikXl_1 = u_1 + u_2. \tag{2.88}$$

The left hand side of equation (2.88) is analytic in the lower half plane and the right hand side is analytic in the lower half plane thus both are equal to a constant. Since $u_1(\alpha)$ and $u_2(\alpha)$ are $O(\alpha^{-1/2})$ at worst it follows that this constant must be zero. It now follows that

$$u_1 + u_2 = 0, \quad l_2 = ikXl_1. \tag{2.89}$$

Substituting back into (2.86) gives

$$(\kappa - ikX)\frac{1}{2}\left(l_1 + \frac{ikXl_1}{\kappa}\right) = u_1 + \frac{\kappa^2 + k^2X^2}{2\pi i(\alpha + k_o)2\kappa}.$$

This can be written as

$$\frac{(\alpha - k_o)}{2\sqrt{k-\alpha}}l_1 + \frac{1}{2\pi i(\alpha + k_o)}\left\{\frac{(\alpha - k_o)}{2\sqrt{k-\alpha}} + \frac{k_o}{\sqrt{k+k_o}}\right\} = \frac{\sqrt{k+\alpha}}{(\alpha + k_o)}u_1 + \frac{k_o}{2\pi i(\alpha + k_o)\sqrt{k+k_o}}. \tag{2.90}$$

Using the usual Wiener-Hopf argument, both sides of this equation must be equal to zero giving

$$u_1 = \frac{-k_o}{2\pi i\sqrt{k+\alpha}\sqrt{k+k_o}}.$$

The scattered field can now be written as

$$\phi_s = \int_{-\infty}^{\infty} \frac{-k_o}{2\pi i\sqrt{k+\alpha}\sqrt{k+k_o}(\kappa - ikX)} e^{i(\alpha x+\kappa y)} d\alpha, \quad y > 0, \tag{2.91}$$

$$= \int_{-\infty}^{\infty} \frac{k_o}{2\pi i\sqrt{k+\alpha}\sqrt{k+k_o}(\kappa + ikX)} e^{i(\alpha x-\kappa y)} d\alpha, \quad y < 0. \tag{2.92}$$

Using the method of stationary phase as before, the diffracted field becomes

$$\phi_D = \sqrt{\frac{\pi}{2kr}} \left(\frac{k_o}{\pi\sqrt{k+k_o}}\right) \frac{\sqrt{k-k\cos\theta}}{k\sin\theta - ikX} e^{ikr+i\pi/4}, \quad 0 < \theta < \pi, \tag{2.93}$$

$$= -\sqrt{\frac{\pi}{2kr}} \left(\frac{k_o}{\pi\sqrt{k+k_o}}\right) \frac{\sqrt{k-k\cos\theta}}{k\sin\theta + ikX} e^{ikr+i\pi/4}, \quad -\pi < \theta < 0. \tag{2.94}$$

There are also pole contributions from expression (2.91). When $\alpha = k_o$ the contribution is

$$\phi_R = \frac{kX}{k+k_o} e^{ik_o x}, \quad x > 0. \tag{2.95}$$

This represents the reflected surface wave on the upper side of the half-plane. The contribution from the pole at $\alpha = -k_o$ is

$$-\phi_i = -e^{-ik_o x}, \quad x < 0. \tag{2.96}$$

This term cancels the incident surface wave in the region $x < 0,\ y = 0^+$. There are no pole contributions from the integral (2.92) thus no transmitted wave exists on the lower surface of the half-plane.

Figure 2.36 shows the magnitude of the reflection coefficient as a function of X. It can be seen that $|\phi_R| \to 1$ as X increases. The diffracted lobes (Figures 2.40-2.38) are identical to those in the case of equal impedance parameters.

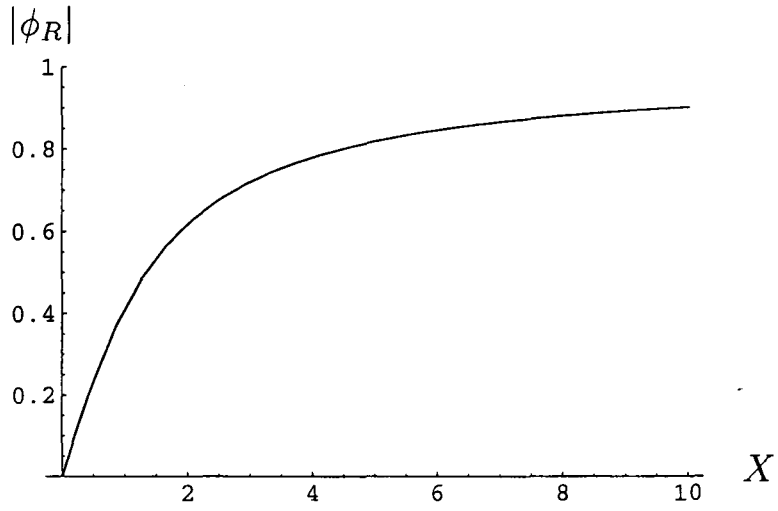

Figure 2.36: Dependence of the reflection coefficient on impedance $X_1 = -X_2 = X$.

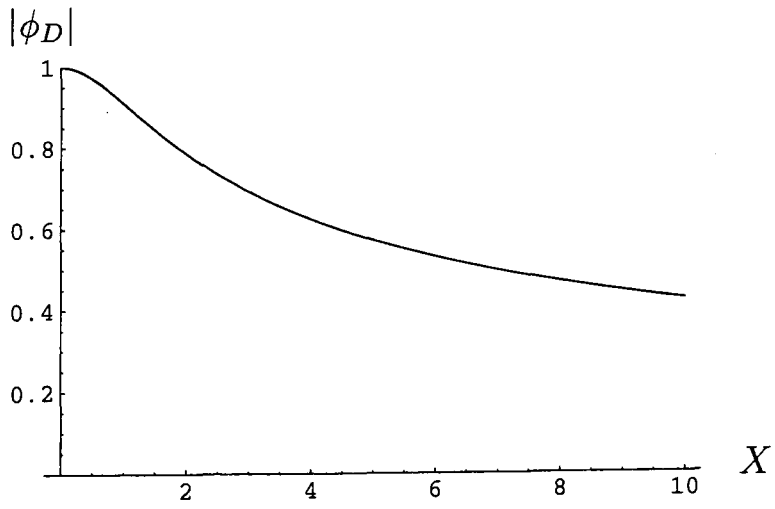

Figure 2.37: Dependence of the diffracted field on impedance $X_1 = -X_2 = X$.

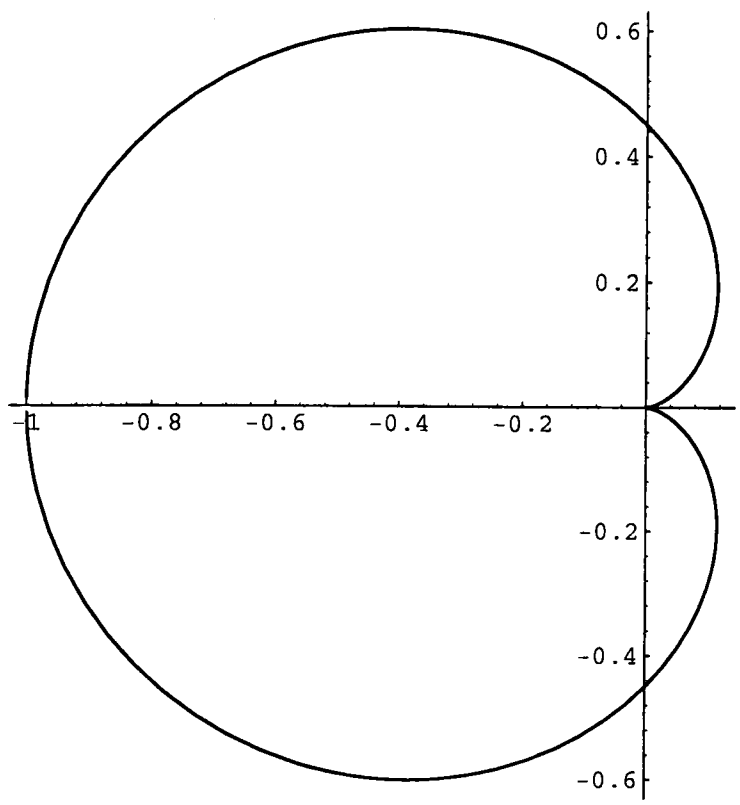

Figure 2.38: Radiation diagram for an incident surface wave, $X_1 = -X_2 = 3$.

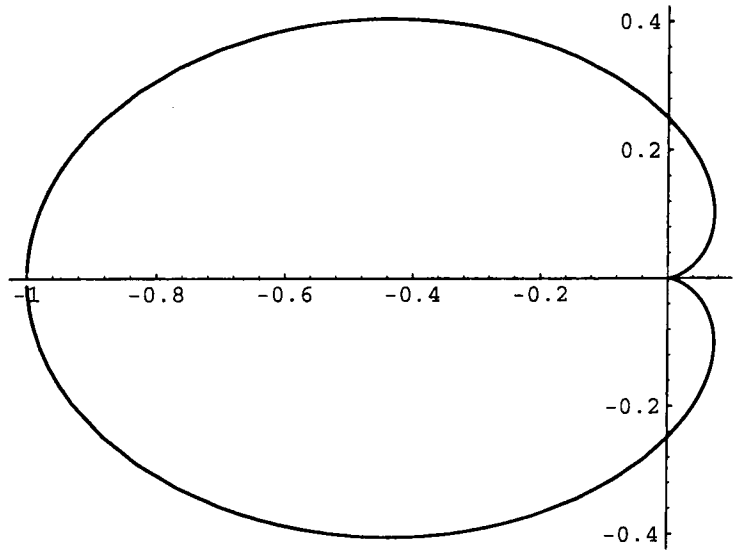

Figure 2.39: Radiation diagram for an incident surface wave, $X_1 = -X_2 = 1$.

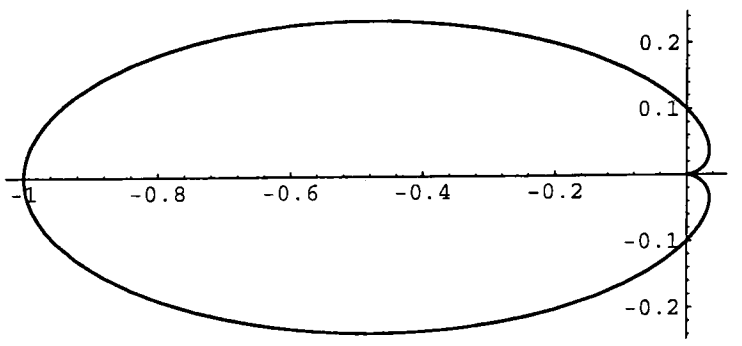

Figure 2.40: Radiation diagram for an incident surface wave, $X_1 = -X_2 = \frac{1}{2}$.

2.12 Conclusions and Further Work

The problem of a plane wave incident on a half-plane with different impedance boundary conditions on each face was examined using the Wiener-Hopf-Hilbert technique. This was done without restriction on the absorbing properties of the faces of the half-plane, thus the solution is valid for both wave-bearing and absorbent half-planes. Explicit expressions were obtained for the total far-field and arising surface waves for an arbitrary angle of incidence. It was shown that the solution given was valid for an incident surface wave in which case the diffracted field takes the form of a lobe. This solution generalises the problem solved by Trenev [32].

An obvious source of further work would be a study of further values of the admittance parameters on either side of the half-plane. Since the problem has been solved without restriction on β_1 and β_2 many cases of physical interest can be examined. The methods employed here can also be extended for more complicated boundary value problems. For example, the problem of the diffraction of sound from a line source by an absorbent half-plane considered by Rawlins [31] can be solved with arbitrary impedance parameter values.

The situation where a finite region near the end of the half-plane was lined with absorbent material could also be considered. This has the advantage of being easier and cheaper to construct than a half-plane with faces entirely coated in absorbent materials. Since the half-plane problem is governed by the conditions at the diffracting edge, it is only necessary to consider an absorbent coating in the vicinity of the edge. The work of the present chapter would act as a first order approximation when the

length of the absorbent tip is large.

More complicated first order boundary conditions on the half-plane can also be dealt with. Such problems arise in acoustics with flow where the Sommerfeld integral method [20] is no longer suitable because of the anisotropic nature of the boundary value problem. This problem is solved in the following chapter.

Chapter 3

Diffraction by a half-plane in a moving fluid

3.1 Introduction

The problem examined in this chapter is more complex than that solved in Chapter 2 in that the half-plane is emersed in a moving fluid. Expressions for the total far-field are derived for both the leading edge and trailing edge situations. In the trailing edge situation ($M > 0$) the problem has the added complication of a trailing vortex sheet or wake. Hence a Kutta-Joukowski edge condition is imposed to ensure that the fluid velocity is finite at the edge and to obtain a unique solution to the problem.

As in the previous problem, in the case where the impedance parameters are such that the half-plane is absorbent, the determinant of the matrix kernel is non-zero. Rawlins [29] obtained explicit expressions for the diffracted and geometrical acoustic field for the diffraction of cylindrical waves from a line source by an absorbing half-plane in the presence of a subsonic flow. However, for wave bearing surfaces, where the impedance parameter can be purely imaginary, the determinant of the matrix kernel has zeros in the cut plane. The solution given here generalises the Wiener-

Hopf-Hilbert approach to deal with both wave-bearing and non-wave-bearing surfaces in the presence of fluid flow and allows different impedance parameters on the upper and lower surfaces of the half-plane.

In Section 3.2 the mathematical boundary value problem is formulated using a generalised boundary condition that arises from the combination of fluid flow and absorbent surfaces. The problem is then reduced to a pair of simultaneous Wiener-Hopf equations in Section 3.3. An explicit factorisation of the Wiener-Hopf kernel is carried out in Section 3.4. In Section 3.5 asymptotic approximations for the far-field are obtained and graphical plots of the modulus of the far-field for various values of the impedance and fluid flow parameters are given in Section 3.7. In the particular case of a still fluid ($M = 0$) and the case where the admittances of the upper and lower faces of the half-plane are equal, it is shown that the results agree with Rawlins [29]. Conclusions are drawn in Section 3.8.

3.2 Formulation of the Boundary Value Problem

To begin with, an introduction is given to the basic equations governing propagation through a homogeneous medium. The density field, ρ, and velocity field, $\mathbf{u}$, satisfy the continuity equation

$$\frac{D\rho}{Dt} + \nabla.(\rho\mathbf{u}) = 0. \tag{3.1}$$

When the medium is inviscid and in the absence of external forces, the Navier-Stokes equation of motion reduces to Euler's equation

$$\frac{D\mathbf{u}}{Dt} = -\frac{1}{\rho}\nabla p. \tag{3.2}$$

An equation of state that describes the incompressibility properties of the medium is also required. It is to be assumed that the pressure, p depends only on the local density

$$p = p(\rho). \tag{3.3}$$

These three equations are linearised by regarding as small all perturbations from a state in which the medium has uniform velocity U in the x direction and has uniform density ρ_o. Retaining only first order terms forms the linearised equations

$$\left(\frac{\partial}{\partial t} - U\frac{\partial}{\partial x}\right)\rho = -\rho_o \nabla.\mathbf{u}, \tag{3.4}$$

$$\left(\frac{\partial}{\partial t} - U\frac{\partial}{\partial x}\right)\mathbf{u} = -\frac{1}{\rho_o}\nabla p, \tag{3.5}$$

$$\frac{\partial p}{\partial t} = c^2\frac{\partial \rho}{\partial t}. \tag{3.6}$$

In the current context, c is the speed of sound. Upon eliminating $\mathbf{u}$ it can be seen that

$$\left(\frac{\partial}{\partial t} - U\frac{\partial}{\partial x}\right)^2 p = c^2\nabla^2 p. \tag{3.7}$$

Taking the curl of equation (3.5) shows that the vorticity $\mathbf{\Omega} = \nabla \wedge \mathbf{u}$ is independent of time. Thus, for an initially irrotational flow, $\mathbf{\Omega} = 0$ for all time and there exists a velocity potential $\psi(\mathbf{x}, t)$ such that $\mathbf{u} = \nabla\psi$. The velocity potential therefore satisfies

$$\frac{\partial^2\psi}{\partial x^2} + \frac{\partial^2\psi}{\partial y^2} - \left(\frac{1}{c}\frac{\partial}{\partial t} - M\frac{\partial}{\partial x}\right)^2 \psi = 0, \tag{3.8}$$

where the Mach number $M = U/c$ and the wave number $k = \omega/c$. If a time harmonic variation $\psi(x, y, t)$ =Re$\{\psi(x, y)e^{-i\omega t}\}$ is assumed and suppressed henceforth

the convective wave equation is formed

$$(1-M^2)\frac{\partial^2\psi}{\partial x^2}+\frac{\partial^2\psi}{\partial y^2}-2ikM\frac{\partial\psi}{\partial x}+k^2\psi=0.$$

In Chapter 2 the field in the region $y=0, x<0$ was subject to the continuity conditions

$$\frac{\partial\psi}{\partial y}(x,0^+)=\frac{\partial\psi}{\partial y}(x,0^-), \quad x<0, \tag{3.9}$$

$$\psi(x,0^+)=\psi(x,0^-), \quad x<0. \tag{3.10}$$

However, in the case where a wake exists (3.10) does not hold. The continuity condition in this situation is derived as follows. Assuming $x<0$ throughout:

$$p(x,0^+)=p(x,0^-),$$

$$\left(i\omega+U\frac{\partial}{\partial x}\right)\psi(x,0^+)=\left(i\omega+U\frac{\partial}{\partial x}\right)\psi(x,0^-),$$

$$\left(i\omega+U\frac{\partial}{\partial x}\right)(\psi(x,0^+)-\psi(x,0^-))=0,$$

$$\left(\frac{\partial}{\partial x}+\frac{i\omega}{U}\right)(\psi(x,0^+)-\psi(x,0^-))=0,$$

$$\frac{\partial}{\partial x}\left(e^{i\omega x/U}(\psi(x,0^+)-\psi(x,0^-))\right)=0,$$

$$\psi(x,0^+)-\psi(x,0^-)=Ce^{-i\omega x/U},$$

$$\psi(x,0^+)-\psi(x,0^-)=Ce^{-ikx/M}, \quad x<0.$$

The problem to be considered is of a plane wave incident on a half-plane in a moving fluid occupying the region $x\geq 0,\ y=0$ (see Figure 3.1). The surfaces are lined with materials such that β_1 and β_2 are the complex specific admittances of the upper and lower surfaces of the half-plane respectively. It is noted that for Re $\beta_{1,2}>0$ the

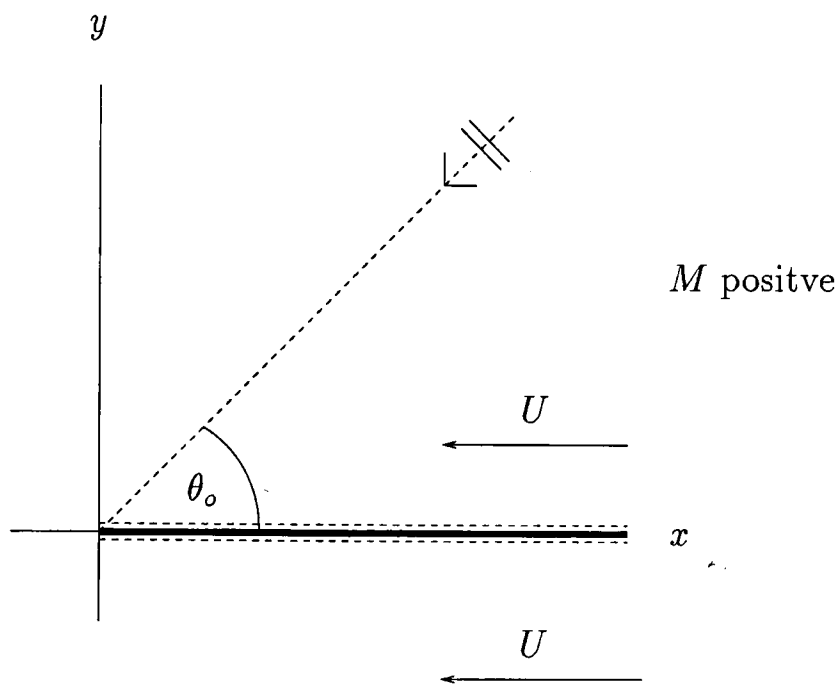

Figure 3.1: A plane wave incident on a half-plane.

surface is absorbent. For Re $\beta_{1,2} = 0$ the surface no longer absorbs energy and can support surface waves provided $\beta_{1,2} = -iX_{1,2}, X_{1,2} > 0$. The problem is one of solving the convective wave equation

$$(1 - M^2)\frac{\partial^2 \psi}{\partial x^2} + \frac{\partial^2 \psi}{\partial y^2} - 2ikM\frac{\partial \psi}{\partial x} + k^2\psi = 0, \tag{3.11}$$

subject to the boundary conditions

$$\left(\frac{\partial}{\partial y} + \beta_1 M\frac{\partial}{\partial x} + ik\beta_1\right)\psi(x, 0^+) = 0, \quad x > 0, \tag{3.12}$$

$$\left(\frac{\partial}{\partial y} - \beta_2 M\frac{\partial}{\partial x} - ik\beta_2\right)\psi(x, 0^-) = 0, \quad x > 0, \tag{3.13}$$

$$\psi(x, 0^+) - \psi(x, 0^-) = 2\pi i C \exp(-ikx/M), \quad x < 0, \tag{3.14}$$

$$\frac{\partial \psi}{\partial y}(x, 0^+) = \frac{\partial \psi}{\partial y}(x, 0^-), \quad x < 0. \tag{3.15}$$

A factor of $2\pi i$ has been introduced to equation (3.14) for convenience later on in the solution. The constant C in this formula will be determined by the requirement

that the velocity at the trailing edge should be finite. This requires the imposition of the Kutta-Joukowski edge condition. Combined with the condition that the field be outgoing at infinity, these conditions ensure that the boundary value problem has a unique solution.

3.3 Solution of the Boundary Value Problem

In the presence of subsonic flow $(-1 < M < 1)$ the following real substitutions can be made

$$x = \sqrt{1-M^2}X, \quad y = Y, \quad k = \sqrt{1-M^2}\,\mathcal{K}, \quad \beta = \sqrt{1-M^2}\,\mathcal{B};$$

which together with

$$\psi(x,y) = \Psi(X,Y)e^{i\mathcal{K}MX}, \tag{3.16}$$

reduces the problem to

$$\frac{\partial^2\Psi}{\partial X^2} + \frac{\partial^2\Psi}{\partial Y^2} + \mathcal{K}^2\Psi = 0, \tag{3.17}$$

subject to the boundary conditions

$$\left(\frac{\partial}{\partial Y} + \mathcal{B}_1 M\frac{\partial}{\partial X} + i\mathcal{K}\mathcal{B}_1\right)\Psi(X,0^+) = 0, \quad X > 0, \tag{3.18}$$

$$\left(\frac{\partial}{\partial Y} - \mathcal{B}_2 M\frac{\partial}{\partial X} - i\mathcal{K}\mathcal{B}_2\right)\Psi(X,0^-) = 0, \quad X > 0, \tag{3.19}$$

$$\Psi(X,0^+) - \Psi(X,0^-) = 2\pi i C\exp(-i\mathcal{K}X/M), \quad X < 0, \tag{3.20}$$

$$\frac{\partial\Psi}{\partial Y}(X,0^+) - \frac{\partial\Psi}{\partial Y}(X,0^-) = 0, \quad X < 0. \tag{3.21}$$

The complex Fourier transform $\hat{\Psi}(\alpha, Y)$ is defined by

$$\hat{\Psi}(\alpha,Y) = \frac{1}{2\pi}\int_{-\infty}^{\infty}\Psi(X,Y)e^{-i\alpha X}dX. \tag{3.22}$$

Applying this transform to the wave equation (3.17) gives

$$\frac{d^2\hat{\Psi}}{dY^2} + \kappa^2\hat{\Psi} = 0. \tag{3.23}$$

The branch of $\kappa = (\mathcal{K}^2 - \alpha^2)^{1/2}$ is chosen such that $\kappa = +\mathcal{K}$ for $\alpha = 0$. A solution of the boundary value problem can now be written as

$$\Psi = \Psi_{go} + \int_{-\infty}^{\infty} A(\alpha)e^{i(\alpha X + \kappa Y)}\, d\alpha, \quad Y > 0, \tag{3.24}$$

$$= \int_{-\infty}^{\infty} B(\alpha)e^{i(\alpha X - \kappa Y)}\, d\alpha, \qquad Y < 0. \tag{3.25}$$

For convenience it shall be assumed that Ψ_{go} consists of the incident plane wave and a reflected wave thus

$$\Psi_{go}(X,Y) = e^{-i\mathcal{K}(X\cos\Theta_o + Y\sin\Theta_o)} + Re^{-i\mathcal{K}(X\cos\Theta_o - Y\sin\Theta_o)}, \tag{3.26}$$

where

$$R = \left(\frac{\sin\Theta_o + \mathcal{B}_1 M\cos\Theta_o - \mathcal{B}_1}{\sin\Theta_o - \mathcal{B}_1 M\cos\Theta_o + \mathcal{B}_1}\right).$$

Applying the conditions (3.20) and (3.21) leads to

$$A(\alpha) - B(\alpha) = l_1(\alpha) - \frac{\sin\Theta_o}{\pi i(\alpha + \mathcal{K}_o)(\sin\Theta_o - \mathcal{B}_1 M\cos\Theta_o + \mathcal{B}_1)} + \frac{C}{(\alpha + \mathcal{K}/M)},$$

$$\kappa(A(\alpha) + B(\alpha)) = l_2(\alpha) + \frac{\mathcal{K}\mathcal{B}_1\sin\Theta_o(1 - M\cos\Theta_o)}{\pi i(\alpha + \mathcal{K}_o)(\sin\Theta_o - \mathcal{B}_1 M\cos\Theta_o + \mathcal{B}_1)},$$

where $\alpha = -\mathcal{K}/M$ and $\alpha = -\mathcal{K}_o = -\mathcal{K}\cos\Theta_o$ lie in the lower half of the complex plane ($\tau_- = \text{Im}\ \alpha \leq 0$) and $l_1(\alpha)$ and $l_2(\alpha)$ are analytic in this region. The capture of the poles at $\alpha = -\mathcal{K}_o$ and $\alpha = -\mathcal{K}/M$ is shown in Figure 3.2. By adding and subtracting these equations it can be seen that

$$A(\alpha) = \frac{1}{2}\left\{l_1(\alpha) + \frac{l_2(\alpha)}{\kappa} - \frac{\sin\Theta_o\{\mathcal{K}\mathcal{B}_1(1 - M\cos\Theta_o)/\kappa - 1\}}{\pi i(\alpha + \mathcal{K}_o)(\sin\Theta_o - \mathcal{B}_1 M\cos\Theta_o + \mathcal{B}_1)} + \frac{C}{(\alpha + \mathcal{K}/M)}\right\}, \tag{3.27}$$

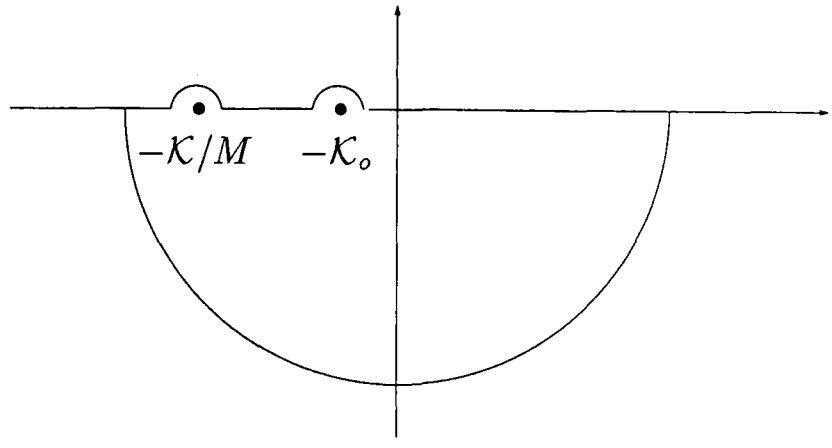

Figure 3.2: The complex plane.

$$B(\alpha) = \frac{1}{2}\left\{-l_1(\alpha) + \frac{l_2(\alpha)}{\kappa} - \frac{\sin\Theta_o\{\mathcal{K}\mathcal{B}_1(1 - M\cos\Theta_o)/\kappa + 1\}}{\pi i(\alpha + \mathcal{K}_o)(\sin\Theta_o - \mathcal{B}_1 M\cos\Theta_o + \mathcal{B}_1)} - \frac{C}{(\alpha + \mathcal{K}/M)}\right\}. \tag{3.28}$$

Applying the boundary conditions (3.18) and (3.19) leads to

$$(\mathcal{K}\mathcal{B}_1 + \kappa + \mathcal{B}_1 M\alpha)A(\alpha) = u_1(\alpha), \tag{3.29}$$

$$(\mathcal{K}\mathcal{B}_2 + \kappa + \mathcal{B}_2 M\alpha)B(\alpha) = u_2(\alpha), \tag{3.30}$$

where $u_1(\alpha)$ and $u_2(\alpha)$ are analytic in the upper half-plane, τ_+: Im $\alpha \geq 0, \alpha \neq -\mathcal{K}_o, \alpha \neq -\mathcal{K}/M$. Substituting (3.27) and (3.28) into these equations eliminates the unknowns $A(\alpha), B(\alpha)$ and leads to the matrix Wiener-Hopf equation

$$G(\alpha)\; l(\alpha) = u(\alpha) + G(\alpha)\frac{P}{(\alpha + \mathcal{K}_o)} - \frac{G(\alpha)}{(\alpha + \mathcal{K}/M)}\begin{pmatrix} C \\ 0 \end{pmatrix}, \tag{3.31}$$

where

$$G(\alpha) = \frac{1}{2}\begin{pmatrix} \kappa + \mathcal{B}_1 M\alpha + \mathcal{K}\mathcal{B}_1 & (\kappa + \mathcal{B}_1 M\alpha + \mathcal{K}\mathcal{B}_1)/\kappa \\ -\kappa - \mathcal{B}_2 M\alpha - \mathcal{K}\mathcal{B}_2 & (\kappa + \mathcal{B}_2 M\alpha + \mathcal{K}\mathcal{B}_2)/\kappa \end{pmatrix}, \tag{3.32}$$

$$P = \frac{\sin\Theta_o}{\pi i(\sin\Theta_o - \mathcal{B}_1 M\cos\Theta_o + \mathcal{B}_1)}\begin{pmatrix} 1 \\ -\mathcal{K}\mathcal{B}_1(1 - M\cos\Theta_o) \end{pmatrix},$$

$$l(\alpha) = \begin{pmatrix} l_1 \\ l_2 \end{pmatrix}, \quad u(\alpha) = \begin{pmatrix} u_1 \\ u_2 \end{pmatrix}.$$

The problem of factorising the matrix $G(\alpha)$ is addressed in a manner similar to that in Chapter 2. Firstly, define $D(\alpha)$ such that

$$D^2(\alpha) = \det G(\alpha) = \frac{1}{2\kappa}(\kappa + \mathcal{B}_1 M\alpha + \mathcal{K}\mathcal{B}_1)(\kappa + \mathcal{B}_2 M\alpha + \mathcal{K}\mathcal{B}_2),$$

and define $K(\alpha)$ by

$$G(\alpha) = D(\alpha)K(\alpha). \tag{3.33}$$

Then

$$K(\alpha) = \sqrt{\frac{\kappa}{2}} \begin{pmatrix} \left(\dfrac{\kappa + \mathcal{B}_1 M\alpha + \mathcal{K}\mathcal{B}_1}{\kappa + \mathcal{B}_2 M\alpha + \mathcal{K}\mathcal{B}_2}\right)^{1/2} & \dfrac{1}{\kappa}\left(\dfrac{\kappa + \mathcal{B}_1 M\alpha + \mathcal{K}\mathcal{B}_1}{\kappa + \mathcal{B}_2 M\alpha + \mathcal{K}\mathcal{B}_2}\right)^{1/2} \\ -\left(\dfrac{\kappa + \mathcal{B}_2 M\alpha + \mathcal{K}\mathcal{B}_2}{\kappa + \mathcal{B}_1 M\alpha + \mathcal{K}\mathcal{B}_1}\right)^{1/2} & \dfrac{1}{\kappa}\left(\dfrac{\kappa + \mathcal{B}_2 M\alpha + \mathcal{K}\mathcal{B}_2}{\kappa + \mathcal{B}_1 M\alpha + \mathcal{K}\mathcal{B}_1}\right)^{1/2} \end{pmatrix}, \tag{3.34}$$

and

$$\det K(\alpha) = 1.$$

The factorisation of $G(\alpha)$ now follows directly from the factorisation of $K(\alpha)$ and $D(\alpha)$.

3.4 Factorisation of the Wiener-Hopf Kernel

Factorisation of $K(\alpha)$

It is required that $K(\alpha) = U(\alpha)L^{-1}(\alpha)$ where $L(\alpha)$ is analytic everywhere except along the line $\mathcal{K} < \alpha < \infty$, $\mathrm{Im}(\alpha) = 0$ and $U(\alpha)$ is analytic everywhere except along $-\infty < \alpha < -\mathcal{K}$, $\mathrm{Im}(\alpha) = 0$. Then it can be written that

$$\left.\begin{aligned} K^+(\xi) &= U^+(\xi)L^{-1}(\xi) \\ K^-(\xi) &= U^-(\xi)L^{-1}(\xi) \end{aligned}\right\} -\infty < \xi < -\mathcal{K} \tag{3.35}$$

since L is continuous across this region. Eliminating $L^{-1}(\xi)$ gives

$$U^+(\xi) = K^+(\xi)[K^{-1}(\xi)]^- U^-(\xi). \tag{3.36}$$

where F^+ denotes values of F on the upper side of the cut and F^- denotes values of F on the lower side of the cut. From equation (3.34) it follows that

$$K^+(\xi) = \sqrt{\frac{i|\kappa|}{2}} \begin{pmatrix} \left(\frac{i|\kappa| - \mathcal{B}_1 M|\xi| + \mathcal{K}\mathcal{B}_1}{i|\kappa| - \mathcal{B}_2 M|\xi| + \mathcal{K}\mathcal{B}_2}\right)^{1/2} & \frac{1}{i|\kappa|}\left(\frac{i|\kappa| - \mathcal{B}_1 M|\xi| + \mathcal{K}\mathcal{B}_1}{i|\kappa| - \mathcal{B}_2 M|\xi| + \mathcal{K}\mathcal{B}_2}\right)^{1/2} \\ -\left(\frac{i|\kappa| - \mathcal{B}_2 M|\xi| + \mathcal{K}\mathcal{B}_2}{i|\kappa| - \mathcal{B}_1 M|\xi| + \mathcal{K}\mathcal{B}_1}\right)^{1/2} & \frac{1}{i|\kappa|}\left(\frac{i|\kappa| - \mathcal{B}_2 M|\xi| + \mathcal{K}\mathcal{B}_2}{i|\kappa| - \mathcal{B}_1 M|\xi| + \mathcal{K}\mathcal{B}_1}\right)^{1/2} \end{pmatrix},$$

$$[K^{-1}(\xi)]^- = \sqrt{\frac{-i|\kappa|}{2}} \begin{pmatrix} \frac{-1}{i|\kappa|}\left(\frac{-i|\kappa| - \mathcal{B}_2 M|\xi| + \mathcal{K}\mathcal{B}_2}{-i|\kappa| - \mathcal{B}_1 M|\xi| + \mathcal{K}\mathcal{B}_1}\right)^{1/2} & \frac{1}{i|\kappa|}\left(\frac{-i|\kappa| - \mathcal{B}_1 M|\xi| + \mathcal{K}\mathcal{B}_1}{-i|\kappa| - \mathcal{B}_2 M|\xi| + \mathcal{K}\mathcal{B}_2}\right)^{1/2} \\ \left(\frac{-i|\kappa| - \mathcal{B}_2 M|\xi| + \mathcal{K}\mathcal{B}_2}{-i|\kappa| - \mathcal{B}_1 M|\xi| + \mathcal{K}\mathcal{B}_1}\right)^{1/2} & \left(\frac{-i|\kappa| - \mathcal{B}_1 M|\xi| + \mathcal{K}\mathcal{B}_1}{-i|\kappa| - \mathcal{B}_2 M|\xi| + \mathcal{K}\mathcal{B}_2}\right)^{1/2} \end{pmatrix}.$$

Substituting these into equation (3.36) gives

$$U^+(\xi) = \begin{pmatrix} 0 & -i\left\{\frac{(\mathcal{K}\mathcal{B}_1 - \mathcal{B}_1 M|\xi|)^2 + |\kappa|^2}{(\mathcal{K}\mathcal{B}_2 - \mathcal{B}_2 M|\xi|)^2 + |\kappa|^2}\right\}^{\frac{1}{2}} \\ -i\left\{\frac{(\mathcal{K}\mathcal{B}_2 - \mathcal{B}_2 M|\xi|)^2 + |\kappa|^2}{(\mathcal{K}\mathcal{B}_1 - \mathcal{B}_1 M|\xi|)^2 + |\kappa|^2}\right\}^{\frac{1}{2}} & 0 \end{pmatrix} U^-(\xi). \tag{3.37}$$

This requires the solution of the following coupled Hilbert problems

$$U_1^+(\xi) = -i\left\{\frac{(\mathcal{K}\mathcal{B}_1 - \mathcal{B}_1 M|\xi|)^2 + |\kappa|^2}{(\mathcal{K}\mathcal{B}_2 - \mathcal{B}_2 M|\xi|)^2 + |\kappa|^2}\right\}^{\frac{1}{2}} U_2^-(\xi), \tag{3.38}$$

$$U_2^+(\xi) = -i\left\{\frac{(\mathcal{K}\mathcal{B}_2 - \mathcal{B}_2 M|\xi|)^2 + |\kappa|^2}{(\mathcal{K}\mathcal{B}_1 - \mathcal{B}_1 M|\xi|)^2 + |\kappa|^2}\right\}^{\frac{1}{2}} U_1^-(\xi). \tag{3.39}$$

If $V(\xi) = U_1(\xi)U_2(\xi)$ and $W(\xi) = \dfrac{U_1(\xi)}{U_2(\xi)}$ then multiplying and dividing the Hilbert equations produces

$$V^+(\xi)/V^-(\xi) = -1, \tag{3.40}$$

$$[\log W(\xi)]^+ + [\log W(\xi)]^- = \log\left[\frac{|\kappa|^2 + (\mathcal{K}\mathcal{B}_1 - \mathcal{B}_1 M|\xi|)^2}{|\kappa|^2 + (\mathcal{K}\mathcal{B}_2 - \mathcal{B}_2 M|\xi|)^2}\right]. \tag{3.41}$$

By inspection, it can be seen that equation (3.40) has a particular solution

$$V(\alpha) = (\mathcal{K} + \alpha)^{-\frac{1}{2}}. \tag{3.42}$$

Equation (3.41) can be written as

$$\left[\frac{\log W(\xi)}{\sqrt{\mathcal{K}+\xi}}\right]^{+} - \left[\frac{\log W(\xi)}{\sqrt{\mathcal{K}+\xi}}\right]^{-} = \frac{-i}{|\mathcal{K}+\xi|^{1/2}} \log\left[\frac{|\kappa|^2 + (\mathcal{K}\mathcal{B}_1 - \mathcal{B}_1 M|\xi|)^2}{|\kappa|^2 + (\mathcal{K}\mathcal{B}_2 - \mathcal{B}_2 M|\xi|)^2}\right]. \quad (3.43)$$

The solution of this equation (see Appendix E) is given by

$$W(\alpha) = \exp\left[-\frac{\sqrt{\mathcal{K}+\alpha}}{2\pi}\int_{-\infty}^{-\mathcal{K}} \frac{1}{|\mathcal{K}+t|^{\frac{1}{2}}} \log\left[\frac{|\kappa|^2 + (\mathcal{K}\mathcal{B}_1 - \mathcal{B}_1 M|t|)^2}{|\kappa|^2 + (\mathcal{K}\mathcal{B}_2 - \mathcal{B}_2 M|t|)^2}\right]\frac{dt}{(t-\alpha)}\right]. \quad (3.44)$$

Now,

$$I(\alpha) = -\frac{1}{2\pi}\int_{-\infty}^{-\mathcal{K}} \frac{1}{|\mathcal{K}+t|^{\frac{1}{2}}} \log\left[\frac{|\kappa|^2 + (\mathcal{K}\mathcal{B}_1 - \mathcal{B}_1 M|t|)^2}{|\kappa|^2 + (\mathcal{K}\mathcal{B}_2 - \mathcal{B}_2 M|t|)^2}\right]\frac{dt}{(t-\alpha)},$$

$$= \frac{1}{2\pi}\int_0^{\infty} \frac{\log(t+\mathcal{K}B_1^+) + \log(t+\mathcal{K}B_1^-) - \log(t+\mathcal{K}B_2^+) - \log(t+\mathcal{K}B_2^-)}{t^{\frac{1}{2}}(t+\mathcal{K}+\alpha)}\,dt$$

$$+\frac{1}{2\pi}\log\left(\frac{1+\mathcal{B}_1^2M^2}{1+\mathcal{B}_2^2M^2}\right)\int_0^{\infty}\frac{dt}{t^{1/2}(t+\mathcal{K}+\alpha)},$$

where

$$B_{1,2}^{\pm} = 1 - \frac{\mathcal{B}_{1,2}^2 M \pm \sqrt{1+\mathcal{B}_{1,2}^2M^2 - \mathcal{B}_{1,2}^2}}{1+\mathcal{B}_{1,2}^2M^2}. \quad (3.45)$$

Using the following results (see Appendix D)

$$\int_0^{\infty}\frac{\log(t+\delta)}{t^{\frac{1}{2}}(t+\gamma)}dt = \frac{2\pi}{\sqrt{\gamma}}\log(\sqrt{\gamma}+\sqrt{\delta}),\ |\arg\gamma|<\pi, |\arg\delta|\le\pi, \quad (3.46)$$

$$\frac{1}{2\pi}\log\left(\frac{1+\mathcal{B}_1^2M^2}{1+\mathcal{B}_2^2M^2}\right)\int_0^{\infty}\frac{dt}{t^{1/2}(t+\mathcal{K}+\alpha)} = \frac{1}{\sqrt{\mathcal{K}+\alpha}}\log\left(\frac{1+\mathcal{B}_1^2M^2}{1+\mathcal{B}_2^2M^2}\right)^{1/2},$$

equation (3.44) reduces to

$$W(\alpha) = \left(\frac{1+\mathcal{B}_1^2M^2}{1+\mathcal{B}_2^2M^2}\right)^{1/2}\frac{\left(\sqrt{\mathcal{K}+\alpha}+\sqrt{\mathcal{K}B_1(+)}\right)\left(\sqrt{\mathcal{K}+\alpha}+\sqrt{\mathcal{K}B_1(-)}\right)}{\left(\sqrt{\mathcal{K}+\alpha}+\sqrt{\mathcal{K}B_2(+)}\right)\left(\sqrt{\mathcal{K}+\alpha}+\sqrt{\mathcal{K}B_2(-)}\right)}. \quad (3.47)$$

Particular solutions of (3.38) and (3.39) are now given by

$$U_1(\alpha) = -[V(\alpha)]^{\frac{1}{2}}[W(\alpha)]^{\frac{1}{2}},$$
$$U_2(\alpha) = -[V(\alpha)]^{\frac{1}{2}}[W(\alpha)]^{-\frac{1}{2}}.$$

A general solution can be obtained by following the method given by Rawlins [31]. This is done by imposing further conditions on the functions $U_1(\alpha)$ and $U_2(\alpha)$. First it is required that

$$U_1(\alpha) = O((k+\alpha)^n), \quad U_2(\alpha) = O((k+\alpha)^{1/2+m}), \quad \text{as } \alpha \to -k,$$

for some $n, m > -1$. The second requirement is that $U_1(\alpha)$ and $U_2(\alpha)$ have finite degree at infinity. These conditions lead to

$$U(\alpha) = U^{(0)}(\alpha)P(\alpha),$$

where $P_{ij}(i,j = 1,2)$ are arbitrary polynomials and

$$U^{(0)}(\alpha) = \begin{pmatrix} -[V(\alpha)]^{\frac{1}{2}}[W(\alpha)]^{\frac{1}{2}} & [V(\alpha)]^{\frac{1}{2}}[W(\alpha)]^{\frac{1}{2}}[k+\alpha]^{\frac{1}{2}} \\ -[V(\alpha)]^{\frac{1}{2}}[W(\alpha)]^{-\frac{1}{2}} & -[V(\alpha)]^{\frac{1}{2}}[W(\alpha)]^{-\frac{1}{2}}[k+\alpha]^{\frac{1}{2}} \end{pmatrix}.$$

To ensure that U is non-singular in the cut plane $\det U$ and hence $\det P$ must be non-zero for all α. The fact that $\det P$ is a polynomial implies that $\det P =$ constant. For simplicity, P is chosen to be the identity matrix. This gives a final expression of

$$U(\alpha) = \begin{pmatrix} -[k+\alpha]^{-\frac{1}{4}}[W(\alpha)]^{\frac{1}{2}} & [k+\alpha]^{\frac{1}{4}}[W(\alpha)]^{\frac{1}{2}} \\ -[k+\alpha]^{-\frac{1}{4}}[W(\alpha)]^{-\frac{1}{2}} & -[k+\alpha]^{\frac{1}{4}}[W(\alpha)]^{-\frac{1}{2}} \end{pmatrix}. \tag{3.48}$$

The matrix $L(\alpha)$ can be found from the expression

$$L(\alpha) = K^{-1}(\alpha)U(\alpha).$$

Factorisation of $D(\alpha)$

$$\begin{aligned} D(\alpha) &= \sqrt{\frac{(\kappa + \mathcal{B}_1 M\alpha + \mathcal{K}\mathcal{B}_1)(\kappa + \mathcal{B}_2 M\alpha + \mathcal{K}\mathcal{B}_1)}{2\kappa}}, \\ &= \left(\frac{\kappa}{2}\right)^{1/2} \left(\frac{\kappa + \mathcal{B}_1 M\alpha + \mathcal{K}\mathcal{B}_1}{\kappa}\right)^{1/2} \left(\frac{\kappa + \mathcal{B}_2 M\alpha + \mathcal{K}\mathcal{B}_2}{\kappa}\right)^{1/2}. \end{aligned}$$

Consider the factorisation of the function $d^n(\alpha)$ given by

$$d^n(\alpha) = \frac{\kappa + \mathcal{B}_n M\alpha + \mathcal{K}\mathcal{B}_n}{\kappa}. \tag{3.49}$$

This function has been factorised explicitly in Rawlins [29]. The upper split function is

$$d^n_+(\mathcal{K}\cos\Theta) = \frac{\sqrt{1+\mathcal{B}_n}}{\sqrt{1+\cos\Theta}} \exp\left\{\frac{\mathcal{B}_n}{2\pi\sqrt{1-\mathcal{B}_n^2+M^2\mathcal{B}_n^2}}\Big[F(v_1)-F(v_2)\Big]\right\}, \quad 0 \le \Theta < \pi, \tag{3.50}$$

where

$$F(v) = -(M+v)\int_{\pi/2}^{\Theta} \frac{u - \frac{\arccos v}{\sqrt{1-v^2}}\sin u\, du}{(v-\cos u)}, \tag{3.51}$$

and

$$v_1 = \frac{-M\mathcal{B}_n^2 + \sqrt{1-\mathcal{B}_n^2+M^2\mathcal{B}_n^2}}{1+\mathcal{B}_n^2M^2}, \quad v_2 = \frac{-M\mathcal{B}_n^2 - \sqrt{1-\mathcal{B}_n^2+M^2\mathcal{B}_n^2}}{1+\mathcal{B}_n^2M^2}. \tag{3.52}$$

The upper split function, $D_+(\alpha)$, can now be written as

$$D_+(\alpha) = \left\{\sqrt{\frac{\mathcal{K}+\alpha}{2}}d_1^+(\alpha)d_2^+(\alpha)\right\}^{1/2}. \tag{3.53}$$

3.5 Asymptotic Expressions for the Far-Field

With the factorisation of $G(\alpha)$ complete, the procedure from equation (3.31) is as follows

$$\begin{aligned}
G(\alpha)l(\alpha) &= u(\alpha) + G(\alpha)\frac{P}{(\alpha+\mathcal{K}_o)} - \frac{G(\alpha)}{(\alpha+\mathcal{K}/M)}\begin{pmatrix}C\\0\end{pmatrix},\\
G_+(\alpha)G_-(\alpha)l(\alpha) &= u(\alpha) + G(\alpha)\frac{P}{(\alpha+\mathcal{K}_o)} - \frac{G(\alpha)}{(\alpha+\mathcal{K}/M)}\begin{pmatrix}C\\0\end{pmatrix},\\
G_-(\alpha)l(\alpha) &= G_+^{-1}(\alpha)u(\alpha) + G_-(\alpha)\frac{P}{(\alpha+\mathcal{K}_o)} - \frac{G_-(\alpha)}{(\alpha+\mathcal{K}/M)}\begin{pmatrix}C\\0\end{pmatrix}.
\end{aligned}$$

This can be written in the form

$$G_-(\alpha)l(\alpha) - \Big[G_-(\alpha) - G_-(-\mathcal{K}_o)\Big]\frac{P}{(\alpha+\mathcal{K}_o)} + \frac{[G_-(\alpha) - G_-(-\mathcal{K}/M)]}{(\alpha+\mathcal{K}/M)}\begin{pmatrix}C\\0\end{pmatrix} = G_+^{-1}(\alpha)u(\alpha) + G_-(-\mathcal{K}_o)\frac{P}{(\alpha+\mathcal{K}_o)} - \frac{G_-(-\mathcal{K}/M)}{(\alpha+\mathcal{K}/M)}\begin{pmatrix}C\\0\end{pmatrix}. \tag{3.54}$$

The left hand side of this expression is analytic in τ_- and the right hand side is analytic in τ_+. Hence both sides of equation (3.54) are equal to an entire function $\mathbf{Q}(\alpha)$. From equations (3.42) and (3.47) it follows that

$$V(\alpha) = O(\alpha^{-\frac{1}{2}}), \quad W(\alpha) = O(1), \quad |\alpha| \to \infty.$$

Therefore

$$G_+(\alpha) = O\begin{pmatrix}1 & \alpha^{\frac{1}{2}}\\ 1 & \alpha^{\frac{1}{2}}\end{pmatrix}, \quad G_-(\alpha) = O\begin{pmatrix}\alpha^{-\frac{1}{2}} & 1\\ \alpha^{\frac{1}{2}} & \alpha^{-1}\end{pmatrix}, \quad |\alpha| \to \infty. \tag{3.55}$$

Combining the edge condition (2.15) with (2.24) it can be shown that the terms of $u(\alpha)$ are $O(\alpha^{-1/2})$ at worst. Using an extension of Liouville's theorem it now follows that $\mathbf{Q}(\alpha) = 0$. Thus

$$l(\alpha) = \frac{\left[G_-^{-1}(\alpha)\, G_-(-\mathcal{K}/M) - \mathrm{I}\right]}{(\alpha+\mathcal{K}/M)}\begin{pmatrix}C\\0\end{pmatrix} - \left[G_-^{-1}(\alpha)G_-(-\mathcal{K}_o) - \mathrm{I}\right]\frac{P}{(\alpha+\mathcal{K}_o)}, \tag{3.56}$$

$$u(\alpha) = \frac{G_+(\alpha)\, G_-(-\mathcal{K}/M)}{(\alpha+\mathcal{K}/M)}\begin{pmatrix}C\\0\end{pmatrix} - G_+(\alpha)G_-(-\mathcal{K}_o)\frac{P}{(\alpha+\mathcal{K}_o)}. \tag{3.57}$$

Combining (3.57) with (3.24) and (3.29) gives

$$\Psi_s(X,Y) = \int_{-\infty}^{\infty} \frac{u_1(\alpha)}{(\kappa + \mathcal{B}_1 M\alpha + \mathcal{K}\mathcal{B}_1)}\, e^{i(\alpha X + \kappa Y)}d\alpha, \quad y > 0. \tag{3.58}$$

As was seen in Chapter 2, the procedure from here is to consider a shift of contour in the α-plane given by

$$\alpha = \mathcal{K}\cos(\Theta + it), \quad (-\infty < t < \infty). \tag{3.59}$$

On applying this to equation (3.58), the scattered field becomes

$$\Psi_s(R,\Theta) = \int_{-\infty}^{\infty} \frac{-i\sin(\Theta+it)\; u_1[\mathcal{K}\cos(\Theta+it)]}{\mathcal{B}_1 + \mathcal{B}_1 M\cos(\Theta+it) + \sin(\Theta+it)} e^{i\mathcal{K}R\cosh t}dt, \quad 0<\Theta<\pi. \tag{3.60}$$

On applying the method of stationary phase, the final expression for the far-field is

$$\Psi(R,\Theta) = \Psi_i(R,\Theta) + \Psi_r(R,\Theta) + \Psi_{d+}(R,\Theta), \qquad 0<\Theta<\pi-\Theta_o, \tag{3.61}$$

$$= \Psi_i(R,\Theta) + \Psi_{d+}(R,\Theta), \qquad \pi-\Theta_o<\Theta<\pi, \tag{3.62}$$

$$= \Psi_i(R,\Theta) + \Psi_{d-}(R,\Theta), \qquad -\pi<\Theta<\Theta_o-\pi, \tag{3.63}$$

$$= \Psi_{d-}(R,\Theta), \qquad \Theta_o-\pi<\Theta<0, \tag{3.64}$$

where

$$\Psi_i(R,\Theta) = e^{-i\mathcal{K}R\cos(\Theta-\Theta_o)}, \tag{3.65}$$

$$\Psi_r(R,\Theta) = \left(\frac{\sin\Theta_o + \mathcal{B}_1 M\cos\Theta_o - \mathcal{B}_1}{\sin\Theta_o - \mathcal{B}_1 M\cos\Theta_o + \mathcal{B}_1}\right) e^{-i\mathcal{K}R\cos(\Theta+\Theta_o)}, \tag{3.66}$$

$$\Psi_{d_+}(R,\Theta) = 2i\sqrt{\frac{\pi}{2\mathcal{K}R}}\left(\frac{\sin\Theta}{\mathcal{B}_1 + \mathcal{B}_1 M\cos\Theta + \sin\Theta}\right) u_1[\mathcal{K}\cos\Theta] e^{i\mathcal{K}R+\frac{\pi i}{4}}, \tag{3.67}$$

$$\Psi_{d_-}(R,\Theta) = -2i\sqrt{\frac{\pi}{2\mathcal{K}R}}\left(\frac{\sin\Theta}{\mathcal{B}_2 + \mathcal{B}_2 M\cos\Theta - \sin\Theta}\right) u_2[\mathcal{K}\cos\Theta] e^{i\mathcal{K}R+\frac{\pi i}{4}}, \tag{3.68}$$

and

$$\cos\Theta = \frac{\cos\theta}{(1-M^2\sin^2\theta)^{1/2}}, \quad R = r\left(\frac{1-M^2\sin^2\theta}{1-M^2}\right)^{1/2}.$$

3.6 The Kutta-Joukowski Condition

In the trailing edge situation ($M > 0$) the unknown C is calculated by applying the Kutta-Joukowski edge condition. In the absence of a wake $C = 0$. The Kutta-Joukowski condition requires that the velocity be finite at the origin which means that

the terms in Ψ that are $O(r^{-1/2})$ must vanish. This in turn implies that the terms of $O(\alpha^{-1/2})$ in $u_1(\alpha)$ and $u_2(\alpha)$ must also vanish. From expression (3.57) it can be seen that

$$u_1(\alpha) = \frac{C\{G_1(\alpha)e + G_2(\alpha)g\}}{(\alpha + \mathcal{K}/M)} - \frac{1}{(\alpha + k_o)}\Big[G_1(\alpha)\{aP_1 + bP_2\} + G_2(\alpha)\{cP_1 + dP_2\}\Big],$$

where

$$G_+(\alpha) = \begin{pmatrix} G_1(\alpha) & G_2(\alpha) \\ G_3(\alpha) & G_4(\alpha) \end{pmatrix}, \; G_-(-\mathcal{K}_o) = \begin{pmatrix} a & b \\ c & d \end{pmatrix}, \; G_-(-\mathcal{K}/M) = \begin{pmatrix} e & f \\ g & h \end{pmatrix}, \; P = \begin{pmatrix} P_1 \\ P_2 \end{pmatrix}.$$

From (3.55) it can be seen that G_1 and G_3 are $O(1)$ whilst G_2 and G_4 are $O(\alpha^{1/2})$ as $|\alpha| \to \infty$. Setting the term that is $O(\alpha^{-1/2})$ to zero in $u_1(\alpha)$ gives

$$cP_1 + dP_2 - gC = 0,$$

$$C = \frac{(cP_1 + dP_2)}{g}. \tag{3.69}$$

3.7 Graphical Results

The diffracted field given by expressions (3.67) and (3.68) becomes infinite on the boundaries $\Theta = \pi - \Theta_o$ and $\Theta = \pi + \Theta_o$ so an alternate expression has been used to give the graphical plots of the modulus of the far-field. See Appendix A for further details.

Figures 3.4-3.7 show the modulus of the far-field for a half-plane with impedance parameters $\beta_1 = \beta_2 = 2/3$ (fibrous sheet), the angle of incidence is taken to be $\pi/2$ and the Mach number, M, takes the values -0.9, 0 and 0.9. As explained in the previous chapter, the field in the region $0 < \theta < \pi/2$ is due primarily to interference

between the incident and reflected waves. The modulus of the reflection coefficient is given by expression (3.66) and $|\Psi_r|$=1. It can be seen that in the region $0 < \theta < \pi/2$ the oscillations about the incident wave magnitude of unity are of the order $|\Psi_r|$. In the trailing edge situation graphs have been obtained in the case where a wake is present (Figure 3.6) and by putting $C = 0$ the case where no wake is present (Figure 3.7). These graphs differ significantly in the region $\pi/2 < \theta < 3\pi/2$. When no wake is present the oscillations about the incident field magnitude of unity are greater in the region $\pi/2 < \theta < \pi$ but less in the region $\pi < \theta < 3\pi/4$ compared to the case where a wake is present. The diffracted field in the shadow region $-\pi/2 < \theta < 0$ varies according to the Mach number. This field is larger in the leading edge situation (Figure 3.4) than in the trailing edge situation, where the fluid flow carries the sound away from the shadow region.

Figures 3.8-3.11 were obtained using $\beta_1 = \beta_2 = 1/(0.5 + i)$ (perforated steel). The trends are the same as those given above and the graphs shown are identical to those in Rawlins [29] (except the half-plane in that work occupies $y = 0$, $x < 0$). It is also noted that Figures 2 and 4 in Rawlins [29] have been transposed.

Figures 3.12-3.15 show the far-field when $\theta_o = \pi/2$ and $\beta_1 = \beta_2 = 0.5 - i$. Figure 3.13 is identical to Figure 2.9 as expected. The modulus of the diffracted field in the shadow region in this case is shown in Figure 3.3. It can be seen that the noise in this region is reduced by the presence of a fluid flow. This is due to the fact that the effective admittance of the half-plane $\mathcal{B} = \beta(1 - M^2)^{-1/2}$ increases as $|M|$ increases. In effect, the half-plane becomes softer as $|M|$ increases. The equivalent graphs for

other values of $\beta_{1,2}$ are omitted due to there similarity to Figure 3.3.

Figures 3.16- 3.19 show the far-field when $\theta_o = \pi/2$ for a surface wave bearing half-plane $\beta_1 = \beta_2 = -i$. Figure 3.17 is for the case of a still fluid and is identical to Figure 2.6 . In the trailing edge situation there is no apparent difference between the case where a wake is present (Figure 3.18) and the case where no wake is assumed (Figure 3.19). This is due to the fact that for these parameter values the value of C is small.

The semi-rigid half-plane problem is re-examined in Figures 3.20-3.27, this time in the presence of fluid flow. Figures 3.20-3.23 are for an angle of incidence $\theta_o = \pi/2$ and in Figures 3.24-3.27 it has been assumed that $\theta_o = \pi/4$. For these latter graphs the interference between the incident wave and the reflected wave is extended to the region $0 < \theta < 3\pi/4$. It is also noted that for given values of β_1, β_2 and θ_o the magnitude of the oscillations in this region of interference have until now shown little dependence on M. However, in Figures 3.24 and 3.25 this is clearly not the case. These oscillations about the incident wave magnitude of unity are of the order $|\Psi_r|$ which is given by (3.66). Therefore, the reason for this behaviour is that in Figure 3.24, $|\Psi_r| = 0.20$ but in Figure 3.25, $|\Psi_r| = 0.88$.

It is of interest to consider the half-plane as a noise barrier and thus to examine the effects of flow to the sound in the shadow region. It can be seen that the magnitude of the sound diffracted into the shadow region is reduced by the presence of flow in comparison to Figures 2.17 and 2.18. Again, the trailing edge situation is the most efficient at minimising the noise in this region.

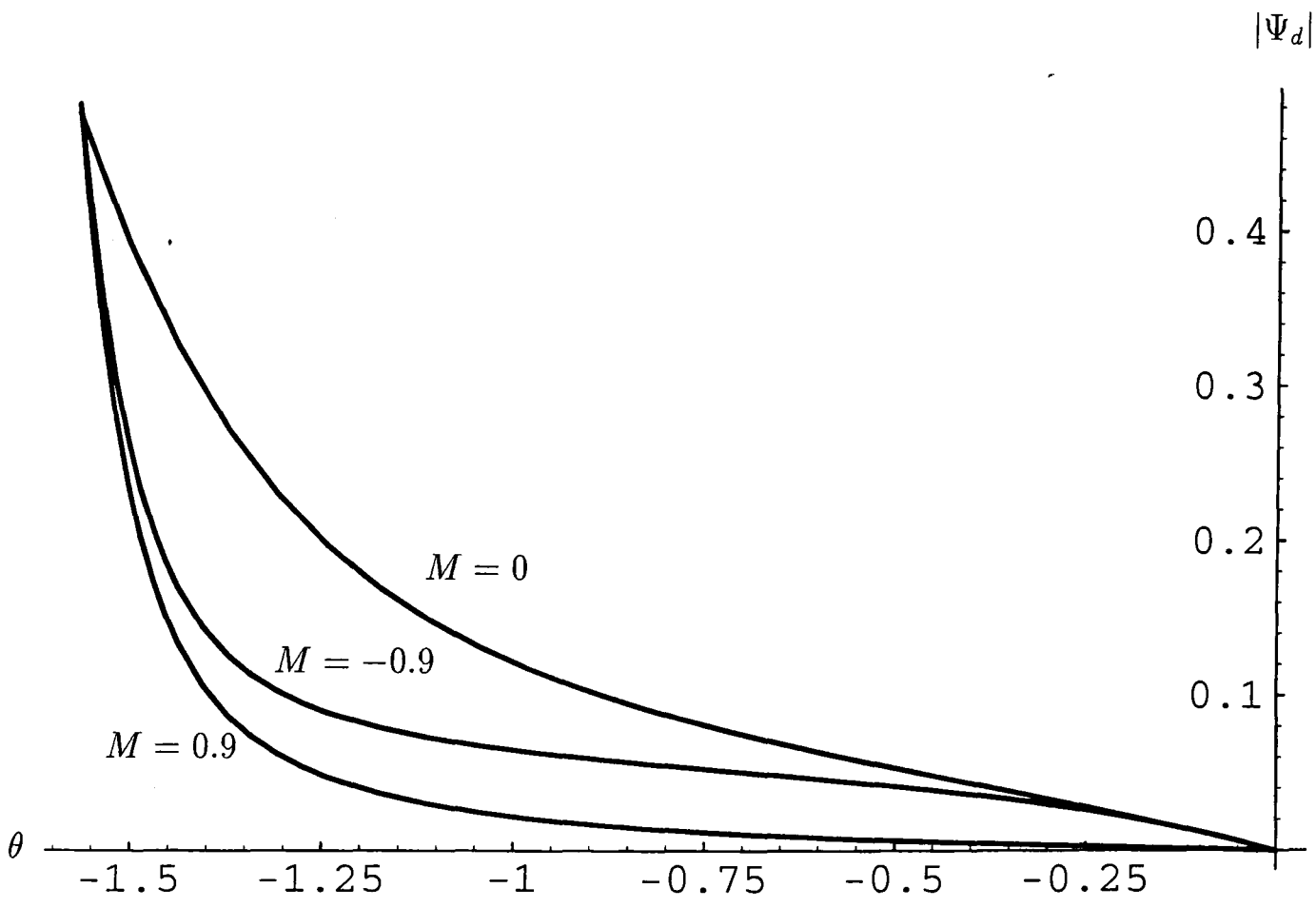

Figure 3.3: The shadow region of a half-plane in a moving fluid, $\beta_1 = \beta_2 = 0.5 - i$.

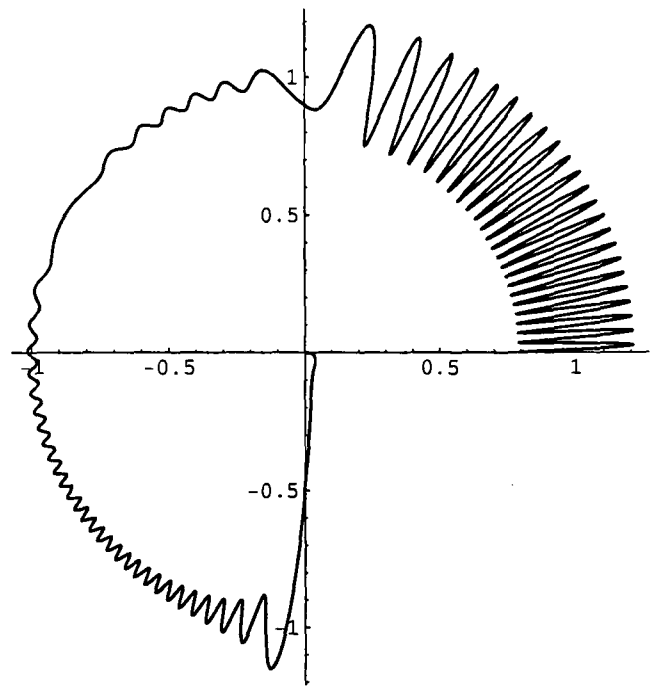

Figure 3.4: $\theta_o = \pi/2$, $\beta_1 = \beta_2 = 2/3$, $M = -0.9$.

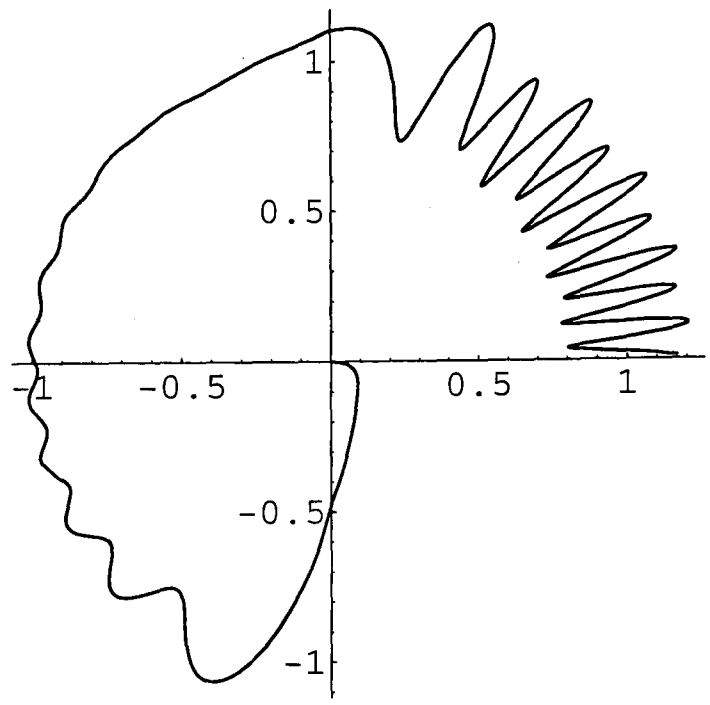

Figure 3.5: $\theta_o = \pi/2$, $\beta_1 = \beta_2 = 2/3$, $M = 0$.

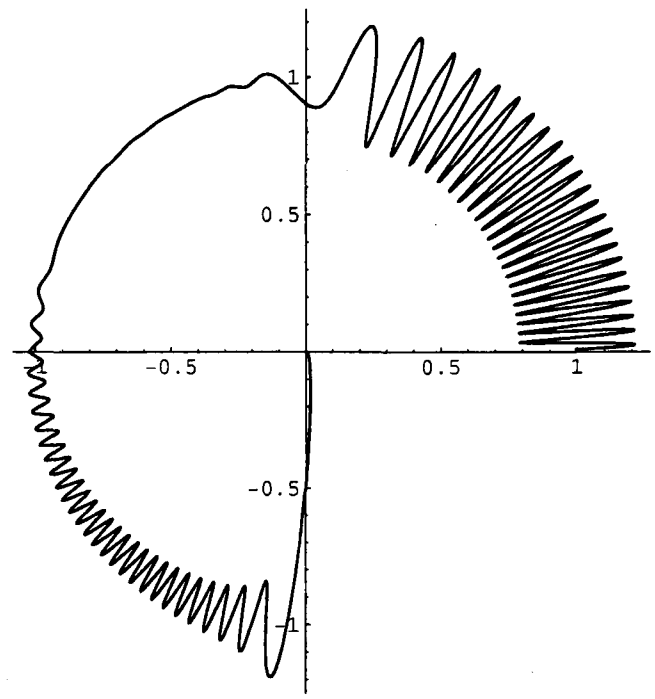

Figure 3.6: $\theta_o = \pi/2$, $\beta_1 = \beta_2 = 2/3$, $M = 0.9$.

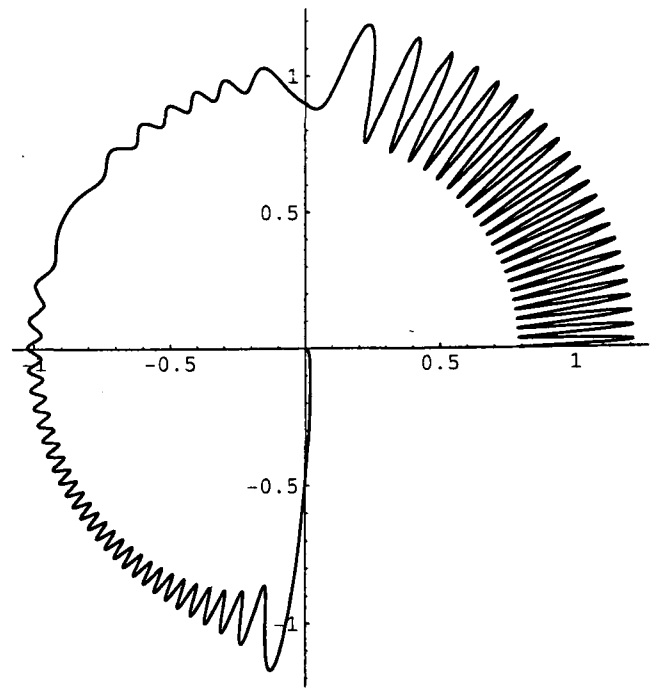

Figure 3.7: $\theta_o = \pi/2$, $\beta_1 = \beta_2 = 2/3$, $M = 0.9, C = 0$.

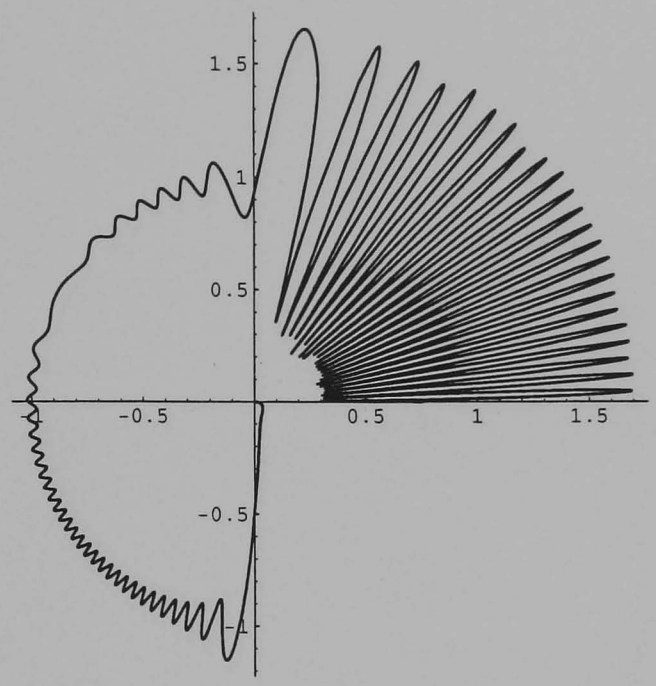

Figure 3.8: $\theta_o = \pi/2$, $\beta_1 = \beta_2 = 1/(0.5+i)$, $M = -0.9$.

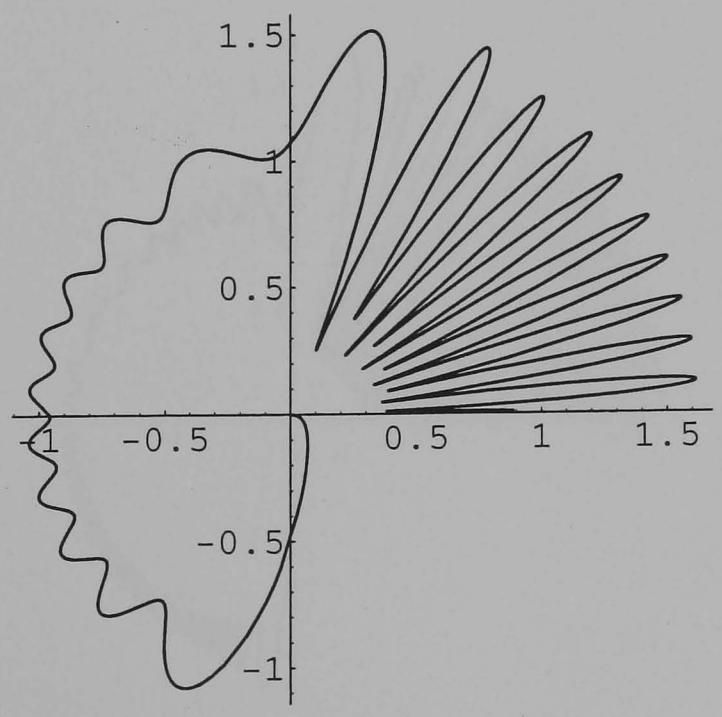

Figure 3.9: $\theta_o = \pi/2$, $\beta_1 = \beta_2 = 1/(0.5+i)$, $M = 0$.

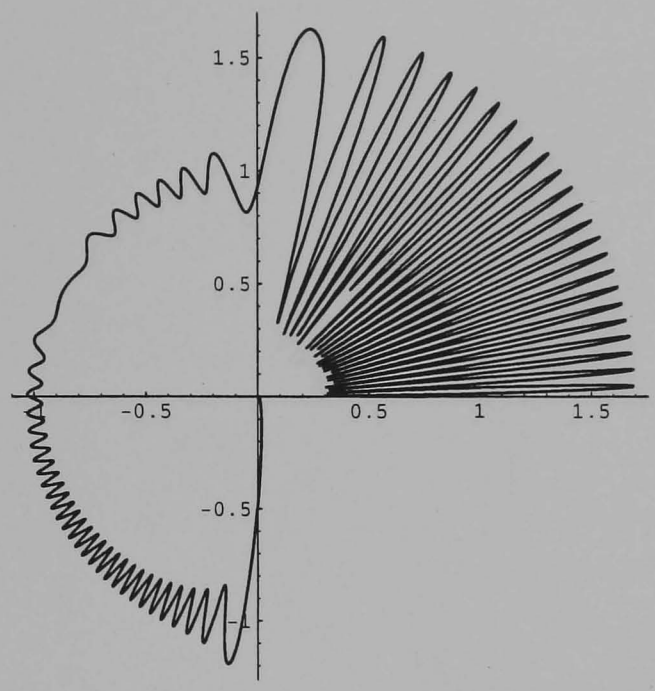

Figure 3.10: $\theta_o = \pi/2$, $\beta_1 = \beta_2 = 1/(0.5+i)$, $M = 0.9$.

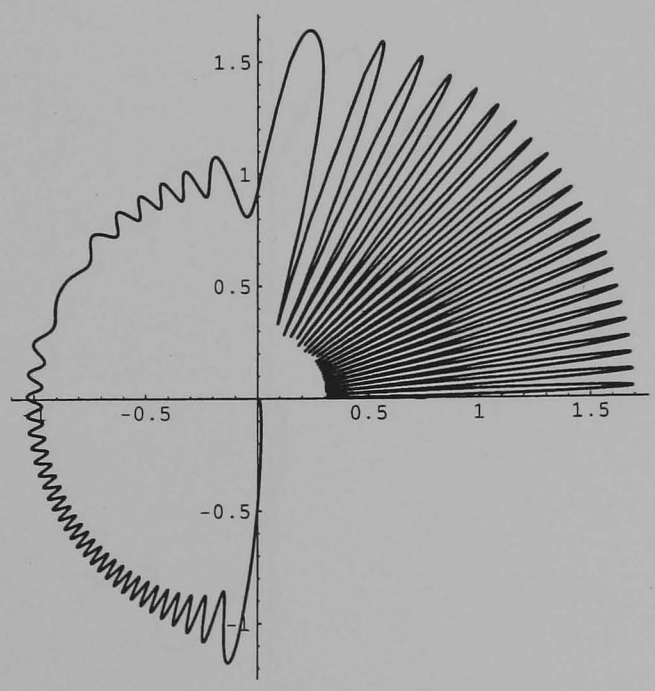

Figure 3.11: $\theta_o = \pi/2$, $\beta_1 = \beta_2 = 1/(0.5+i)$, $M = 0.9, C = 0$.

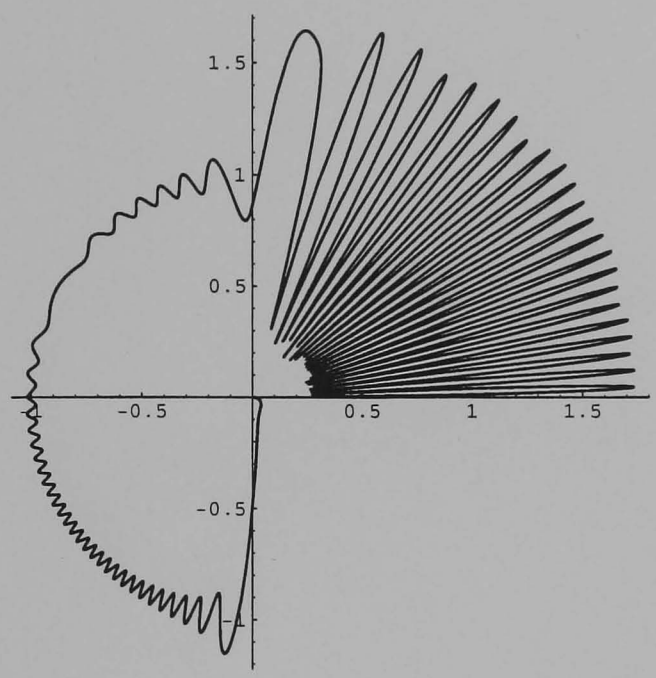

Figure 3.12: $\theta_o = \pi/2$, $\beta_1 = \beta_2 = 0.5 - i$, $M = -0.9$.

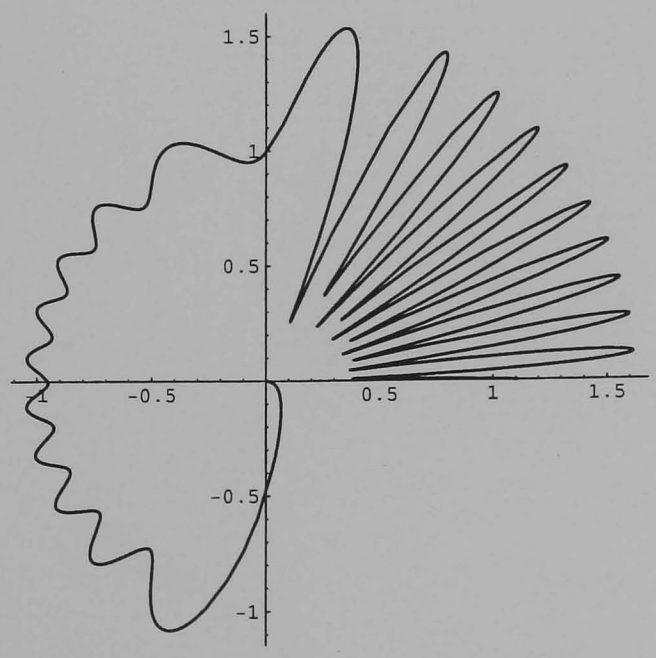

Figure 3.13: $\theta_o = \pi/2$, $\beta_1 = \beta_2 = 0.5 - i$, $M = 0$.

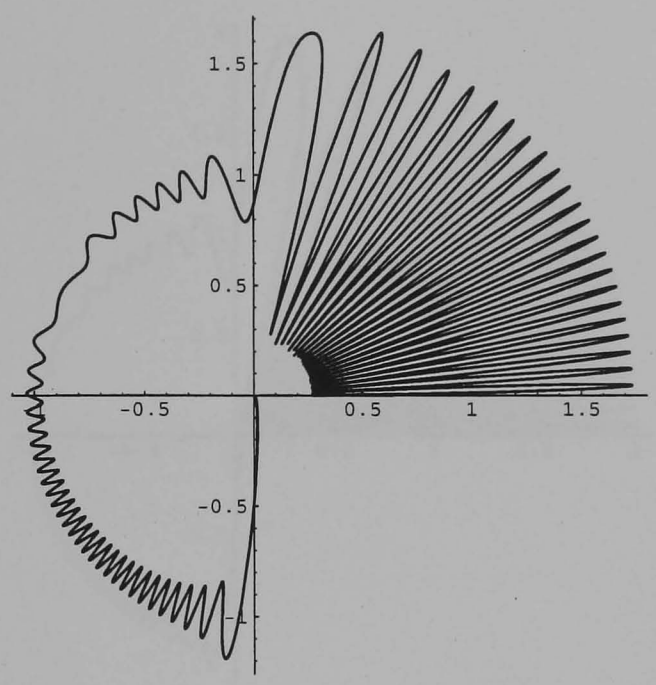

Figure 3.14: $\theta_o = \pi/2$, $\beta_1 = \beta_2 = 0.5 - i$, $M = 0.9$.

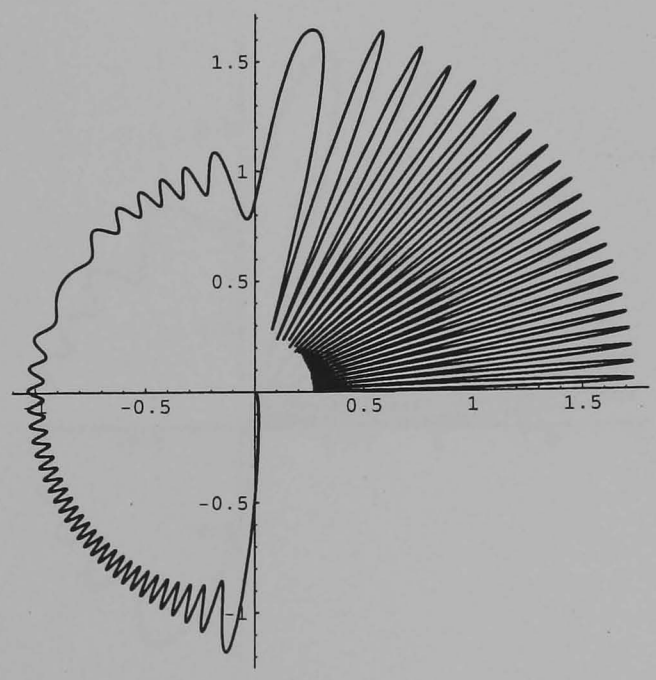

Figure 3.15: $\theta_o = \pi/2$, $\beta_1 = \beta_2 = 0.5 - i$, $M = 0.9, C = 0$.

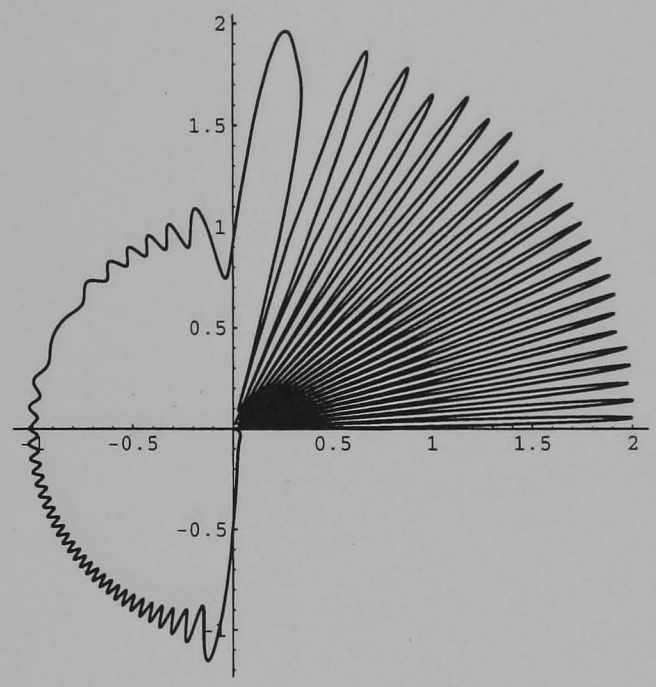

Figure 3.16: $\theta_o = \pi/2$, $\beta_1 = \beta_2 = -i$, $M = -0.9$.

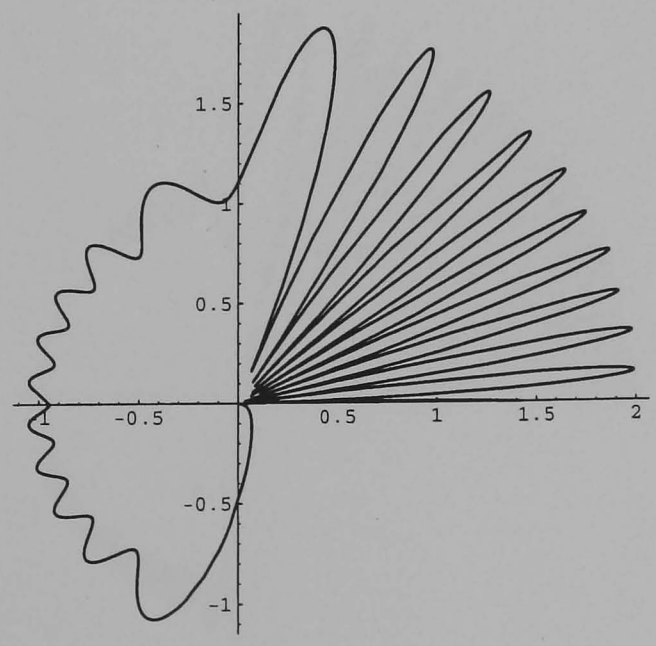

Figure 3.17: $\theta_o = \pi/2$, $\beta_1 = \beta_2 = -i$, $M = 0$.

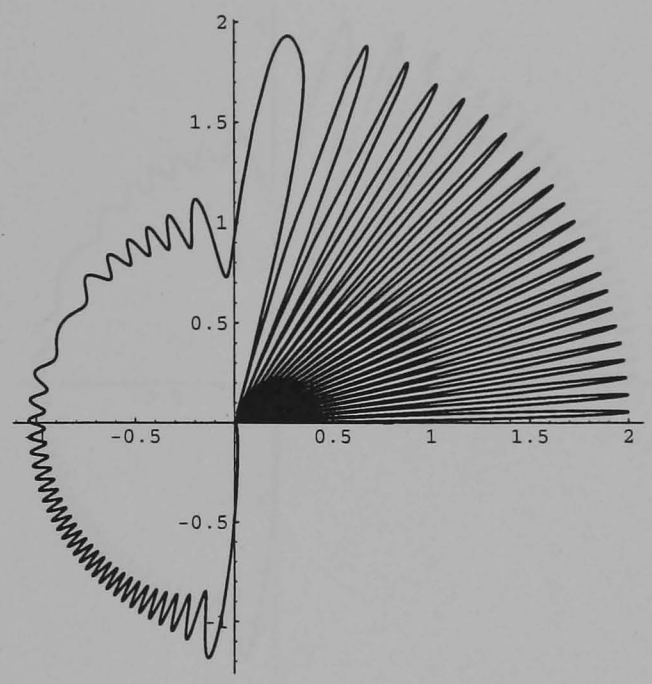

Figure 3.18: $\theta_o = \pi/2$, $\beta_1 = \beta_2 = -i$, $M = 0.9$.

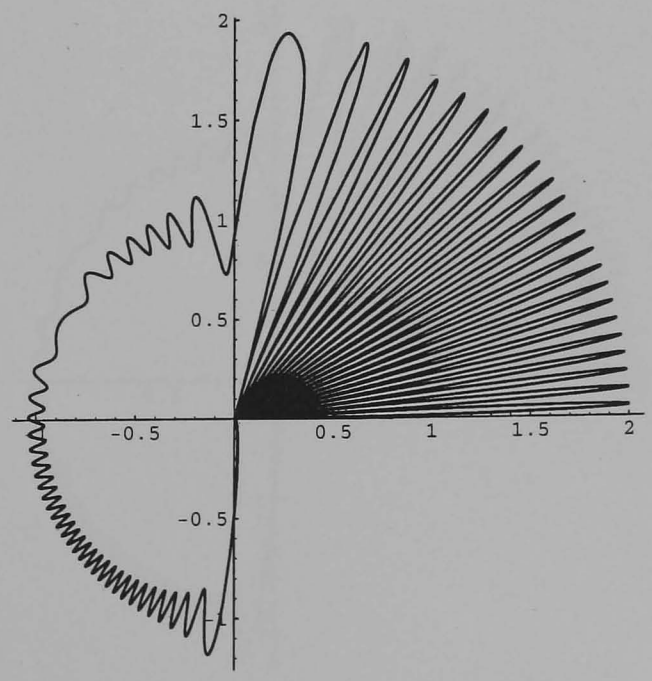

Figure 3.19: $\theta_o = \pi/2$, $\beta_1 = \beta_2 = -i$, $M = 0.9, C = 0$.

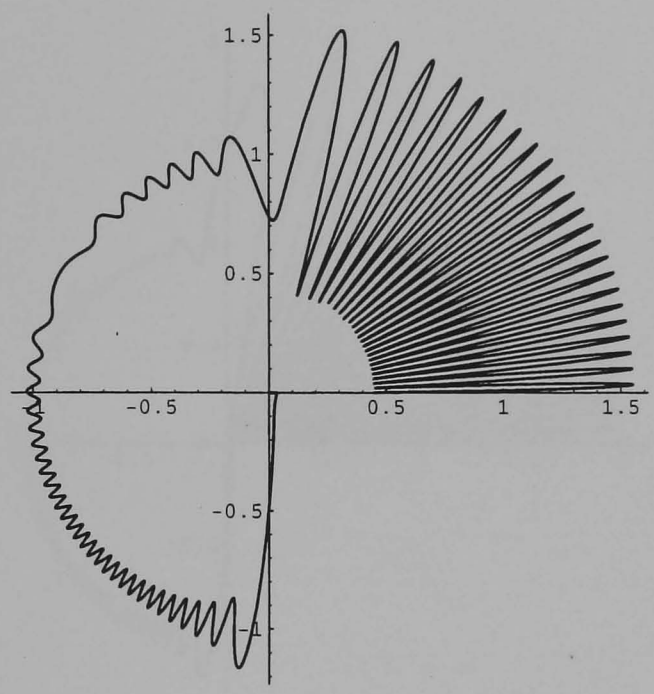

Figure 3.20: $\theta_o = \pi/2$, $\beta_1 = 1.5, \beta_2 = 0$, $M = 0.9, C = 0$.

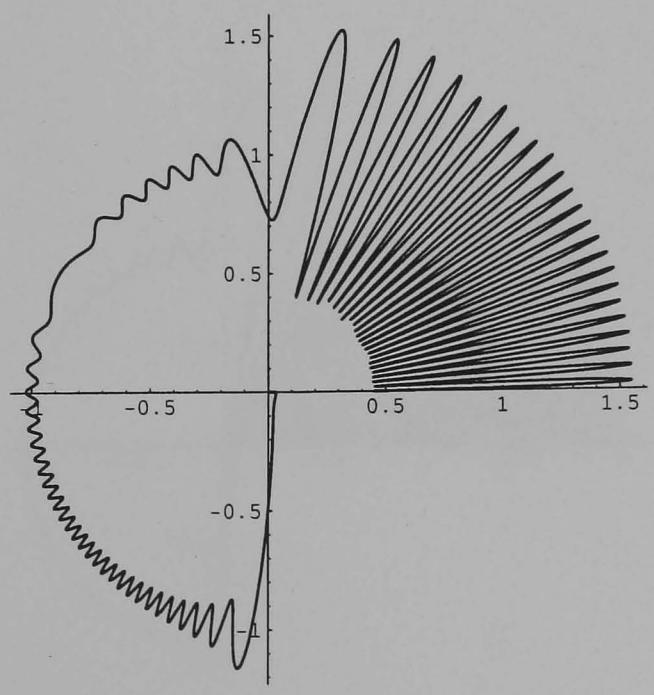

Figure 3.21: $\theta_o = \pi/2$, $\beta_1 = 1.5, \beta_2 = 0$, $M = -0.9$.

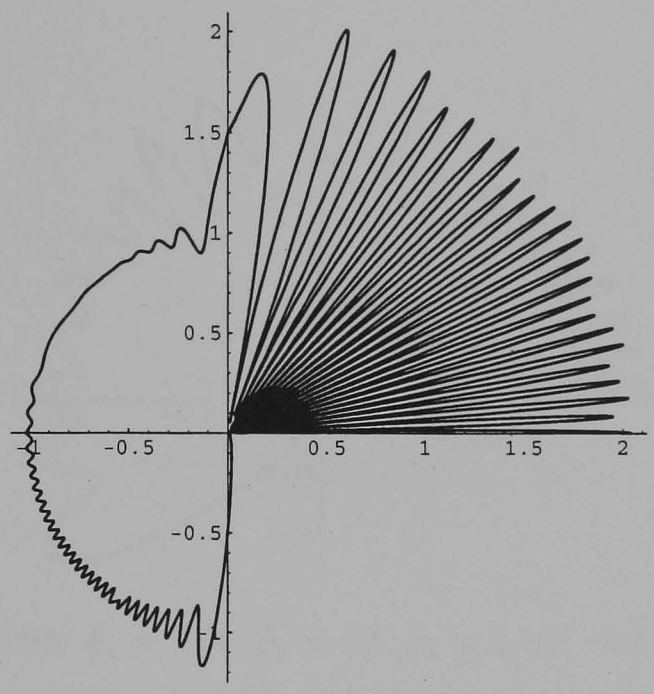

Figure 3.22: $\theta_o = \pi/2$, $\beta_1 = 0, \beta_2 = 1.5$, $M = 0.9, C = 0$.

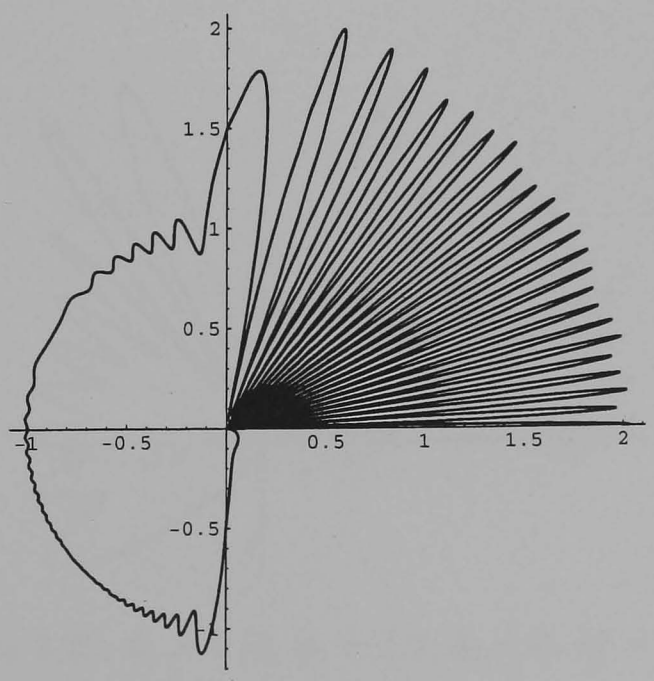

Figure 3.23: $\theta_o = \pi/2$, $\beta_1 = 0, \beta_2 = 1.5$, $M = -0.9$.

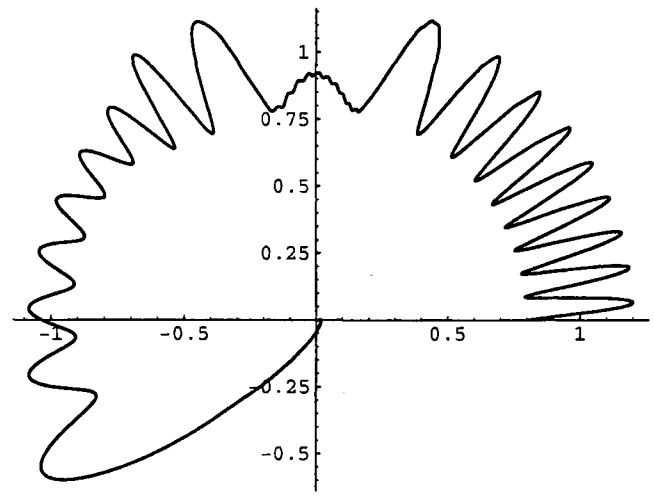

Figure 3.24: $\theta_o = \pi/4$, $\beta_1 = 1.5, \beta_2 = 0$, $M = 0.9, C = 0$.

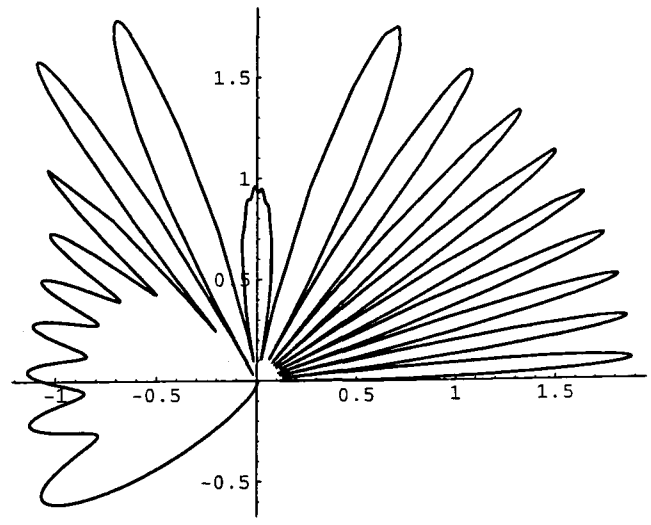

Figure 3.25: $\theta_o = \pi/4$, $\beta_1 = 1.5, \beta_2 = 0$, $M = -0.9$.

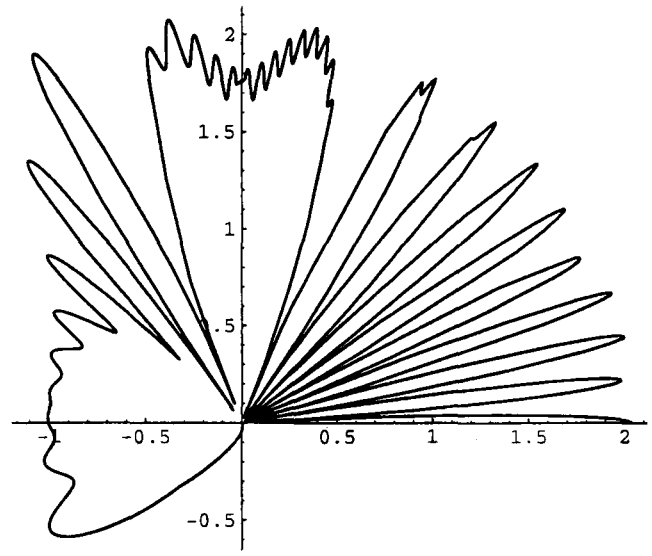

Figure 3.26: $\theta_o = \pi/4$, $\beta_1 = 0, \beta_2 = 1.5$, $M = 0.9, C = 0$.

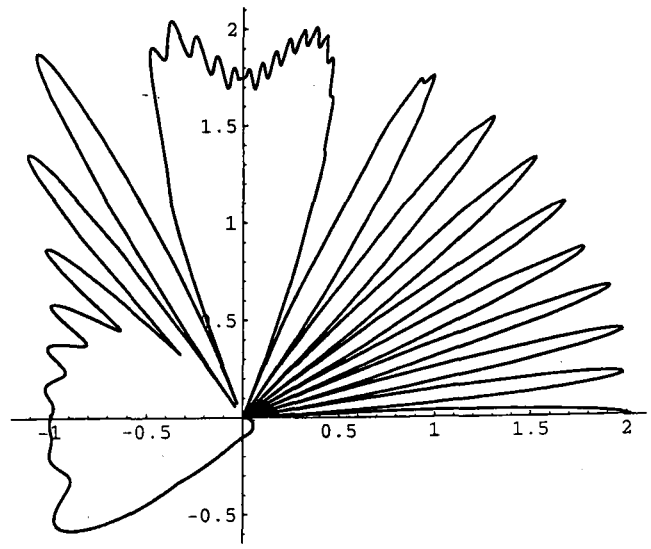

Figure 3.27: $\theta_o = \pi/4$, $\beta_1 = 0, \beta_2 = 1.5$, $M = -0.9$.

3.8 Conclusions

The problem of a plane wave incident on a half-plane in a moving fluid has been solved without restriction on the impedance parameters of the half-plane. In particular, both absorbent and inductive half-planes can be considered with incident plane or surface waves. Moreover, the solution is valid for subsonic values of the Mach number M, and taking $M = 0$ reduces the solution to that of a half-plane in a still fluid.

The solution contains an explicit factorisation of the matrix kernel using the Wiener-Hopf-Hilbert technique. Asymptotic expressions for the far-field were obtained leading to graphical results, which agree with Rawlins [29], and results from Chapter 2.

The half-plane in a moving fluid problem has been solved without restriction on β_1 and β_2. Further work could be done therefore on an inductive half-plane in a moving fluid. An examination could be carried out on the surface waves arising on the upper and lower surfaces of the half-plane similar to those in Chapter 2. Moreover, results for an incident surface wave can be obtained from the work in Chapter 3. A more complicated fluid problem is one where the fluid speed differs in the different halves of the plane. This problem is not solvable by the Maliuzhinets method, which assumes a Sommerfeld integral representation of the field throughout the entire plane.

A problem with more practical applications is one of a strip with an absorbent tip in a moving fluid. This would be a model for an aeroplane wing and has the advantage of being cheaper to construct than a strip with faces entirely coated in absorbent materials. Since the problem is governed by the conditions at the diffracting edge,

one needs only to consider an absorbent coating in the vicinity of the edge. The work of the present chapter would act as a first order approximation when the length of the absorbent tip is large.

The results obtained here could also be applied to the problem of the radiation of high frequency sound from a circular cylinder in a moving fluid (see Munt [25]). This is of practical importance as a model of a jet engine in motion. One could investigate noise shielding by examining the effects of lining the cylinder with absorbent materials. To high frequency sound, the edge of the cylinder is locally plane and an application of Keller's geometrical theory of diffraction would give an approximate answer to a mathematically insoluble problem.

Chapter 4

Radiation from an inductive wave-guide

4.1 Introduction

The problem considered here is of an electromagnetically radiating parallel plate waveguide where the inside walls are inductively loaded and the outside walls are capacitively loaded. This mathematical problem serves as a model for an inductively loaded horn antenna. Expressions are obtained for the reflection coefficient at the waveguide mouth and far-field radiation diagrams.

Useful information about the properties of various radiating structures can often be obtained from exact solutions of simple canonical problems. A canonical problem for an interesting antenna is the impedance-walled structure shown in Figure 4.1. The incident field is taken to be lowest order TM wave, proceeding to the left in the waveguide region, with the parameters a, β_1, and β_2 chosen so that only this TM wave propagates. When β_1 and β_2 are purely inductive, that is β_1 and β_2 purely imaginary, so that a surface wave can propagate along the inside walls of the duct a model for an impedance horn is obtained. The imposition of the $\pm\beta$ impedance condition on

each waveguide half plane means that one surface of each half plane will then support a surface wave (inductive condition), whilst the other cannot (capacitive condition). Thus the investigation is that of an inductively loaded open waveguide.

In Section 4.2 the mathematical boundary value problem is formulated. The problem is then reduced to a matrix Wiener-Hopf equation in Section 4.3. The factorisation of the Wiener-Hopf matrix kernel is carried out in Section 4.4 by the Wiener-Hopf-Hilbert method. It was thought that the Wiener-Hopf-Hilbert method would be inapplicable due to the poles contained in the matrix kernel. These poles correspond to the modes that propagate in the duct region. However, this problem is overcome to obtain an explicit factorisation of the matrix. In Section 4.5 expressions are obtained for the field in the different regions. These are simplified in Section 4.6 where the special case of a rigid wave-guide is examined. Conclusions are drawn and future work discussed in Section 4.7.

4.2 Formulation of the Boundary Value Problem

The configuration to be considered is shown in Figure 4.1. A TM wave is incident from $x = \infty$ in the parallel plate region, and the problem is to find the radiated and reflected fields. A time dependence of $e^{-i\omega t}$ is assumed and suppressed henceforth. Although it is clear that $\beta_{1,2} = iX_{1,2}$ where $X_{1,2} \geq 0$, so that surface waves can propagate on the inner walls of the duct, this notation shall be introduced later on in the solution for convenience.

To begin with, a brief reminder of the equations governing electromagnetic wave

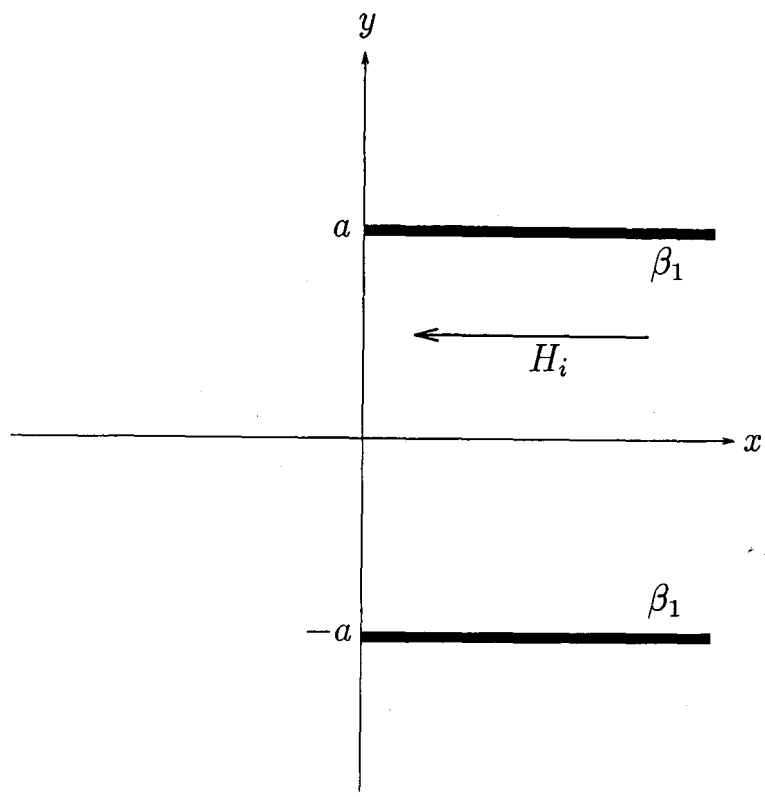

Figure 4.1: An impedance loaded wave-guide.

propagation is given. A comprehensive guide can be found in Jones [16]. The magnetic intensity $\mathbf{H}$ and electric intensity $\mathbf{E}$ can be represented by Maxwell's equations

$$\text{curl}\mathbf{E} = i\mu_o\omega\mathbf{H}, \quad \text{curl}\mathbf{H} = -i\epsilon_o\omega\mathbf{E},$$

where ϵ_o is the dielectric constant and μ_o is the permeability. If a transverse magnetic (TM) polarisation is assumed, so that the magnetic field has no component in the direction of propagation, then only three field components (E_x, E_y and H_z) are non-zero. They satisfy

$$E_x = \frac{i}{\omega\epsilon_o}\frac{\partial H_z}{\partial y}, \quad E_y = \frac{-i}{\omega\epsilon_o}\frac{\partial H_z}{\partial x}, \tag{4.1}$$

$$\frac{\partial^2 H_z}{\partial x^2} + \frac{\partial^2 H_z}{\partial y^2} + k^2 H_z = 0, \quad k = \omega\sqrt{\epsilon_o\mu_o}.$$

At $y = a$ the fields satisfy the impedance boundary condition

$$\frac{E_x}{H_z} = Z_1.$$

Using (4.1) this can be written in the form

$$\frac{\partial H_z}{\partial y}(x, a_\pm) + ik\beta_1 H_z(x, a_\pm) = 0,$$

where $k\beta_1 = \omega\epsilon_o Z_1$. At $y = -a$ the fields satisfy

$$\frac{E_x}{H_z} = Z_2.$$

Writing $k\beta_2 = \omega\epsilon_o Z_2$ and using (4.1) allows this to be written in the form

$$\frac{\partial H_z}{\partial y}(x, -a_\pm) - ik\beta_2 H_z(x, -a_\pm) = 0.$$

The problem can be written as the solution of the Helmholtz equation

$$\frac{\partial^2 H_z}{\partial x^2} + \frac{\partial^2 H_z}{\partial y^2} + k^2 H_z = 0, \tag{4.2}$$

subject to the boundary conditions

$$\frac{\partial H_z}{\partial y}(x, a_\pm) + ik\beta_1 H_z(x, a_\pm) = 0, \quad x > 0, \tag{4.3}$$

$$\frac{\partial H_z}{\partial y}(x, -a_\pm) - ik\beta_2 H_z(x, -a_\pm) = 0, \quad x > 0. \tag{4.4}$$

The field must also satisfy the continuity conditions

$$\frac{\partial H_z}{\partial y}(x, \pm a_+) = \frac{\partial H_z}{\partial y}(x, \pm a_-), \quad x < 0, \tag{4.5}$$

$$H_z(x, \pm a_+) = H_z(x, \pm a_-), \quad x < 0, \tag{4.6}$$

and the edge condition

$$H_z = O(1), \quad \nabla H_z = O(r^{-1/2}), \quad \text{as } r \to 0. \tag{4.7}$$

Combined with the condition that the diffracted field be outgoing at infinity, these conditions ensure that the boundary value problem has a unique solution.

4.3 Reduction to a Matrix Wiener-Hopf Equation

As before, the Fourier transform is applied to the wave equation (4.2) to give

$$\frac{d^2\hat{H}_z}{dy^2} + \kappa^2 \hat{H}_z = 0. \tag{4.8}$$

The branch of $\kappa = (k^2 - \alpha^2)^{1/2}$ is chosen such that $\kappa = +k$ for $\alpha = 0$. The incident field is written as

$$H_i = \phi_o(y, \kappa_o) e^{-i\alpha_o x}, \tag{4.9}$$

where

$$\phi_o(y, \kappa) = \cos\kappa(y-a) - \frac{ik\beta_1}{\kappa} \sin\kappa(y-a), \tag{4.10}$$

and α_o is chosen so that only the dominant order TM wave propagates. A discussion of the incident field is given in Appendix B. A solution of the boundary value problem can now be written as

$$H_z = \int_{-\infty}^{\infty} A(\alpha) e^{i\alpha x + i\kappa(y-a)}\, d\alpha, \qquad y \geq a, \tag{4.11}$$

$$= H_i + \int_{-\infty}^{\infty} B(\alpha) e^{i(\alpha x + \kappa y)} + C(\alpha) e^{i(\alpha x - \kappa y)}\, d\alpha, \qquad -a < y < a, \tag{4.12}$$

$$= \int_{-\infty}^{\infty} D(\alpha) e^{i\alpha x - i\kappa(y+a)}\, d\alpha, \qquad y \leq -a. \tag{4.13}$$

Applying the boundary conditions (4.3) and (4.4) leads to

$$(\kappa + k\beta_1)A(\alpha) = u_1(\alpha), \tag{4.14}$$

$$(\kappa + k\beta_2)D(\alpha) = u_2(\alpha), \tag{4.15}$$

where $u_1(\alpha)$ and $u_2(\alpha)$ are analytic in the upper half of the α-plane, $\mathrm{Im}(\alpha) \geq 0$. Now, from (4.3)-(4.6) it can be seen that $\partial H_z/\partial y + k\beta_1 H_z$ and $\partial H_z/\partial y - k\beta_2 H_z$ must be continuous across $y = a$ and $y = -a$ respectively for all x. Applying this to the scattered field gives

$$A(\alpha)(\kappa + k\beta_1) = B(\alpha)(\kappa + k\beta_1)e^{i\kappa a} + C(\alpha)(-\kappa + k\beta_1)e^{-i\kappa a}, \tag{4.16}$$

$$D(\alpha)(\kappa + k\beta_2) = B(\alpha)(-\kappa + k\beta_2)e^{-i\kappa a} + C(\alpha)(\kappa + k\beta_2)e^{i\kappa a}. \tag{4.17}$$

These can be written as

$$A(\alpha) = B(\alpha)e^{i\kappa a} + \left(\frac{-\kappa + k\beta_1}{\kappa + k\beta_1}\right) C(\alpha)e^{-i\kappa a}, \tag{4.18}$$

$$D(\alpha) = \left(\frac{-\kappa + k\beta_2}{\kappa + k\beta_2}\right) B(\alpha)e^{-i\kappa a} + C(\alpha)e^{i\kappa a}. \tag{4.19}$$

Applying the continuity condition (4.6) leads to

$$-A(\alpha) + B(\alpha)e^{i\kappa a} + C(\alpha)e^{-i\kappa a} = l_2(\alpha) + \frac{\phi_o(a, \kappa_o)}{2\pi i(\alpha + \alpha_o)}, \tag{4.20}$$

$$-D(\alpha) + B(\alpha)e^{-i\kappa a} + C(\alpha)e^{i\kappa a} = l_1(\alpha) + \frac{\phi_o(-a, \kappa_o)}{2\pi i(\alpha + \alpha_o)}, \tag{4.21}$$

where $l_1(\alpha)$ and $l_2(\alpha)$ are analytic in the lower half of the complex plane, $\mathrm{Im}(\alpha) \leq 0$. It is also noted that $\alpha = -\alpha_o$ lies in the lower half plane (Figure 4.2). Eliminating $A(\alpha)$ and $D(\alpha)$ from equations (4.18)-(4.21) gives

$$C(\alpha)e^{-i\kappa a} - \left(\frac{-\kappa + k\beta_1}{\kappa + k\beta_1}\right) C(\alpha)e^{-i\kappa a} = l_2(\alpha) + \frac{\phi_o(a, \kappa_o)}{2\pi i(\alpha + \alpha_o)},$$

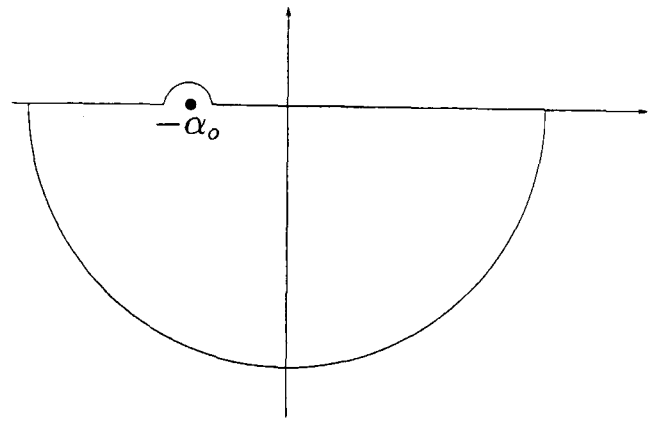

Figure 4.2: The complex plane.

$$\kappa\left\{B(\alpha)e^{-i\kappa a}-\left(\frac{-\kappa+k\beta_2}{\kappa+k\beta_2}\right)\ B(\alpha)e^{-i\kappa a}\right\}=l_1(\alpha)+\frac{\phi_o(-a,\kappa_o)}{2\pi i(\alpha+\alpha_o)}.$$

These can be written in the form

$$C(\alpha)=\frac{e^{i\kappa a}(\kappa+k\beta_1)}{2\kappa}\ l_2(\alpha)+\frac{e^{i\kappa a}(\kappa+k\beta_1)}{2\kappa}\frac{\phi_o(a,\kappa_o)}{2\pi i(\alpha+\alpha_o)}, \tag{4.22}$$

$$B(\alpha)=\frac{e^{i\kappa a}(\kappa+k\beta_2)}{2\kappa}\ l_1(\alpha)+\frac{e^{i\kappa a}(\kappa+k\beta_2)}{2\kappa}\frac{\phi_o(-a,\kappa_o)}{2\pi i(\alpha+\alpha_o)}. \tag{4.23}$$

Combining these with (4.14) and (4.15) and writing $\psi = e^{i\kappa a}$ leads to the matrix Wiener-Hopf equation

$$G(\alpha)l(\alpha)=u(\alpha)+G(\alpha)\frac{P}{(\alpha+\alpha_o)}, \tag{4.24}$$

where

$$G(\alpha)=\frac{1}{2\kappa}\begin{pmatrix}(\kappa+k\beta_1)(\kappa+k\beta_2)\psi^2 & k^2\beta_1^2-\kappa^2\\ k^2\beta_2^2-\kappa^2 & (\kappa+k\beta_1)(\kappa+k\beta_2)\psi^2\end{pmatrix}, \tag{4.25}$$

$$P=\frac{-1}{2\pi i}\begin{pmatrix}\phi_o(-a,\kappa_o)\\ \phi_o(a,\kappa_o)\end{pmatrix},\quad l(\alpha)=\begin{pmatrix}l_1\\ l_2\end{pmatrix},\quad u(\alpha)=\begin{pmatrix}u_1\\ u_2\end{pmatrix}.$$

Define $D(\alpha)$ such that

$$D^2(\alpha)=\det G(\alpha)=\frac{\psi^4(\kappa+k\beta_1)^2(\kappa+k\beta_2)^2-(k^2\beta_1^2-\kappa^2)(k^2\beta_2^2-\kappa^2)}{4\kappa^2},$$

and define $K(\alpha)$ by

$$G(\alpha) = D(\alpha)K(\alpha). \tag{4.26}$$

Then

$$K(\alpha) = \frac{(\kappa + k\beta_1)(\kappa + k\beta_2)\psi^2}{D(\alpha)} \begin{pmatrix} 1 & \left(\frac{k\beta_1 - \kappa}{k\beta_2 + \kappa}\right)\psi^{-2} \\ \left(\frac{k\beta_2 - \kappa}{k\beta_1 + \kappa}\right)\psi^{-2} & 1 \end{pmatrix}, \tag{4.27}$$

and

$$\det K(\alpha) = 1.$$

The factorisation of $G(\alpha)$ now follows directly from the factorisation of $K(\alpha)$ and $D(\alpha)$.

4.4 Factorisation of the Matrix Kernel

Factorisation of $K(\alpha)$

The requirement is that $K(\alpha) = U(\alpha)L^{-1}(\alpha)$ where $L(\alpha)$ is analytic everywhere except $k < \alpha < \infty$, $\mathrm{Im}(\alpha) = 0$ and $U(\alpha)$ is analytic everywhere except $-\infty < \alpha < -k$, $\mathrm{Im}(\alpha) = 0$. Then it is not difficult to see that

$$\left.\begin{aligned} K^+(\xi) &= U^+(\xi)L^{-1}(\xi) \\ K^-(\xi) &= U^-(\xi)L^{-1}(\xi) \end{aligned}\right\} -\infty < \xi < -k \tag{4.28}$$

since L is continuous across this region. Eliminating $L^{-1}(\xi)$ gives

$$U^+(\xi) = K^+(\xi)[K^{-1}(\xi)]^- U^-(\xi), \tag{4.29}$$

where F^+ denotes values of F on the upper side of the cut and F^- denotes values of F on the lower side of the cut. From equation (4.27) it follows that

$$K^+(\xi) = \frac{(k\beta_1 + i|\kappa|)(k\beta_2 + i|\kappa|)e^{-|\kappa|a}}{D^+(\alpha)} \begin{pmatrix} 1 & \left(\frac{k\beta_1 - i|\kappa|}{k\beta_2 + i|\kappa|}\right)e^{2|\kappa|a} \\ \left(\frac{k\beta_2 - i|\kappa|}{k\beta_1 + i|\kappa|}\right)e^{2|\kappa|a} & 1 \end{pmatrix}, \tag{4.30}$$

$$[K^{-1}(\xi)]^- = \frac{(k\beta_1 - i|\kappa|)(k\beta_2 - i|\kappa|)e^{|\kappa|a}}{D^-(\alpha)} \begin{pmatrix} 1 & -\left(\frac{k\beta_1+i|\kappa|}{k\beta_2-i|\kappa|}\right) e^{-2|\kappa|a} \\ -\left(\frac{k\beta_2+i|\kappa|}{k\beta_1-i|\kappa|}\right) e^{-2|\kappa|a} & 1 \end{pmatrix}, \tag{4.31}$$

Equation (4.29) then becomes

$$U^+(\xi) = \frac{(k^2\beta_1^2+\kappa^2)(k^2\beta_2^2+\kappa^2)}{D^+D^-} \begin{pmatrix} 0 & \left(\frac{k\beta_1-i|\kappa|}{k\beta_2+i|\kappa|}\right) e^{2|\kappa|a} - \left(\frac{k\beta_1+i|\kappa|}{k\beta_2-i|\kappa|}\right) e^{-2|\kappa|a} \\ \left(\frac{k\beta_2-i|\kappa|}{k\beta_1+i|\kappa|}\right) e^{2|\kappa|a} - \left(\frac{k\beta_2+i|\kappa|}{k\beta_1-i|\kappa|}\right) e^{-2|\kappa|a} & 0 \end{pmatrix} U^-(\xi).$$

Simplifying leads to

$$U^+(\xi) = \left\{ \frac{1}{(k^2\beta_1^2 + |\kappa|^2)(k^2\beta_2^2 + |\kappa|^2)} \right\}^{\frac{1}{2}} \begin{pmatrix} 0 & -i(k^2\beta_1^2 + |\kappa|^2) \\ -i(k^2\beta_2^2 + |\kappa|^2) & 0 \end{pmatrix} U^-(\xi).$$

This further simplifies to give

$$U^+(\xi) = \begin{pmatrix} 0 & -i\sqrt{\frac{k^2\beta_1^2+|\kappa|^2}{k^2\beta_2^2+|\kappa|^2}} \\ -i\sqrt{\frac{k^2\beta_2^2+|\kappa|^2}{k^2\beta_1^2+|\kappa|^2}} & 0 \end{pmatrix} U^-(\xi). \tag{4.32}$$

This equation was solved in Chapter 2 and has the following solution.

$$U(\alpha) = \begin{pmatrix} -[k+\alpha]^{-\frac{1}{4}}[W(\alpha)]^{\frac{1}{2}} & [k+\alpha]^{\frac{1}{4}}[W(\alpha)]^{\frac{1}{2}} \\ -[k+\alpha]^{-\frac{1}{4}}[W(\alpha)]^{-\frac{1}{2}} & -[k+\alpha]^{\frac{1}{4}}[W(\alpha)]^{-\frac{1}{2}} \end{pmatrix}, \tag{4.33}$$

where

$$W(\alpha) = \frac{\left(\sqrt{k+\alpha} + \sqrt{kB_1(+)}\right)\left(\sqrt{k+\alpha} + \sqrt{kB_1(-)}\right)}{\left(\sqrt{k+\alpha} + \sqrt{kB_2(+)}\right)\left(\sqrt{k+\alpha} + \sqrt{kB_2(-)}\right)}. \tag{4.34}$$

and $B_{1,2}(\pm) = 1 \pm \sqrt{1-\beta_{1,2}^2}$. The matrix $L(\alpha)$ can be found from the expression

$$L(\alpha) = K^{-1}(\alpha)U(\alpha).$$

Factorisation of $D(\alpha)$

The function $D(\alpha)$ can be written as

$$D(\alpha) = -\frac{(\kappa + k\beta_1)(\kappa + k\beta_2)}{2\kappa} \left\{ \frac{(k\beta_1 - \kappa)(k\beta_2 - \kappa)}{(k\beta_1 + \kappa)(k\beta_2 + \kappa)} - e^{4i\kappa a} \right\}^{1/2}. \tag{4.35}$$

Now, in Chapter 2 a factorisation was given for the function $d^n(\alpha)$ given by

$$d^n(\alpha) = \frac{\kappa + k\beta_n}{\kappa}. \tag{4.36}$$

Thus it remains only to factorise

$$\Delta(\alpha) = \frac{(k\beta_1 - \kappa)(k\beta_2 - \kappa)}{(k\beta_1 + \kappa)(k\beta_2 + \kappa)} - e^{4i\kappa a}. \tag{4.37}$$

Now, $\Delta(\alpha) \to 1$ as $|\alpha| \to \infty$. Applying Theorem C from Noble [27] produces

$$\Delta_+(\alpha) = \Delta(\alpha)^{1/2} \exp\left\{\frac{1}{2\pi i}\int_{-\infty}^{\infty} \frac{\log \Delta(\xi)}{\xi - \alpha} d\xi\right\}. \tag{4.38}$$

It now follows that the upper split function can be written in the form

$$D_+(\alpha) = \sqrt{\frac{k+\alpha}{2}}\, d_+^1(\alpha)\, d_+^2(\alpha)\Delta_+(\alpha)^{1/2}. \tag{4.39}$$

This completes the factorisation of $D(\alpha)$.

4.5 The Field in Different Regions

Having factorised the matrix kernel, the usual Wiener-Hopf arguments lead to

$$l(\alpha) = \left[\mathrm{I} - G_-^{-1}(\alpha)G_-(-\alpha_o)\right]\frac{P}{(\alpha + \alpha_o)}, \tag{4.40}$$

$$u(\alpha) = -G_+(\alpha)G_-(-\alpha_o)\frac{P}{(\alpha + \alpha_o)}. \tag{4.41}$$

The scattered field now reduces to

$$H_z(x,y) = \int_{-\infty}^{\infty} \frac{u_1(\alpha)}{\kappa + k\beta_1} e^{i(\alpha x + \kappa(y-a))} d\alpha, \qquad y \geq a, \tag{4.42}$$

$$= \int_{-\infty}^{\infty} \frac{\kappa + k\beta_1}{2\kappa}\left\{l_2(\alpha) - \frac{\phi_o(a,\kappa_o)}{2\pi i(\alpha + \alpha_o)}\right\} e^{i(\alpha x - \kappa(y-a))} d\alpha$$

$$+ \int_{-\infty}^{\infty} \frac{\kappa + k\beta_2}{2\kappa}\left\{l_1(\alpha) - \frac{1}{2\pi i(\alpha + \alpha_o)}\right\} e^{i(\alpha x + \kappa(y+a))} d\alpha, \quad -a < y < a, \tag{4.43}$$

$$= \int_{-\infty}^{\infty} \frac{u_2(\alpha)}{\kappa + k\beta_2} e^{i(\alpha x - \kappa(y+a))} d\alpha, \qquad y \leq a. \tag{4.44}$$

As in Chapters 2 and 3, the method of stationary phase is applied to the above integrals. The total far-field can now be written as

$$H_z(r,\theta) = 2i\sqrt{\frac{\pi}{2kr}}\left(\frac{\sin\theta}{\beta_1+\sin\theta}\right)u_1[k\cos\theta]e^{ikr+\frac{\pi i}{4}}, \quad y \geq a, \tag{4.45}$$

$$= -2i\sqrt{\frac{\pi}{2kr}}\left(\frac{\sin\theta}{\beta_2-\sin\theta}\right)u_2[k\cos\theta]e^{ikr+\frac{\pi i}{4}}, \quad y \leq a. \tag{4.46}$$

The field in the duct region is now considered. Using (4.18) and (4.19), the field in this region can be expressed in terms of the functions u_1 and u_2 thus

$$H_z(x,y) = \int_{-\infty}^{\infty}\left\{-\frac{u_1(\alpha)\psi(k\beta_2+\kappa)}{f(\alpha)} + \frac{u_2(\alpha)\psi^{-1}(k\beta_1-\kappa)}{f(\alpha)}\right\}e^{i(\alpha x+\kappa y)}d\alpha$$
$$+\int_{-\infty}^{\infty}\left\{\frac{u_1(\alpha)\psi^{-1}(k\beta_2-\kappa)}{f(\alpha)} - \frac{u_2(\alpha)\psi(k\beta_1+\kappa)}{f(\alpha)}\right\}e^{i(\alpha x-\kappa y)}d\alpha, \quad |y| < a. \tag{4.47}$$

In the above expression it has been assumed that

$$f(\alpha) = (k\beta_1-\kappa)(k\beta_2-\kappa)\psi^{-2} - (k\beta_1+\kappa)(k\beta_2+\kappa)\psi^2.$$

For $x > 0$ the contour of integration is closed in the upper half of the complex plane. The singularities in this region come from the zeros of $f(\alpha)$ which are denoted as $\alpha_n, n = 0,1,2...$ The residues at these poles give the waveguide modes that can propagate in the duct region.

$$R = 2\pi i\sum_{n=0}^{\infty}\frac{1}{f'(\alpha_n)}\Big\{-u_1(\alpha_n)\psi_n(k\beta_2+\kappa_n) + u_2(\alpha_n)\psi_n^{-1}(k\beta_1-\kappa_n)$$
$$+u_1(\alpha_n)\psi_n^{-1}(k\beta_2-\kappa_n) - u_2(\alpha_n)\psi_n(k\beta_1+\kappa_n)\Big\}, \quad |y| < a. \tag{4.48}$$

The terms in this expression represent the reflected field modes in the waveguide. The dominant surface wave reflected mode R_0 is given by

$$R_0 = \frac{2\pi i}{f'(\alpha_o)}\Big\{-u_1(\alpha_o)\psi_o(k\beta_2+\kappa_o) + u_2(\alpha_o)\psi_o^{-1}(k\beta_1-\kappa_o).$$
$$+u_1(\alpha_o)\psi_o^{-1}(k\beta_2-\kappa_o) - u_2(\alpha_o)\psi_o(k\beta_1+\kappa_o)\Big\}. \tag{4.49}$$

The dominant mode is of particular interest since this mode transports most of the acoustic energy down the wave-guide. The power that is transmitted out of the duct will be proportional to $1-|R|^2$ when only the dominant surface wave mode propagates in the semi-infinite duct.

4.6 A Rigid Duct

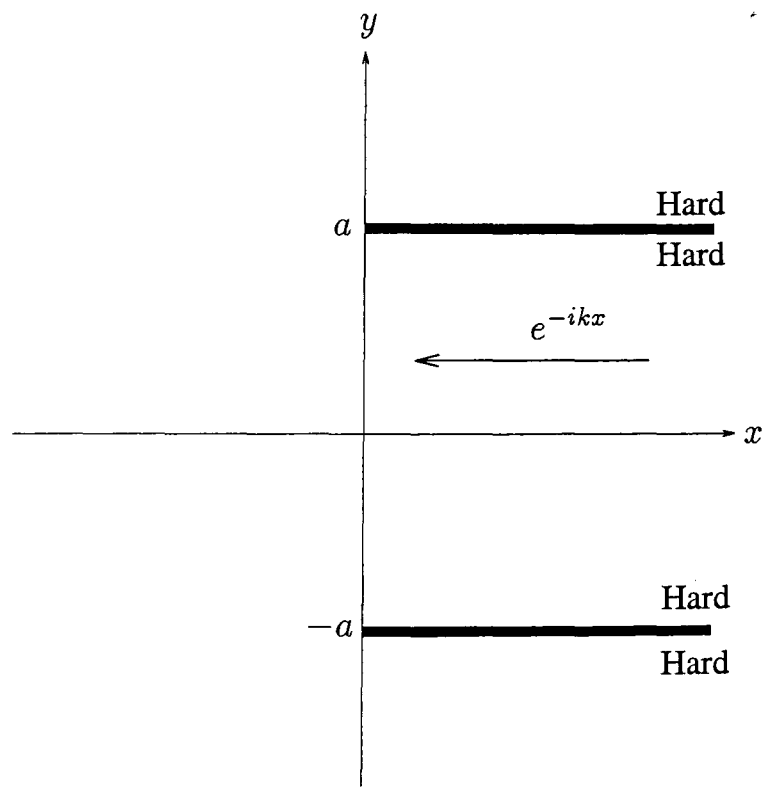

Figure 4.3: A rigid wave-guide.

In this section, the special case of a rigid duct is examined, as shown in Figure 4.3. By writing $\beta_1 = \beta_2 = 0$ the coupled Wiener-Hopf equations simplify to

$$u_1(\alpha) = \frac{\kappa}{2}(\psi^2 l_1(\alpha) - l_2(\alpha)) + \frac{\kappa}{4\pi i(\alpha+k)}(1-\psi^2),$$

$$u_2(\alpha) = \frac{\kappa}{2}(-l_1(\alpha) + \psi^2 l_2(\alpha)) + \frac{\kappa}{4\pi i(\alpha+k)}(1-\psi^2).$$

Upon making the substitutions $u_3 = u_1 + u_2, u_4 = u_1 - u_2, l_3 = l_1 + l_2$ and $l_4 = l_1 - l_2$ it becomes clear that $u_3(\alpha)$ and $u_4(\alpha)$ are analytic in the upper half plane whilst $l_3(\alpha)$ and $l_4(\alpha)$ are analytic in the lower half plane. Adding and subtracting the above equations yields

$$u_3(\alpha) = l_3(\alpha)\frac{\kappa}{2}(\psi^2 - 1) + \frac{\kappa(1-\psi^2)}{2\pi i(\alpha + k)}, \tag{4.50}$$

$$u_4(\alpha) = l_4(\alpha)\frac{\kappa}{2}(\psi^2 + 1). \tag{4.51}$$

Applying Liouville's theorem to (4.51) gives

$$u_3 = u_4 = 0.$$

This implies that $u_1 = u_2$ and $l_1 = l_2$. Substituting back into (4.50) produces

$$G(\alpha)l_1(\alpha) = u_1(\alpha) + G(\alpha)P(\alpha),$$

where

$$G(\alpha) = \frac{\kappa(\psi^2 - 1)}{2}, \quad P(\alpha) = \frac{1}{2\pi i(\alpha + k)}.$$

This equation is now rearranged in the usual manner and Liouville's theorem is applied. The functions $u_1(\alpha)$ and $l_1(\alpha)$ can be written as

$$u_1(\alpha) = -G_+(\alpha)G_-(-k)P(\alpha),$$

$$l_1(\alpha) = [\mathrm{I} - G_-^{-1}(\alpha)G_-(-k)]P(\alpha).$$

In the case of a rigid wave-guide, the far-field takes the form

$$H_z(r,\theta) = 2i\sqrt{\frac{\pi}{2kr}}u_1[k\cos\theta]e^{ikr+\frac{\pi i}{4}}, \quad y \geq a, \tag{4.52}$$

$$= -2i\sqrt{\frac{\pi}{2kr}}u_2[k\cos\theta]e^{ikr+\frac{\pi i}{4}}, \quad y \leq a. \tag{4.53}$$

The field reflected at the wave-guide mouth reduces to

$$R = \sum_{n=0}^{\infty} \frac{-2\pi i}{f'(\alpha_n)} \Big\{ u_1(\alpha_n)\psi_n\kappa_n + u_2(\alpha_n)\psi_n^{-1}\kappa_n + u_1(\alpha_n)\psi_n^{-1}\kappa_n + u_2(\alpha_n)\psi_n\kappa_n \Big\}, \quad |y| < a, \tag{4.54}$$

where

$$f(\alpha) = \kappa^2\psi^{-2} - \kappa^2\psi^2.$$

The terms in this expression represent the reflected field modes in the waveguide. The dominant reflected wave mode R_0 is given by

$$R_0 = \frac{-2\pi i\kappa_o}{f'(\alpha_o)}(u_1(\alpha_o) + u_2(\alpha_o))(\psi_o + \psi_o^{-1}). \tag{4.55}$$

4.7 Conclusions

A new diffraction problem has been solved by means of the Wiener-Hopf-Hilbert Technique. The solution generalises that of Rulf and Hurd [12]. It was thought that the Wiener-Hopf-Hilbert method was not applicable due to the pole singularities in the matrix kernel. However, it has been shown that an explicit factorisation can be carried out.

The wave-guide problem solved here can be extended in several ways. A problem involving higher order modes in the wave-guide region provides a natural extension to this work. The situation could also be considered where the inner walls of the duct are capacitive and the outer walls inductive. This would simply require a change of sign in $\beta_{1,2}$ in the current solution.

A plane wave incident on a wave-guide can be solved using the Wiener-Hopf-Hilbert method (to be published by Rawlins). The solution to this problem closely follows the solution in the current chapter.

It would be of interest to consider more complicated boundary conditions on the faces of the waveguide. In particular, the techniques used in this work could be used in the case of a wave-guide in a moving fluid. The problem of a cylindrical semi-infinite waveguide with an inductive inner surface and capacitive outer surface might also be examined.

Appendix A

An Alternative Expression for the Diffracted Field

The diffracted field given by expressions (3.67) and (3.68) becomes infinite on the boundaries $\Theta = \pi - \Theta_o$ and $\Theta = \pi + \Theta_o$ so an alternate expression has been used to give the graphical plots of the modulus of the far-field. It is noted that Noble [27] gives the following result

$$\mathcal{I} = 2i \sin\left(\frac{\Theta_o}{2}\right) \int_{-\infty}^{\infty} \frac{\sin\frac{1}{2}(\Theta + it) e^{i\mathcal{K}R\cosh t}}{\cos(\Theta + it) + \cos\Theta_o} dt = -2iH(\Theta - \Theta_o) + 2iH(\Theta + \Theta_o),$$

where

$$H(\lambda) = \begin{cases} \pi^{\frac{1}{2}} e^{-\frac{i\pi}{4}} \mathcal{F}\left[\sqrt{2\mathcal{K}R}\cos(\lambda/2)\right] e^{-i\mathcal{K}R\cos\lambda}, & \cos(\lambda/2) > 0, \\ -\pi^{\frac{1}{2}} e^{-\frac{i\pi}{4}} \mathcal{F}\left[-\sqrt{2\mathcal{K}R}\cos(\lambda/2)\right] e^{-i\mathcal{K}R\cos\lambda}, & \cos(\lambda/2) < 0, \end{cases}$$

and

$$\mathcal{F}[v] = \int_v^{\infty} e^{iu^2} du.$$

This result, combined with (3.58) gives the following expression for the diffracted field

in the upper half of the plane.

$$\Psi_+(R,\Theta) = \frac{\cos(\Theta/2)u_1[\mathcal{K}\cos\Theta]\{\cos\Theta+\cos\Theta_o\}}{(\mathcal{B}_1-\mathcal{B}_1 M\cos\Theta+\sin\Theta)\sin(\Theta_o/2)}J_1, \qquad 0<\Theta<\pi-\Theta_o,$$
$$= \frac{\cos(\Theta/2)u_1[\mathcal{K}\cos\Theta]\{\cos\Theta+\cos\Theta_o\}}{(\mathcal{B}_1-\mathcal{B}_1 M\cos\Theta+\sin\Theta)\sin(\Theta_o/2)}J_2, \qquad \pi-\Theta_o<\Theta<\pi.$$

Where

$$J_1 = 2i\pi^{\frac{1}{2}}e^{-\frac{i\pi}{4}}\Big(e^{-i\mathcal{K}R\cos(\Theta+\Theta_o)}\mathcal{F}\left[\sqrt{2\mathcal{K}R}\cos\tfrac{1}{2}(\Theta+\Theta_o)\right] - e^{-i\mathcal{K}R\cos(\Theta-\Theta_o)}\mathcal{F}\left[\sqrt{2\mathcal{K}r}\cos\tfrac{1}{2}(\Theta-\Theta_o)\right]\Big),$$

$$J_2 = J_1 - 2\pi i e^{-i\mathcal{K}R\cos(\Theta+\Theta_o)}.$$

In the case of Chapter 2, Section 2.6, the alternate expressions are obtained by putting $M=0$ in the above results.

Appendix B

The Incident TM Wave

Here a discussion is given concerning the derivation of the incident wave (4.9) in Chapter 4. The incident wave is required to be the lowest order TM wave. A wave of the form

$$H_i = (A\cos\kappa y + B\sin\kappa y)e^{-i\alpha x}, \tag{B.1}$$

satisfies (4.2). Applying the boundary conditions (4.3) and (4.4) gives

$$A = B\left(\frac{\kappa\cos\kappa a - kX_1\sin\kappa a}{\kappa\sin\kappa a + kX_1\cos\kappa a}\right), \tag{B.2}$$

and

$$A = B\left(\frac{kX_2\sin\kappa a - \kappa\cos\kappa a}{kX_2\cos\kappa a + \kappa\sin\kappa a}\right). \tag{B.3}$$

Eliminating A and B and simplifying gives

$$\left(\kappa - \frac{k^2X_1X_2}{\kappa}\right)\sin 2\kappa a + k(X_1+X_2)\cos 2\kappa a = 0. \tag{B.4}$$

Equation (B.4) has an infinite number of roots. The only case of interest is where a single imaginary root exists, corresponding to the lowest propagating mode. Under the restriction $a < (X_1+X_2)/X_1X_2$ (Rulf and Hurd [12]), (B.4) possesses a single

imaginary root κ_o given by

$$\kappa_o = i\sigma_o, \quad \alpha_o = (k^2 + \sigma_o^2)^{1/2}, \tag{B.5}$$

where

$$\tanh 2\sigma_o a = \frac{k(X_1 + X_2)\sigma_o}{\sigma_o^2 + X_1 X_2}. \tag{B.6}$$

Also, substituting (B.2) into (B.1) allows the incident field to be written as

$$H_i = \phi_o(y, \kappa_o) e^{-i\alpha_o x},$$

where

$$\phi_o(y, \kappa) = \cos \kappa(y - a) + \frac{kX_1}{\kappa} \sin \kappa(y - a).$$

Appendix C

Mathematica Programs

The following programs were used in Mathematica to produce the graphical results within this work. Whilst Mathematica version 2.2 was used to plot the graphs, the programs have been converted to Mathematica version 3 for clarity.

Program 1 is an example of a program used to plot a radiated lobe for an incident surface wave. Program 2 gives the far-field plot for a half-plane in a moving fluid. The Kutta-Joukowski condition was used in Program 3, which is used for a half-plane in a moving fluid with a trailing vortex sheet.

```
* PROGRAM 1 : Radiated lobe for an incident surface wave *
thetao := ArcSin[beta1]
k := 1
r := 10 π
beta1 := -I
beta2 := -.5 I
```

$$u[y\_] := \begin{pmatrix} -\sqrt{v[x]}\ \sqrt{w[x]} & \sqrt{v[x]}\ \sqrt{w[x]}\ \sqrt{k+x} \\ -\frac{\sqrt{v[x]}}{\sqrt{w[x]}} & -\frac{\sqrt{v[x]}\ \sqrt{k+x}}{\sqrt{w[x]}} \end{pmatrix}$$

$$v[x\_] := \frac{1}{\sqrt{k+x}}$$

$$w[x\_] := \frac{\left(\sqrt{k+x} + \sqrt{k+k\sqrt{1-beta1^2}}\right)\left(\sqrt{k+x} + \sqrt{k-k\sqrt{1-beta1^2}}\right)}{\left(\sqrt{k+x} + \sqrt{k+k\sqrt{1-beta2^2}}\right)\left(\sqrt{k+x} + \sqrt{k-k\sqrt{1-beta2^2}}\right)}$$

$$int[x\_, y\_] := \int_{\frac{\pi}{2}}^{ArcCos[\frac{x}{k}]} a - \frac{Sin[a]\ ArcCos[y]}{\sqrt{1-y^2}} \Big/ \left(y - Cos[a]\right) da$$

$$lplus[x\_, b\_] := \sqrt{\frac{1+b}{1+\frac{x}{k}}}\ Exp\left[-\frac{b\left(int\left[x, \sqrt{1-b^2}\right] + int\left[x, -\sqrt{1-b^2}\right]\right)}{2\pi}\right]$$

```
lminus[x_, b_] := rawl[x, b] / lplus[x, b]
rawl[x_, b_] := 1 + (k b / Sqrt[k^2 - x^2])
```

$$matrixk[x\_] := \frac{1}{\sqrt{2}} \begin{pmatrix} \sqrt{kappa[x]}\ \sqrt{\frac{kappa[x]+k\,beta1}{kappa[x]+k\,beta2}} & \frac{\sqrt{\frac{kappa[x]+k\,beta1}{kappa[x]+k\,beta2}}}{\sqrt{kappa[x]}} \\ -\sqrt{kappa[x]}\ \sqrt{\frac{kappa[x]+k\,beta2}{kappa[x]+k\,beta1}} & \frac{\sqrt{\frac{kappa[x]+k\,beta2}{kappa[x]+k\,beta1}}}{\sqrt{kappa[x]}} \end{pmatrix}$$

$$kappa[x\_] := -I\ Abs\left[\sqrt{k^2 - x^2}\right]$$

```
gplus[x_] := dplus[x] u[x]
gminus[x_] := dminus[x] Inverse[u[x]] . matrixk[x]
```

$$dminus[x\_] := \sqrt{\sqrt{\frac{k-x}{2}}}\ \sqrt{lminus[x, beta1]}\ \sqrt{lminus[x, beta2]}$$

$$\text{dplus}[x\_] := \sqrt{\sqrt{\frac{k+x}{2}}}\ \sqrt{\text{lplus}[x, \text{beta1}]}\ \sqrt{\text{lplus}[x, \text{beta2}]}$$

$$\text{matrixu}[x\_] := -\frac{\text{Sin}[\text{thetao}]\ (\text{gplus}[x] \cdot \text{gminus}[-k\,\text{Cos}[\text{thetao}]]) \cdot p}{(\pi\,I)\ (\text{beta1} + \text{Sin}[\text{thetao}])\ (x + \text{Cos}[\text{thetao}])}$$

$$p := \begin{pmatrix} 1 \\ -\text{beta1} \end{pmatrix}$$

```
u1[x_] := matrixu[x][[1]]

u2[x_] := matrixu[x][[2]]
```

$$\text{psi3}[t\_] := \frac{2\,I\,\sqrt{\frac{\pi}{2\,k\,r}}\ \text{Sin}[t]\ \text{Exp}[I\,k\,r + \frac{I\,\pi}{4}]\ \text{u1}[k\,\text{Cos}[t]]}{\text{Sin}[t] + \text{beta1}}$$

$$\text{psi4}[t\_] := -\frac{2\,I\,\sqrt{\frac{\pi}{2\,k\,r}}\ \text{Sin}[t]\ \text{Exp}[I\,k\,r + \frac{I\,\pi}{4}]\ \text{u2}[k\,\text{Cos}[t]]}{-\text{Sin}[t] + \text{beta2}}$$

```
<< "Graphics`Graphics`"

r5 := PolarPlot[Abs[psi3[x]^2 / psi3[3.14]^2], {x, 0, 3.14}]

r6 := PolarPlot[Abs[ psi4[x]^2 / psi4[-3.14]^2], {x, -3.14, 0}]

Show[r5, r6]
```

```
* PROGRAM 2 : Far - field for a plane wave incident on a half - plane in a moving fluid *
Off[General::"spell"]
Off[General::"spell1"]
thetao := bt[π/2]
k := 1/√(1 - m^2)
m := 0.9
beta1 := 1/((.5 + I) √(1 - m^2))
beta2 := 1/((.5 + I) √(1 - m^2))
u[y_] := ( -√v[x] √w[x]        √v[x] √w[x] √k + x
           -√v[x]/√w[x]        -√v[x] √k+x/√w[x] )
v[x_] := 1/√(k + x)
bplus[b_] := √(k - (k b^2 m + k √(1 + b^2 m^2 - b^2))/(1 + b^2 m^2))
bminus[b_] := √(k - (k b^2 m - k √(1 + b^2 m^2 - b^2))/(1 + b^2 m^2))
w[x_] := √((1+beta1^2 m^2)/(1+beta2^2 m^2)) ((√k + x + bplus[beta1]) (√k + x + bminus[beta1]))
         / ((√k + x + bplus[beta2]) (√k + x + bminus[beta2]))
int[x_, y_] := N[-(m + y) ∫_{π/2}^{ArcCos[x/k]} (a - Sin[a] ArcCos[y]/√(1-y^2))/(y - Cos[a]) da]
lplus[x_, b_] := √((1 + b)/(1 + x/k)) Exp[b (int[x, v1[b]] - int[x, v2[b]])/(2 π √(1 - b^2 + (b m)^2))]
lminus[x_, b_] := lplus[-x, b]
```

$$v1[b\_] := \frac{-m\,b^2 + \sqrt{1 - b^2 + (m\,b)^2}}{1 + (b\,m)^2}$$

$$v2[b\_] := \frac{-m\,b^2 - \sqrt{1 - b^2 + (m\,b)^2}}{1 + (b\,m)^2}$$

$$\text{matrixk}[x\_] := (1 / \text{Sqrt}[2]) \left\{\left\{\sqrt{\text{kappa}[x]}\ \sqrt{\frac{\text{kappa}[x] + \text{beta1}\,m\,x + k\,\text{beta1}}{\text{kappa}[x] + \text{beta2}\,m\,x + k\,\text{beta2}}},\ \frac{\sqrt{\frac{\text{kappa}[x]+\text{beta1}\,m\,x+k\,\text{beta1}}{\text{kappa}[x]+\text{beta2}\,m\,x+k\,\text{beta2}}}}{\sqrt{\text{kappa}[x]}}\right\},\ \left\{-\sqrt{\text{kappa}[x]}\ \sqrt{\frac{\text{kappa}[x] + \text{beta2}\,m\,x + k\,\text{beta2}}{\text{kappa}[x] + \text{beta1}\,m\,x + k\,\text{beta1}}},\ \frac{\sqrt{\frac{\text{kappa}[x]+\text{beta2}\,m\,x+k\,\text{beta2}}{\text{kappa}[x]+\text{beta1}\,m\,x+k\,\text{beta1}}}}{\sqrt{\text{kappa}[x]}}\right\}\right\}$$

$$\text{kappa}[x\_] := \sqrt{k^2 - x^2}$$

$$l[x\_] := \text{Inverse}[u[x]] \,.\, \text{matrixk}[x]$$

$$\text{gminus}[x\_] := \text{dminus}[x]\ l[x]$$

$$\text{dminus}[x\_] := \sqrt{\sqrt{\frac{k - x}{2}}}\ \sqrt{\text{lminus}[x, \text{beta1}]}\ \sqrt{\text{lminus}[x, \text{beta2}]}$$

$$\text{dplus}[x\_] := \sqrt{\sqrt{\frac{k + x}{2}}}\ \sqrt{\text{lplus}[x, \text{beta1}]}\ \sqrt{\text{lplus}[x, \text{beta2}]}$$

$$\text{gplus}[x\_] := \text{dplus}[x]\ u[x]$$

$$\text{matrixu}[x\_] := \left(\text{gplus}[x] \,.\, \text{gminus}\left[-\frac{k}{m}\right]\right) \,.\, q[x] - (\text{gplus}[x] \,.\, \text{gminus}[-k\,\text{Cos}[\text{thetao}]]) \,.\, \frac{p}{x + k\,\text{Cos}[\text{thetao}]}$$

$$p := \frac{\text{Sin}[\text{thetao}]\ \{1,\ -k\,\text{beta1}\ (1 - m\,\text{Cos}[\text{thetao}])\}}{\pi\,I\ (\text{Sin}[\text{thetao}] - \text{beta1}\,m\,\text{Cos}[\text{thetao}] + \text{beta1})}$$

$$u1[x\_] := \text{matrixu}[x]\,[\![1]\!]$$
$$u2[x\_] := \text{matrixu}[x]\,[\![2]\!]$$

$$i1[t\_,\ r\_] := I\sqrt{\pi}\ \text{Exp}\left[-\frac{I\,\pi}{4}\right] \left(-\text{Exp}[-I\,k\,r\,\text{Cos}[t - \text{thetao}]]\ f\left[\sqrt{2\,k\,r}\ \text{Cos}\left[\frac{t - \text{thetao}}{2}\right]\right] + \text{Exp}[-I\,k\,r\,\text{Cos}[t + \text{thetao}]]\ f\left[\sqrt{2\,k\,r}\ \text{Cos}\left[\frac{t + \text{thetao}}{2}\right]\right]\right)$$

$$f[t\_] := \int_t^{\infty} \text{Exp}[I\,v^2]\ dv$$

```
psi1[t_, r_] := Exp[-I k r Cos[t - thetao]]

psi2[t_, r_] := (beta1 m Cos[thetao] + Sin[thetao] - beta1) Exp[-I k r Cos[t + thetao]] / (-beta1 m Cos[thetao] + Sin[thetao] + beta1)

psi5[t_, r_] := (2 Cos[t/2]) u1[k Cos[t]] (Cos[t] + Cos[thetao]) i1[t, r] / ((beta1 + Sin[t] + beta1 m Cos[t]) Sin[thetao/2])

psi7[t_, r_] := (2 Cos[t/2]) u1[k Cos[t]] (Cos[t] + Cos[thetao]) (i1[t, r] - I π Exp[-I r k Cos[t + thetao]]) / ((beta1 + Sin[t] + beta1 m Cos[t]) Sin[thetao/2])

psi6[t_, r_] := -(2 Cos[t/2]) u2[k Cos[t]] (Cos[t] + Cos[thetao]) i1[t, r] / ((beta2 - Sin[t] + beta2 m Cos[t]) Sin[thetao/2])

psi8[t_, r_] := -(2 Cos[t/2]) u2[k Cos[t]] (Cos[t] + Cos[thetao]) (i1[t, r] + I π Exp[-I r k Cos[t - thetao]]) / ((beta2 - Sin[t] + beta2 m Cos[t]) Sin[thetao/2])

<< "Graphics`Graphics`"

bt[x_] := ArcCos[Cos[x] / Sqrt[1 - (m Sin[x])^2]]

br[x_] := 10 π Sqrt[(1 - (m Sin[x])^2) / (1 - m^2)]

r1 := PolarPlot[Abs[psi1[bt[x], br[x]] + psi2[bt[x], br[x]] + psi5[bt[x], br[x]]],
  {x, 0, 3.14 - thetao}, PlotPoints → 50]
r2 := PolarPlot[Abs[psi1[bt[x], br[x]] + psi7[bt[x], br[x]]],
  {x, 3.14 - thetao, 3.14}, PlotPoints → 50]
r3 := PolarPlot[Abs[psi1[-bt[x], br[x]] + psi8[-bt[x], br[x]]],
  {x, -3.14, -3.14 + thetao}, PlotPoints → 50]
r4 := PolarPlot[Abs[psi6[-bt[x], br[x]]], {x, -3.14 + thetao, 0}, PlotPoints → 50]

Show[r1, r2, r3, r4]
```

```
* PROGRAM 3 : Far - field for a plane wave incident on a half - plane in a moving fluid *

Off[General::"spell"]
Off[General::"spell1"]
```

$$\text{thetao} := \text{bt}\left[\frac{\pi}{2}\right]$$

$$k := \frac{1}{\sqrt{1 - m^2}}$$

$$m := 0.9$$

$$\text{beta1} := \frac{0.5 - I}{\sqrt{1 - m^2}}$$

$$\text{beta2} := \frac{0.5 - I}{\sqrt{1 - m^2}}$$

$$\text{bplus}[b\_] := \sqrt{k - \frac{k\,b^2\,m + k\sqrt{1 + b^2\,m^2 - b^2}}{1 + b^2\,m^2}}$$

$$\text{bminus}[b\_] := \sqrt{k - \frac{k\,b^2\,m - k\sqrt{1 + b^2\,m^2 - b^2}}{1 + b^2\,m^2}}$$

$$v[x\_] := \frac{1}{\sqrt{k + x}}$$

$$w[x\_] := \frac{\sqrt{\frac{1+\text{beta1}^2\,m^2}{1+\text{beta2}^2\,m^2}}\ \left(\left(\sqrt{k + x} + \text{bplus}[\text{beta1}]\right)\left(\sqrt{k + x} + \text{bminus}[\text{beta1}]\right)\right)}{\left(\sqrt{k + x} + \text{bplus}[\text{beta2}]\right)\left(\sqrt{k + x} + \text{bminus}[\text{beta2}]\right)}$$

$$u[y\_] := \begin{pmatrix} -\sqrt{v[x]}\ \sqrt{w[x]} & \sqrt{v[x]}\ \sqrt{w[x]}\ \sqrt{k + x} \\ -\frac{\sqrt{v[x]}}{\sqrt{w[x]}} & -\frac{\sqrt{v[x]}\ \sqrt{k+x}}{\sqrt{w[x]}} \end{pmatrix}$$

$$\text{int}[x\_, y\_] := N\left[-(m + y)\int_{\frac{\pi}{2}}^{\text{ArcCos}\left[\frac{x}{k}\right]} a - \frac{\text{Sin}[a]\,\text{ArcCos}[y]}{\sqrt{1-y^2}}}{y - \text{Cos}[a]}\,da\right]$$

$$\text{lplus}[x\_, b\_] := \sqrt{\frac{1 + b}{1 + \frac{x}{k}}}\ \text{Exp}\left[\frac{b\,(\text{int}[x, \text{v1}[b]] - \text{int}[x, \text{v2}[b]])}{2\,\pi\sqrt{1 - b^2 + (b\,m)^2}}\right]$$

$$\text{lminus}[x\_, b\_] := \text{lplus}[-x, b]$$

$$\text{v1}[b\_] := \frac{-m\,b^2 + \sqrt{1 - b^2 + (m\,b)^2}}{1 + (b\,m)^2}$$

$$v2[b\_] := \frac{-m\,b^2 - \sqrt{1 - b^2 + (m\,b)^2}}{1 + (b\,m)^2}$$

$$matrixk[x\_] := (1 / Sqrt[2])\left\{\left\{\sqrt{kappa[x]}\,\sqrt{\frac{kappa[x] + beta1\,m\,x + k\,beta1}{kappa[x] + beta2\,m\,x + k\,beta2}},\ \frac{\sqrt{\frac{kappa[x]+beta1\,m\,x+k\,beta1}{kappa[x]+beta2\,m\,x+k\,beta2}}}{\sqrt{kappa[x]}}\right\},\ \left\{-\sqrt{kappa[x]}\,\sqrt{\frac{kappa[x] + beta2\,m\,x + k\,beta2}{kappa[x] + beta1\,m\,x + k\,beta1}},\ \frac{\sqrt{\frac{kappa[x]+beta2\,m\,x+k\,beta2}{kappa[x]+beta1\,m\,x+k\,beta1}}}{\sqrt{kappa[x]}}\right\}\right\}$$

$$kappa[x\_] := \sqrt{k^2 - x^2}$$

$$l[x\_] := Inverse[u[x]] \,.\, matrixk[x]$$

$$gminus[x\_] := dminus[x]\,l[x]$$

$$dminus[x\_] := \sqrt{\sqrt{\frac{k - x}{2}}}\ \sqrt{lminus[x, beta1]}\ \sqrt{lminus[x, beta2]}$$

$$dplus[x\_] := \sqrt{\sqrt{\frac{k + x}{2}}}\ \sqrt{lplus[x, beta1]}\ \sqrt{lplus[x, beta2]}$$

$$gplus[x\_] := dplus[x]\,u[x]$$

$$matrixu[x\_] := \left(gplus[x] \,.\, gminus\left[-\frac{k}{m}\right]\right) \,.\, q[x] - (gplus[x] \,.\, gminus[-k\,Cos[thetao]]) \,.\, \frac{p}{x + k\,Cos[thetao]}$$

$$p := \frac{Sin[thetao]\,\{1,\ -k\,beta1\,(1 - m\,Cos[thetao])\}}{\pi\,I\,(Sin[thetao] - beta1\,m\,Cos[thetao] + beta1)}$$

$$u1[x\_] := matrixu[x]\llbracket 1\rrbracket$$
$$u2[x\_] := matrixu[x]\llbracket 2\rrbracket$$

$$cform := N\left[\frac{gminus[-k\,Cos[thetao]]\llbracket 2,\ 1\rrbracket\,p\llbracket 1\rrbracket + gminus[-k\,Cos[thetao]]\llbracket 2,\ 2\rrbracket\,p\llbracket 2\rrbracket}{gminus\left[-\frac{k}{m}\right]\llbracket 2,\ 1\rrbracket}\right]$$

$$q[x\_] := \frac{cform\,\{1,\ 0\}}{x + \frac{k}{m}}$$

$$i1[t\_,\ r\_] := I\,\sqrt{\pi}\ Exp\left[-\frac{I\,\pi}{4}\right]\left(-Exp[-I\,k\,r\,Cos[t - thetao]]\ f\left[\sqrt{2\,k\,r}\ Cos\left[\frac{t - thetao}{2}\right]\right] + Exp[-I\,k\,r\,Cos[t + thetao]]\ f\left[\sqrt{2\,k\,r}\ Cos\left[\frac{t + thetao}{2}\right]\right]\right)$$

$$f[t\_] := \int_t^{\infty} Exp[I\,v^2]\,dv$$

$$psi1[t\_,\ r\_] := N[Exp[-I\,k\,r\,Cos[t - thetao]]]$$

$$\text{psi2}[t\_, r\_] := \frac{(\text{beta1 m Cos}[\text{thetao}] + \text{Sin}[\text{thetao}] - \text{beta1})\ \text{Exp}[-\text{I k r Cos}[t + \text{thetao}]]}{-\text{beta1 m Cos}[\text{thetao}] + \text{Sin}[\text{thetao}] + \text{beta1}}$$

$$\text{psi3}[t\_, r\_] := \frac{2\,\text{I}\sqrt{\frac{\pi}{2\,k\,r}}\ \text{Sin}[t]\ \text{Exp}[\text{I k r} + \frac{\text{I}\pi}{4}]\ \text{u1}[k\,\text{Cos}[t]]}{\text{Sin}[t] + \text{beta1 m Cos}[t] + \text{beta1}}$$

$$\text{psi4}[t\_, r\_] := -\frac{2\,\text{I}\sqrt{\frac{\pi}{2\,k\,r}}\ \text{Sin}[t]\ \text{Exp}[\text{I k r} + \frac{\text{I}\pi}{4}]\ \text{u2}[k\,\text{Cos}[t]]}{-\text{Sin}[t] + \text{beta2 m Cos}[t] + \text{beta2}}$$

$$\text{psi5}[t\_, r\_] := \frac{(2\,\text{Cos}[\frac{t}{2}])\ \text{u1}[k\,\text{Cos}[t]]\ (\text{Cos}[t] + \text{Cos}[\text{thetao}])\ \text{i1}[t, r]}{(\text{beta1} + \text{Sin}[t] + \text{beta1 m Cos}[t])\ \text{Sin}[\frac{\text{thetao}}{2}]}$$

$$\text{psi7}[t\_, r\_] := \frac{(2\,\text{Cos}[\frac{t}{2}])\ \text{u1}[k\,\text{Cos}[t]]\ (\text{Cos}[t] + \text{Cos}[\text{thetao}])\ (\text{i1}[t, r] - \text{I}\,\pi\,\text{Exp}[-\text{I r k Cos}[t + \text{thetao}]])}{(\text{beta1} + \text{Sin}[t] + \text{beta1 m Cos}[t])\ \text{Sin}[\frac{\text{thetao}}{2}]}$$

$$\text{psi6}[t\_, r\_] := -\frac{(2\,\text{Cos}[\frac{t}{2}])\ \text{u2}[k\,\text{Cos}[t]]\ (\text{Cos}[t] + \text{Cos}[\text{thetao}])\ \text{i1}[t, r]}{(\text{beta2} - \text{Sin}[t] + \text{beta2 m Cos}[t])\ \text{Sin}[\frac{\text{thetao}}{2}]}$$

$$\text{psi8}[t\_, r\_] := -\frac{(2\,\text{Cos}[\frac{t}{2}])\ \text{u2}[k\,\text{Cos}[t]]\ (\text{Cos}[t] + \text{Cos}[\text{thetao}])\ (\text{i1}[t, r] + \text{I}\,\pi\,\text{Exp}[-\text{I r k Cos}[t - \text{thetao}]])}{(\text{beta2} - \text{Sin}[t] + \text{beta2 m Cos}[t])\ \text{Sin}[\frac{\text{thetao}}{2}]}$$

```
<< "Graphics`Graphics`"
```

$$\text{bt}[x\_] := \text{ArcCos}\left[\frac{\text{Cos}[x]}{\sqrt{1 - (\text{m Sin}[x])^2}}\right]$$

$$\text{br}[x\_] := 10\,\pi\sqrt{\frac{1 - (\text{m Sin}[x])^2}{1 - \text{m}^2}}$$

```
r1 := PolarPlot[Abs[psi1[bt[x], br[x]] + psi2[bt[x], br[x]] + psi5[bt[x], br[x]]],
   {x, 0, 3.14 - thetao}, PlotPoints → 50]
r2 := PolarPlot[Abs[psi1[bt[x], br[x]] + psi7[bt[x], br[x]]],
   {x, 3.14 - thetao, 3.14}, PlotPoints → 50]
r3 := PolarPlot[Abs[psi1[-bt[x], br[x]] + psi8[-bt[x], br[x]]],
   {x, -3.14, -3.14 + thetao}, PlotPoints → 50]
r4 := PolarPlot[Abs[psi6[-bt[x], br[x]]], {x, -3.14 + thetao, 0}, PlotPoints → 50]

Show[r1, r2, r3, r4]
```

Appendix D

Calculation of $I(\alpha)$ and $J(\alpha)$

In this appendix a derivation is given for the integral

$$I(\alpha) = \int_0^\infty \frac{\log(t+\delta)}{t^{\frac{1}{2}}(t+\gamma)} dt. \tag{D.1}$$

If it is assumed that γ and δ are real and positive then

$$\begin{aligned} I(\alpha) &= \int_0^\infty \frac{\log|t+\delta|}{t^{\frac{1}{2}}(t+\gamma)} dt, \\ &= 2\int_0^\infty \frac{\log|u^2+\delta|}{u^2+\gamma} du, \\ &= \int_{-\infty}^\infty \frac{\log|u^2+\delta|}{u^2+\gamma} du, \\ &= \int_{-\infty}^\infty \frac{\log|u+i\sqrt{\delta}|}{u^2+\gamma} du + \int_{-\infty}^\infty \frac{\log|u-i\sqrt{\delta}|}{u^2+\gamma} du, \\ &= 2\int_{-\infty}^\infty \frac{\log|u+i\sqrt{\delta}|}{u^2+\gamma} du = 2\mathrm{Re}\int_{-\infty}^\infty \frac{\log(u+i\sqrt{\delta})}{u^2+\gamma} du. \end{aligned}$$

Now consider the integral

$$2\int_\Gamma \frac{\log(z+i\sqrt{\delta})}{z^2+\gamma} dz,$$

where Γ is shown in Figure D.1. Using the fact that the contribution from the circular arc is zero and capturing the simple pole at $i\sqrt{\gamma}$ yields

$$2\int_{-\infty}^\infty \frac{\log(u+i\sqrt{\delta})}{u^2+\gamma} du = 2\pi i \lim_{z\to i\sqrt{\gamma}} \frac{\log(z+i\sqrt{\delta})}{z+i\sqrt{\gamma}},$$

Appendix E

Throughout this work the following theorem is required. If $F(\dot{z})$ is a holomorphic function of z in $-\pi < arg(z+k) \leq \pi$; $F(z) = O(z^{-\epsilon})(\epsilon > 0)$ as $|z| \to \infty$ in $-\pi < \arg(z+k) \leq \pi$ and $F(z)$ satisfies

$$F^+(\xi) - F^-(\xi) = g(\xi), \quad -\infty < \xi < -k,$$

where $g(\xi)$ is a known function then

$$F(z) = \frac{1}{2\pi i}\int_{-\infty}^{-k} \frac{g(\xi)}{\xi - z} d\xi, \quad -\pi < arg(z+k) \leq \pi.$$

The proof of this theorem is as follows. For Γ_2 as shown in Figure E.1, Cauchy's theorem for z inside Γ_2 states that

$$F(z) = \frac{1}{2\pi i}\int_{\Gamma_2} \frac{F(\xi)}{\xi - z} d\xi.$$

Since $F(z) = O(z^{-\epsilon})$ as $|z| \to \infty(\epsilon > 0)$ the contribution to the above integral from the circular arc is zero. The branch cut contribution gives

$$\begin{aligned} F(z) &= \frac{1}{2\pi i}\int_{-\infty}^{-k} \frac{F^+(\xi)}{\xi - z} d\xi + \frac{1}{2\pi i}\int_{-k}^{-\infty} \frac{F^-(\xi)}{\xi - z} d\xi, \\ &= \frac{1}{2\pi i}\int_{-\infty}^{-k} \frac{F^+(\xi) - F^-(\xi)}{\xi - z} d\xi, \\ &= \frac{1}{2\pi i}\int_{-\infty}^{-k} \frac{g(\xi)}{\xi - z} d\xi. \end{aligned}$$

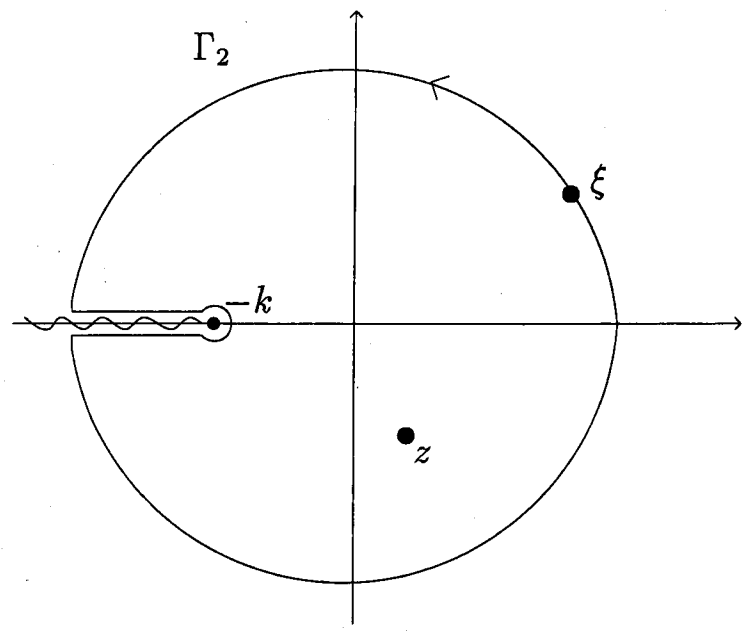

Figure E.1: The contour Γ_2 in the complex plane.

References

[1] Abrahams, I. D. and Wickham, G. R. "On the scattering of sound by two semi-infinite parallel staggered plates I. Explicit matrix Wiener-Hopf factorization", *Proc. Roy. Soc. London.* **420** 131-156 (1988).

[2] Abrahams, I. D. and Wickham, G. R. "Acoustic scattering by two parallel slightly staggered rigid plates", *Wave Motion.* **12** 281-297 (1990).

[3] Abrahams, I. D. and Wickham, G. R. "The scattering of sound by two semi-infinite parallel staggered plates II. Evaluation of the velocity potential for an incident plane wave and an incident duct mode", *Proc. Roy. Soc. London.* **427** 139-171 (1990).

[4] Copson, E. T. *Asymptotic Expansions.* Cambridge UP, (1965).

[5] Daniele, V. G. "On the Factorization of Wiener-Hopf Matrices in Problems Solvable with Hurd's Method", *IEEE Trans. Ant. Prop.* **26** 614-616 (1978).

[6] Erdelyi, A. *Asymptotic Expansions.* New York: Dover, (1956).

[7] Hashimoto, M. Idemen, M. and Tretyakov, O. A. *Analytical and Numerical Methods in Electromagnetic Wave Theory.* Science House Co. (1993).

[8] Heins, A. E. "The radiation and transmission properties of a pair of semi-infinite parallel plates - I", *Q. Appl. Math.* **6** 157-166 (1948).

[9] Heins, A. E. "The radiation and transmission properties of a pair of semi-infinite parallel plates - II", *Q. Appl. Math.* **6** 215-220 (1948).

[10] Heins, A. E. *Proceedings of Symposia in Applied Math.* New York: McGraw-Hill, (1950).

[11] Hurd, R. A. "The Wiener-Hopf-Hilbert method for diffraction problems", *Can. J. Phys.* **54** 775 (1976).

[12] Hurd, R. A. and Rulf, B. "Radiation from an Open Waveguide with Reactive Walls", *IEEE Trans. Ant. Prop.* **26** 668-673 (1978).

[13] Hurd, R. A. and Przeździecki, S. "Diffraction by a half-plane perpendicular to the distinguished axis of a general gyrotropic medium", *J. Math. Phys.* **17** 1838 (1976).

[14] Hurd, R. A. and Przeździecki, S. "Diffraction by a half-plane with different face impedances - a re-examination", *Can. J. Phys.* **59** 1337 (1981).

[15] Jones, D. S. *The Theory of Electromagnetism.* Oxford: Pergamon Press, (1964).

[16] Jones, D. S. "The mathematical theory of noise shielding", *Progr. Aerospace Sci.* **17** 149-229 (1977).

[17] Khrapkov, A. A. "Certain cases of the elastic equilibrium of an infinite wedge with a non-symmetric notch at the vertex, subjected to concentrated forces", *Prikl. Math. Mekh.* **35** 625-637 (1971).

[18] Lüneburg, E. and Hurd, R. A. "On the diffraction problem of a half-plane with different face impedances", *Can. J. Phys.* **62** 853 (1984).

[19] Lüneburg, E. and Hurd, R. A. "Diffraction by an anisotropic impedance half plane", *Can. J. Phys.* **63** 1135 (1985).

[20] Maliuzhinets, G. D. "Excitation, reflection and emission of surface waves from a wedge with given face impedances", *Sov. Phys. Dokl. Engl. Trans.* **3** 752-755 (1958).

[21] McIver, P. and Rawlins, A. D. "Diffraction by a rigid barrier with a soft or perfectly absorbent end face", *Wave Motion* **22** 387-402 (1995).

[22] Meister, E. and Speck, F. -O. "Diffraction problems with impedance conditions", *Appl. Anal.* **22** 193-211 (1986).

[23] Mittra, R. and Lee, S. W. *Analytical Techniques in the Theory of Guided Waves.* New York: Macmillan, (1971).

[24] Morse, P. M. and Ingard, K. U. *Encycl. Phys., Acoustics I.* Berlin: Springer Verlag, (1961).

[25] Munt, R. M. "Acoustic Radiation from a Circular Cylinder in a Subsonic Stream", *J. Inst. Maths. Applics.* **16** 1-10 (1975).

[26] Muskhelishvili, N. I. *Singular Integral Equations.* Groningen: Noordhoff, (1953).

[27] Noble, B. *Methods Based on the Wiener-Hopf Technique.* London: Pergamon, (1958).

[28] Rawlins, A. D. "Acoustic Diffraction by an Absorbing Semi-Infinite Half-Plane in a Moving Fluid", *Proc. R. S. E.* **72** 337-357 (1975).

[29] Rawlins, A. D. "Acoustic Diffraction by an Absorbing Semi-Infinite Plane in a Moving Fluid, II", *Proc. R. S. E.* **75** 83-95 (1975).

[30] Rawlins, A. D. and Williams, W. E. "Matrix Wiener-Hopf Factorisation", *Q. Journal Mech. Appl. Math.* **34** 1-8 (1981).

[31] Rawlins, A. D. "The solution of a mixed boundary value problem in the theory of diffraction", *Journal of Engineering Mathematics.* **18** 37-62 (1984).

[32] Trenev, N. G. "Diffraction of Surface Electromagnetic Waves on a Semi-Infinite Impedance Plane", *Radiotekhnika i elektronika 3.* **2** 163-171 (1958).

[33] Wiener, N. and Hopf, E. "Über eine Klasse singulärer Integralgeichungen", *S. B. Preuss. Akad. Wiss.* **3** 696-706 (1931).

$$I(\alpha) = \frac{2\pi}{\sqrt{\gamma}} \log(\sqrt{\gamma} + \sqrt{\delta}), \quad \gamma, \delta > 0. \tag{D.2}$$

Analytic continuation is now invoked to extend the range of applicability of this result.

$$\int_0^\infty \frac{\log(t+\delta)}{t^{1/2}(t+\gamma)} dt = \frac{2\pi}{\sqrt{\gamma}} \log(\sqrt{\gamma} + \sqrt{\delta}), \ |\arg\gamma| < \pi, |\arg\delta| \leq \pi. \tag{D.3}$$

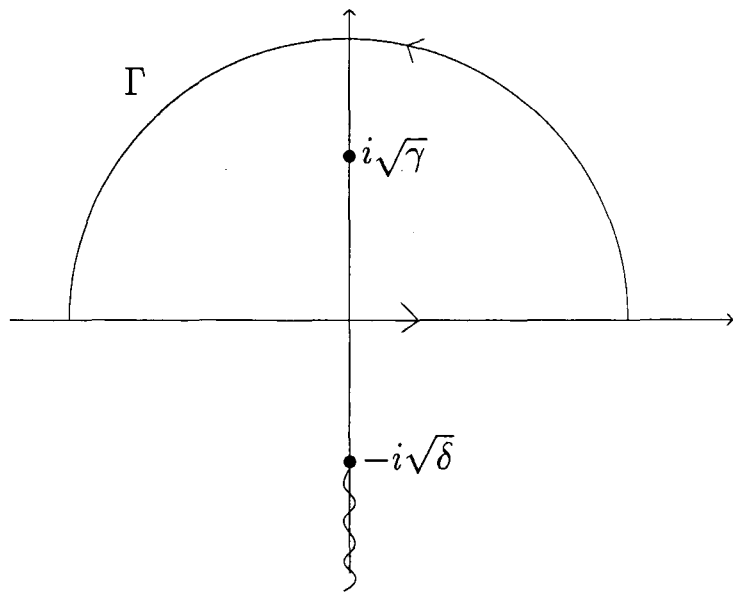

Figure D.1: Pole capture in the complex plane.

In Section 3.4 it is also required that

$$\begin{aligned}
J(\alpha) &= \int_0^\infty \frac{dt}{t^{1/2}(t+\mathcal{K}+\alpha)}, \\
&= 2\int_0^\infty \frac{du}{u^2+\mathcal{K}+\alpha}, \\
&= \frac{1}{\sqrt{\mathcal{K}+\alpha}} \int_0^\infty \left\{ \frac{1}{u+i\sqrt{\mathcal{K}+\alpha}} - \frac{1}{u-i\sqrt{\mathcal{K}+\alpha}} \right\} du, \\
&= \frac{1}{i\sqrt{\mathcal{K}+\alpha}} \left[\log\left(\frac{u-i\sqrt{\gamma}}{u+i\sqrt{\gamma}} \right) \right]_0^\infty, \\
&= \frac{\pi}{\sqrt{\mathcal{K}+\alpha}}.
\end{aligned}$$